Synergistic Effects of Oct4-Induced Reprogramming and PE2max-Mediated Prime Editing on Myelination and Restoration of GALC activity in Krabbe disease

Kim, Jinyoung

Department of Biomedical Engineering

Graduate School

Yonsei University

Synergistic Effects of Oct4-Induced Reprogramming and PE2max-Mediated Prime Editing on Myelination and Restoration of GALC activity in Krabbe disease

Advisor Cho, Sung-Rae

A Master's Thesis
Submitted to the Department of Biomedical Engineering
and the Committee on Graduate School
of Yonsei University in Partial Fulfillment of the
Requirements for the Degree of
Master of Biomedical Engineering

Kim, Jinyoung

July 2025

Synergistic Effects of Oct4-Induced Reprogramming and PE2max-Mediated Prime Editing on Myelination and Restoration of GALC activity in Krabbe disease

This certifies that the Master's Thesis of Kim, Jinyoung is Approved

Committee Chair	**Cho, Sung-Rae**
Committee Member	**Kim, Hyongbum**
Committee Member	**Yoo, Heechan**

Department of Biomedical Engineering
Graduate School
Yonsei University
June 2025

TABLE OF CONTENTS

LIST OF FIGURES

LIST OF TABLES

ABSTRACT

Synergistic Effects of Oct4-Induced Reprogramming and PE2max-Mediated Prime Editing on Myelination and Restoration of GALC activity in Krabbe disease

ABSTRACT

Krabbe disease (KD) is a fatal lysosomal storage disorder caused by a loss-of-function mutation in the *galactosylceramidase* (*GALC*) gene, resulting in impaired myelin metabolism and cytotoxic metabolite psychosine accumulation. This study aimed to investigate the therapeutic potential of a combinational approach that involves prime editing and *in vivo* cellular reprogramming in the KD Twitcher mouse model. The prime editor PE2max was used to correct the point mutation in the *Galc* gene, and Oct4 overexpression was induced through intracerebroventricular injection of AAV9 on postnatal day 1 (PD 1). Further, systemic delivery of AAVPHP.eB-PE2max was performed via facial vein injection. Behavioral assessments, including rotarod, hanging wire, cylinder, clasping, were conducted on PD21, PD28, and PD35. Animals were sacrificed on PD38, and subsequent molecular and histological analyses were conducted, including reverse quantitative transcription polymerase chain reaction, immunohistochemistry, electron microscopy, and magnetic resonance imaging, to assess Galc expression, remyelination (myelin basic protein), and cell fate markers such as Nestin, Olig2, Tuj1, and GFAP. BrdU labeling (PD7–9) confirmed that Oct4 induced neural precursor cell proliferation. The result revealed that Oct4 overexpression significantly increased the markers of the oligodendrocyte lineage and neural stem cell populations while reducing astrogliosis. Gene correction via PE2max restored the enzymatic activity of *Galc* and reduced psychosine accumulation. Combined treatment

resulted in superior outcomes in myelin restoration, behavioral improvement, and extended survival compared with monotherapies and control groups. These results indicate that dual therapy combining Oct4-mediated reprogramming and PE2max-based gene correction represents a synergistic and promising therapeutic strategy for KD, addressing both cellular regeneration and the underlying enzymatic deficiency.

Key words: Krabbe disease, galactocerebrosidase, *Galc* gene editing, Oct4-mediated in vivo reprogramming, Oligodendrocyte differentiation, myelination, Combination therapy

1. Introduction

Krabbe disease (KD), also known as globoid cell leukodystrophy, is a rare and fatal lysosomal storage disorder caused by *galactosylceramidase (Galc)* gene mutations.[1] The loss of the enzymatic activity of GALC results in the accumulation of psychosine, which is a cytotoxic metabolite that disrupts myelin sheath development and maintenance.[2,3] This causes widespread demyelination in both the central and peripheral nervous systems (CNS and PNS, respectively), clinically manifesting as developmental regression, spasticity, feeding difficulties, seizures, and early death. In murine models, such as the Twitcher mouse—which harbors a naturally occurring point mutation in the *Galc* gene—symptoms appear around postnatal day (PD) 21, with a life expectancy of approximately 40 days.[4]

The current treatment strategies for KD remain limited despite intensive research efforts. Hematopoietic stem cell transplantation provides partial benefit when administered presymptomatically; however, it fails to reverse existing neurological damage or effectively address the underlying molecular defects. Hence, therapies that correct the genetic basis of the disease and promote remyelination and functional recovery of affected neural circuits are urgently needed.

Recent advances in gene editing and regenerative medicine have opened new therapeutic possibilities. Prime editing, particularly the PE2max system, enables precise correction of point mutations without inducing double-strand DNA breaks. This method holds particular promise for treating monogenic diseases such as KD.[5-7] In parallel, *in vivo* cellular reprogramming using transcription factors, such as Oct4, has stimulated endogenous neurogenesis and glial lineage differentiation, which may support remyelination in demyelinating conditions.[8,9]

In this study, we employed a combinational therapeutic method in the Twitcher mouse model, integrating systemic delivery of PE2max via AAVPHP.eB vectors to correct the *Galc* gene, alongside intracerebroventricular (ICV) AAV9-Oct4 injection to promote neural reprogramming.[10,11] Oct4 was administered on PD 1, whereas behavioral assessments were conducted at PD21, PD28, and PD35.[12,13] After the sacrifice at PD38, we conducted

histological and molecular analyses—including quantitative reverse transcription polymerase chain reaction (qRT-PCR), immunohistochemistry (IHC), electron microscopy (EM), and magnetic resonance imaging (MRI)—to assess Galc expression, remyelination (myelin basic protein [MBP]), and the presence of neural stem and glial lineage markers (Nestin, Olig2, Tuj1, and GFAP). BrdU labeling was used from PD7 to PD9 to trace proliferating cells that are induced by Oct4 expression.[14,15]

This study aims to investigate the therapeutic potential of combining prime editing with transcriptional reprogramming as a novel strategy for treating KD by assessing both gene correction efficiency and cellular remodeling capacity. We hypothesize that this dual method may synergistically address both the genetic defect and the regenerative deficit underlying KD pathology.

2. Materials and methods

2.1. Mouse Strains and Environmental Conditions

Twitcher mouse (C57BL/6, *Galc*^{twi}), carrying a heterozygous point mutation in the *Galc* gene at codon 355 (G to A transition, resulting in a tryptophan-to-stop codon substitution, p.W355*), were obtained from Jackson Laboratory and maintained on a C57BL/6 background. Disease onset typically occurs around postnatal day 20, presenting symptoms such as head tremors, reduced body weight, and decreased activity. Due to a deficiency in functional galactosylceramidase (GALC), these mice express only a truncated, non-functional form of the enzyme, and their lifespan is typically limited to approximately 40 days. To generate homozygous Twitcher mouse, heterozygous breeders were housed in standard cages (27 × 22.5 × 14 cm³) under controlled conditions in an animal facility accredited by the Association for Assessment and Accreditation of Laboratory Animal Care (AAALAC). All animals were maintained on a 12-hour light/dark cycle, and all procedures were conducted with approval from the Institutional Animal Care and Use Committee of Yonsei University College of Medicine (IACUC No. 2022-0307).

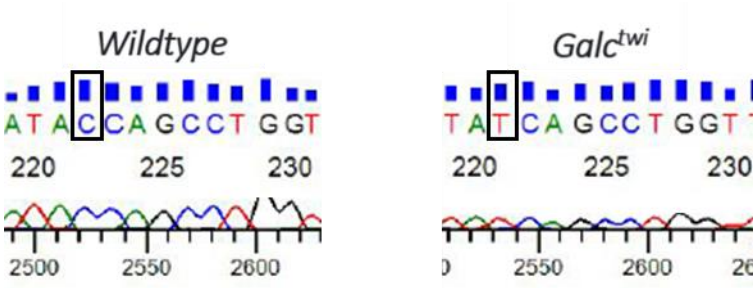

Figure 1. Genotyping for identification of Twitcher mice

PCR-based genotyping was performed to identify the *Galc* mutation in mice. The wild-type allele contains a homozygous cytosine (*CCAGCCT*), whereas the mutant *Galc*^{twi} allele contains a homozygous thymine (*TCAGCCT*). Mice homozygous for the *Galc*^{twi} allele exhibits the disease phenotype.

2.2. Structure of the AAV9 Vector Encoding Oct4

AAV9 vectors that encode the *Oct4* gene (*mPou5f1*; reference sequence: NM_013633.3) were designed using a CMV promoter and obtained from VectorBuilder (Chicago, USA).

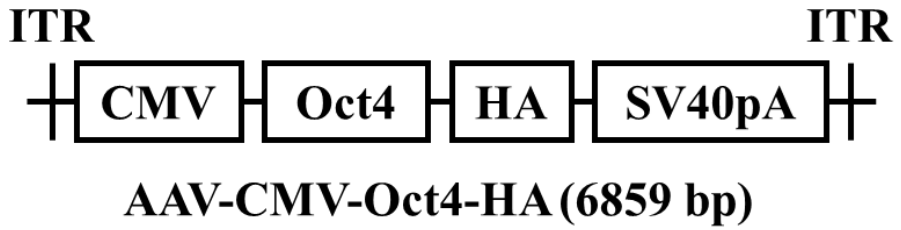

Figure 2. AAV Vector Construct Encoding HA-Tagged Oct4

Design of an AAV expression cassette encoding the HA-tagged *Oct4* gene. The construct consists of the CMV promoter, which drives robust, constitutive expression in mammalian cells; *Oct4*, the transcription factor gene used for cellular reprogramming; an HA (hemagglutinin) tag fused at the C-terminal end of Oct4 for immunodetection; and the SV40 polyadenylation signal (SV40pA) to ensure proper transcriptional termination and mRNA stability.

2.3. Intracerebroventricular (ICV) injection of AAV9-Oct4 on PD 1

ICV AAV9-Oct4 was injected into Twitcher mice within 24 h postnatal (PD 1). Neonatal mice were placed on ice for 5 min, and a 1-μL volume of viral solution (1×10^{10} vg/μL) was slowly injected into both lateral ventricles for 1 min using a 32-gauge Hamilton syringe for anesthesia. The stereotaxic coordinates used were anteroposterior (AP) +1.5 mm and mediolateral (ML) ±0.8 mm from the lambda, and dorsoventral (DV) −1.5 mm from the dura mater (Figure 2). After the injection, the needle was left in place for 1 min to prevent backflow. The pups were allowed to recover on a heating pad and were then returned to their home cage with the dam after completing the procedure. BrdU was administered to the injected group at 250 mg/mouse once daily from PD7 to PD9. Figure 3 illustrates the overall experimental scheme. Further, to verify viral expression, AAV9-GFP was used, and GFP expression was observed in the septum, frontal cortex (FC), and basal ganglia.

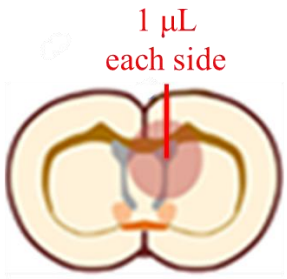

AAV9-Oct4:1μL
(10^{10}viral particles per μL)

Injection site
AP+1.55mm
ML±0.8mm
DV-1.5mm

Figure 3. Intracerebroventricular (ICV) injection of AAV9-Oct4 on postnatal day 1. The AAV9-Oct4 was injected intracerebroventricularly (ICV) into Twitcher mice on postnatal day 1 (PD 1). (A) Schematic image depicting the site of stereotaxic injection: AP +1.5 mm; ML ±0.8 mm; DV −1.5 mm. Procedure for ICV injection of the virus on PD 1 in Twitcher mice. ICV injection was performed on a PD 1 Twitcher mouse.

2.4. Design of PHP.eB-Based PE2max Delivery System

A split PE2max delivery system using AAV-PHP.eB vectors was developed to enable intein-mediated protein reconstitution, and the configuration of the prime editing guide RNA was optimized separately to enhance editing efficiency.

(A)

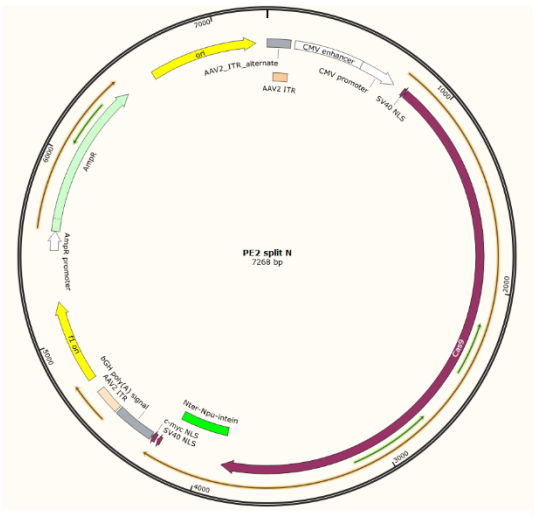

PE2max_N plasmid map

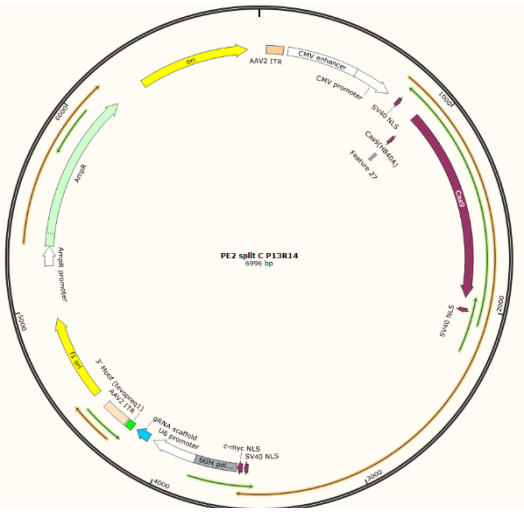

PE2max_C_epegRNA plasmid map

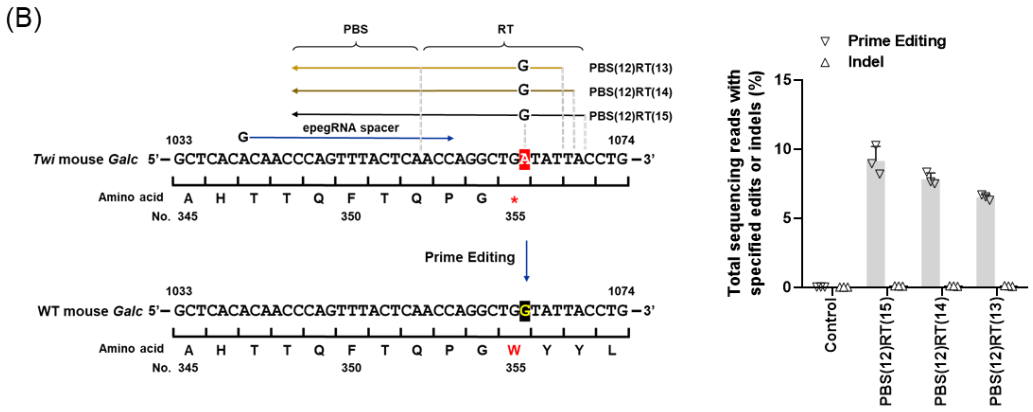

Figure 4. Design and functional elements of the split PE2max vector.

(A) The full-length PE2max construct cannot be packaged into a single AAV vector due to its size; thus, the sequence was divided and cloned into two separate AAV-compatible plasmids. Npu intein was utilized to enable protein reconstitution. After n infection, each plasmid expresses its respective protein fragments, which undergoes intein-mediated protein splicing to reconstitute a functional full-length PE2max protein in the host cell.

(B) To identify the optimal design for prime editing, various combinations of primer binding site (PBS) and reverse transcription (RT) template lengths were systematically tested. The design with a 12-nucleotide PBS and a 15-nucleotide RT template yielded the highest editing efficiency among the different configurations. This combination was selected as the most effective condition for subsequent experiments because it consistently produced robust and precise gene correction outcomes. These dual AAV constructs (AAV-PHP.eB-PE2max) were kindly provided by Prof. Heechan Yoo (Chung-Ang University).

2.5. Facial vein injection of AAV PHP.eB PE2max on PD 1

On PD 1, AAV-PHP.eB-PE2max (4×10^{10} vg/μL, 10 μL) was administered via facial vein injection using a 32-gauge insulin syringe. Evans blue dye was added to the viral solution to monitor vascular leakage or rupture, enabling visual confirmation through changes in the skin color of the pup.

2.6. Experimental Timeline of Animal Study

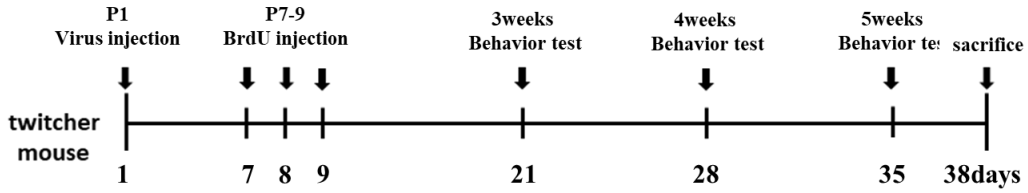

Figure 5. The experimental scheme.

Remyelination was induced by overexpression of Oct4 under the control of the AAV9 vector. AAV9-Oct4 was administered in KD mice on postnatal day 1 (PD 1) via intracerebroventricular injection. The PE2max prime editor, in either the AAVPHP.eB-PE2max vectors, was injected into the facial vein on PD 1 of KD mice. Behavioral tests were conducted on PD 21, 28, and 35, with molecular and histological analyses conducted at PD 37 to confirm the extent of remyelination. Additionally, to determine the presence of newly generated cells resulting from Oct4 overexpression, BrdU was administered via intraperitoneal injection from PD 7 to 9.

2.7. Behavioral assessments

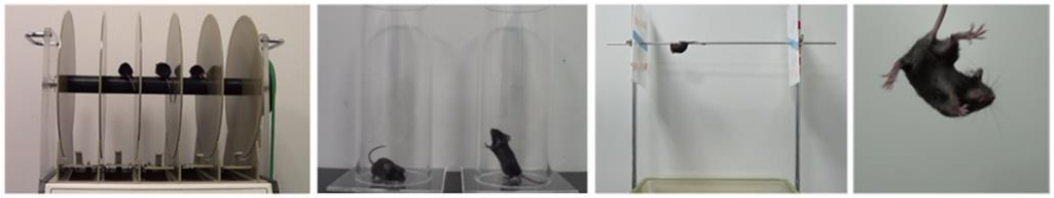

Figure 6. List of behavioral assessments conducted in the mouse model of Krabbe disease.

(A) Rotarod test, (B) Cylinder test, (C) Hanging wire test, (D) Clasping test

The schematic representation of ICV injection of AAV9-Oct4 and facial vein injection AAV PHP.eB-PE2max on postnatal day 1 in the twitcher

2.7.1. Rotarod test

The rotarod test was conducted to assess motor coordination and locomotor function. Mice were placed on a rotarod treadmill (Ugo Basile, Gemonio, Italy), and the latency to fall was recorded as the time each mouse remained on the rotating rod. Tests were performed at 3, 4, and 5 weeks of age under two conditions: an accelerating speed (4 to 40 rpm) and constant speeds (4 and 12 rpm). Each test was conducted twice per condition, with a maximum trial duration of 300 seconds.

2.7.2. Hanging wire test

The hanging wire test was performed to evaluate muscle strength in mice. Each mouse was placed on a 4-mm thick metal wire securely suspended between two vertical stands. Plastic barriers at both ends of the wire prevented escape, and a cage filled with wood shavings was placed 35 cm below to cushion any falls. The latency to fall was recorded, with a maximum duration of 300 seconds per trial. Each mouse underwent three trials, with a 10-minute rest interval between trials.

2.7.3. Clasping test

Hindlimb clasping, a phenotype commonly observed in neurodegenerative mouse models such as the Twitcher mouse, was evaluated. Each mouse was gently lifted by the base of the tail, ensuring no contact with surrounding surfaces, and suspended for 10seconds. Hindlimb posture was assessed during this period and scored as follows:
0: Hindlimbs consistently splayed outward. 1: One hindlimb retracted toward the abdomen for 1–5 seconds. 2: Both hindlimbs partially retracted for 5–9 seconds. 3: Both hindlimbs fully retracted and touched the abdomen for the full 10 seconds. After the assessment, mice were returned to their cages, and scores were recorded accordingly. Hindlimb clasping, a phenotype commonly observed in neurodegenerative mouse models such as the Twitcher mouse, was evaluated. Each mouse was gently lifted by the base of the tail, ensuring no contact with surrounding surfaces, and suspended for 10seconds. Hindlimb posture was assessed during this period and scored as follows:

2.7.4. Cylinder test

Mice were placed individually in a transparent plexiglass cylinder (8 cm diameter × 18 cm height; Jeung Do B&P, Seoul, Korea), and their behavior was videorecorded for later analysis. During a 5-minute observation period, the number of instances in which mice reared upright, fully supporting themselves on their hind legs, was counted.

2.8. RNA Extraction and Quantitative Real-Time Reverse Transcription Polymerase Chain Reaction (qRT-PCR)

Total RNA was extracted from both in vitro and in vivo samples using TRIzol reagent (Thermo Fisher Scientific, Waltham, MA, USA) according to the manufacturer's instructions. The concentration and purity of the isolated RNA were measured using a NanoDrop spectrophotometer (Thermo Fisher Scientific). Quantitative real-time reverse transcription PCR (RT-qPCR) was performed to validate the transcriptomic analysis results. Complementary DNA (cDNA) was synthesized from total RNA using the ReverTra Ace® qPCR RT Master Mix with gDNA Remover (Toyobo, Osaka, Japan), following the manufacturer's protocol. RT-qPCR was conducted using the qPCRBIO SyGreen Mix Hi-ROX (PCR BIOSYSTEMS, London, UK) on a StepOnePlus Real-Time PCR System (Applied Biosystems, Foster City, CA, USA). The thermal cycling conditions were as follows: initial denaturation at 95°C for 2 minutes, followed by 40 cycles of denaturation at 95°C for 5 seconds and annealing/extension at 60°C for 30 seconds. A melting curve analysis was performed at the end of the reaction to confirm amplification specificity. Relative gene expression levels were calculated using the $2^{-\Delta\Delta Ct}$ method, and the primer sequences used are listed in Table1.

2.9. RNA sequencing data processing and analysis

Paired-end sequencing reads were generated on the NovaSeqX platform (Illumina). Trimmomatic version 0.38 was used to remove adapter sequences and trim bases with poor base quality before conducting the analysis. The cleaned reads were aligned to the Mus musculus (10 mm) using HISAT version 2.1.0. The reference genome sequence and gene annotation data were downloaded from the National Center for Biotechnology Information Genome assembly and National Center for Biotechnology Information Reference Sequence (RefSeq) database, respectively. The aligned data (SAM file format) were sorted and indexed using SAMtools version 1.9. After alignment, StringTie version 21.3b was used to assemble and quantify the transcripts. Gene- and transcript-level quantifications were calculated as raw read count, fragments per kilobase of transcript per million mapped reads, and transcripts per million (TPM).

2.10. Differential analysis of gene expression

Statistical analyses of differential gene expression were conducted using edgeR version 3.26.8 with raw counts as input. Genes with non-zero counts in all samples were selected in the QC step. Principal component analysis and multidimensional scaling plots were generated to confirm the similarity of expression between samples. The filtered dataset was subjected to TMM normalization to correct the variation of library sizes among samples. Statistical significance of differential expressions of the gene was identified using the edgeR exactTest. Fold change and p-value were extracted from the exactTest. All p-values are adjusted based on the Benjamini–Hochberg algorithm to control the false discovery rate (FDR). A significant gene list was filtered according to |fold change| of ≥ 2 and raw p-value of <0.05. Hierarchical clustering on rlog-transformed values for significant genes was obtained using the following parameters (distance metric = Euclidean distance, linkage method = complete). Gene-enrichment and functional annotation analysis for significant genes were conducted using gProfiler (https://biit.cs.ut.ee/gprofiler/orth) against the Gene Ontology (GO) database. The adjusted p-values reported from the gProfiler result were

derived using a one-sided hypergeometric test and corrected by the Benjamini–Hochberg method. R version 4.2.2 (www.r-project.org) was used for all data analysis and visualization of differentially expressed genes (DEGs).

2.11. GALC Enzyme Activity Assay Using HMU-β-Gal

GALC enzyme activity was measured using the fluorogenic substrate 6-hexadecanoylamino-4-methylumbelliferyl-β-D-galactipyranoside(HMU-β-Gal; Carbosynth, EH05989). Substrate films were prepared by dissolving HMU-β-Gal in a mixture of chloroform/methanol (2:1, v/v), then mixing with oleic acid (0.6% w/v in n-hexane) and sodium taurocholate (3% w/v in chloroform/methanol). The mixture was aliquoted into microtubes (462 μL/tube), dried using a nitrogen evaporator at 36°C, and stored at −80°C until use. Prior to the assay, brain tissues were homogenized in distilled water using a pellet pestle, followed by sonication (Q-sonica 4423, metal tip; amplitude 20–30%, 20 seconds, 2 times) on ice. Total protein concentrations were determined using a BSA assay, and homogenates were diluted to 2 mg/mL with distilled water. The substrate buffer (McIlvaine buffer, pH 5.2) was prepared with 0.2 M Na_2HPO_4, 0.1 M citric acid, and 0.02% sodium azide. To prepare the substrate solution, a thawed substrate film tube was mixed with 660 μL of substrate buffer and sonicated twice (same conditions as above) at room temperature. The solution was incubated at room temperature on a rocker for 10 minutes and used within 1 hour. For the enzyme reaction, 10 μL of tissue homogenate (test group) or 0.2% BSA (blank) was mixed with 20 μL of substrate solution in a 96-well black plate with a clear bottom (Corning 3603). After sealing, the plate was incubated at 37°C for 17 hours. The reaction was stopped by adding 200 μL of stop buffer (0.5 M $NaHCO_3$, 0.5 M Na_2CO_3, 0.25% Triton X-100). A standard curve was generated using serial dilutions of 4-methylumbelliferone (MU; Sigma M1508) in distilled water at final concentrations of 0, 10, 50, 100, 200, 500, and 1000 pmol/well. Fluorescence was measured using an EnVision HTS multimode plate reader (PerkinElmer) with excitation at 404 nm and emission at 460 nm.

2.12. Immunofluorescence staining

BrdU-treated mice received daily intraperitoneal injections of 5-bromo-2'-deoxyuridine (BrdU; 250 μg/mouse, Sigma-Aldrich, St. Louis, MO, USA) from PD 7 to PD 9. At PD37, both BrdU-treated and untreated Twitcher mouse were euthanized by transcardial perfusion with cold 1× PBS, followed by fixation with 4% paraformaldehyde (PFA; BPP-9004, Tech & Innovation, Chuncheon-si, Korea).

Fixed brains were post-fixed in 4% PFA at 4°C for 24 hours, then subjected to cryoprotection by sequential immersion in 6% and 30% sucrose solutions (S5390, Sigma-Aldrich) at 4°C until the tissue sank. The sucrose-infiltrated brains were then embedded in optimal cutting temperature (OCT) compound, rapidly frozen, and stored at −80°C until sectioning. Frozen brains were sectioned coronally at a thickness of 16 μm using a cryostat (Leica CM1860, Leica Biosystems, Germany). Tissue sections were mounted on adhesion slides and stored at −20°C until use. Fluorescent signal was visualized using a secondary antibody specific to the host species of the primary antibody. Immunofluorescent images were acquired using a confocal laser scanning microscope (LSM700, Zeiss, Göttingen, Germany) and analyzed using ZEN Black and Blue software (Zeiss). Four representative sections per mouse were used for analysis. All antibodies were diluted in the standard solution, and details are provided in Table 2.

2.13. Magnetic Resonance Imaging (MRI)

Magnetic resonance imaging was performed on PD37 using a 9.4T BioSpec scanner (Bruker BioSpin GmbH, Germany) equipped with ParaVision 5.1 software. Mice were anesthetized with 3–3.5% isoflurane for induction and maintained with 1.5–2% isoflurane during scanning. A mouse brain surface coil with an 86 mm transmit coil was used. Anatomical images were obtained using the RARE protocol. Diffusion-weighted images were acquired using a DTI-EPI sequence with the following parameters: slice thickness =

0.32 mm, number of slices = 20, matrix = 128×128, resolution = 0.156×0.156 mm², diffusion time/gradient duration = 4/10 ms, 30 directions, b = 670 s/mm², and TE/TR = 23.5/5000 ms. DTI data was processed with DSI Studio and analyzed using MATLAB to obtain fractional anisotropy (FA) and diffusivity values. T2-weighted images were acquired using the following parameters: slice thickness = 0.16 mm, number of slices = 30, matrix = 128×128, resolution = 0.125×0.125 mm², and TE/TR = 20/2100 ms. T2 images were processed using ParaVision 5.1.

2.14. Transmission electron microscopy

Transmission electron microscopy specimens were fixed for 12 hours in 2% glutaraldehyde, 2% paraformaldehyde in 0.1M phosphate buffer (pH 7.4) and washed in 0.1M phosphate buffer, post-fixed with 1% OsO4 in 0.1M phosphate buffer for 2 hours and dehydrated with an ascending ethanol series (50, 60, 70, 80, 90, 95, 100, 100%) for 10 minutes each, and infiltrated with propylene oxide for 10 minutes. Specimens were embedded with a Poly/Bed 812 kit (08792-1, Polysciences, Warrington, PA, USA), polymerized in an electron microscope oven (TD-700, DOSAKA, Kyoto Japan) at 65°C for 12 hours. The block is equipped with a diamond knife in the Ultra-microtome (UC7, Leica Microsystems Ltd, Wetzlar, Germany), and is cut into 200nm semi–thin section and stained toluidine blue for observation of optical microscope. The region of interest was then cut into 80nm thin sections using the ultra-microtome, placed on copper grids, double stained with 5% uranyl acetate for 20 minutes and 3% lead citrate for 7 minutes staining, and imaged with a transmission electron microscopy (JEM-1011, JEOL, Tokyo, Japan) at the acceleration voltage of 80kV equipped with a Veleta G3 camera (EMSIS, Münster, Germany).

2.15. Luxol fast blue Periodic acid-Schiff staining

Luxol Fast Blue (LFB) staining was performed to visualize myelinated fibers in brain sections. Paraffin-embedded tissue sections were deparaffinized in xylene (2 changes, 10 minutes each) and rehydrated through a graded ethanol series (100%, 95%, and 70%). The sections were then incubated in a 0.1% Luxol Fast Blue solution (1 g Luxol Fast Blue [Sigma, S3382], 1000 mL of 95% ethanol, and 5 mL of 10% acetic acid [Sigma, A6283]) at 70°C for 2 hours, with the lid tightly sealed to prevent evaporation. Following staining, the sections were rinsed in 95% ethanol for 1 minute and washed in running tap water for 10 minutes, taking care to avoid direct water flow onto the tissue. Differentiation was performed using a 0.05% lithium carbonate solution (0.5 g lithium carbonate [Sigma, 431559] in 1000 mL of distilled water) for 20 seconds, followed by 70% ethanol (3 changes; 1 minute each in the first and second dishes). During this process, individual slides were agitated manually with forceps (forward, backward, up, down, left, and right) to ensure uniform decolorization. The extent of differentiation was monitored microscopically. If necessary, the lithium carbonate and ethanol steps were repeated to achieve pale staining of the gray matter while preserving the blue color in the white matter. Prior to PAS staining or dehydration, the sections were washed again in running tap water for 10 minutes. After LFB staining, PAS (Periodic Acid-Schiff) staining was performed in the same sections. The procedure began with acidification using a 0.05% periodic acid solution prepared in 1N hydrochloric acid, followed by three washes with distilled water. The sections were then incubated in Schiff's reagent for 15 minutes to promote staining, followed by two 2-minute rinses in sulfurous rinse solution. Afterward, the tissue was washed under running tap water for 10 minutes. For nuclear counterstaining, Mayer's hematoxylin solution was applied for 1 minute. The sections were then rinsed with 1X Tris-buffered saline (TBS) and again washed with tap water for 10 minutes. The stained sections were gradually dehydrated using ethanol and xylene and mounted with a water-resistant mounting medium. The stained tissue sections were examined under a microscope, and the mean gray value of

myelin fibers as well as the area and number of globoid cells were quantitatively analyzed using ImageJ software.

2.16. Quantification of psychosine

Quantification of psychosine (galactosylsphingosine) was performed from mouse brain hemispheres using a modified methanol/chloroform extraction protocol followed by LC-MS analysis. Brain hemispheres were weighed and homogenized in 1.2 mL of 1X phosphate-buffered saline (PBS) using a glass homogenizer, and total protein concentration was measured using the Bradford assay. For lipid extraction, 2 mL of methanol, 1 mL of chloroform, and 1000 ppb of internal standard (N,N-dimethyl-D-galactosyl-β1-1′-D, Avanti, #860579P) were added sequentially. The mixture was sonicated at room temperature for 60 seconds (20 seconds on, 0 pulse, amplitude 20%) and incubated overnight at 48°C in a water bath. The following day, after cooling to room temperature, 452 µL of 1 M KOH was added, followed by another 60-second sonication under the same conditions. The samples were then incubated at 37°C for 2 hours. Once cooled, 24.4 µL of glacial acetic acid was added and vortexed for 20 seconds. The samples were then dried completely using a cold trap (Eyela UT-2000), and the dried residues were resuspended in 400 µL of a 2:1 methanol:chloroform mixture. The samples were centrifuged at 1800 × g for 15 minutes at 4°C, and the supernatants were transferred to new low-adhesion tubes and stored at –20°C until LC-MS analysis. High-resolution liquid chromatography–mass spectrometry (LC-MS) analysis was outsourced to the Core Facility at Yonsei University College of Medicine (3rd-floor Shared Equipment Laboratory) and performed using the Exploris 240 system (Thermo Fisher Scientific). All samples were prepared in advance for LC and MS analysis and stored at –20°C prior to injection.

2.17. Statistical Analysis

The All data are represented as the mean ± standard error of the mean (SEM), and each experiment was conducted at least four times with four technical replicates per group. Statistical analyses were performed using the Statistical Package for Social Sciences version 28.0 (IBM Corp. Released 2015. IBM SPSS Statistics for Windows, v.28.0. Armonk, NY, USA). The significance of differences between groups was determined using Student's paired t-test, one-way analysis of variance (ANOVA), or two-way ANOVA, as appropriate. Additionally, The Chi-square test was used to assess differences in survival rates between groups. A p-value of less than 0.05 was considered statistically significant.

Table 1. Primer sequences for PCR

Gene	Primer sequence
Oct4	Forward: 5'- AGA CCA CCA TCT GTC GCT TC -3' Reverse: 5'- CTC CAC CTC ACA CGG TTC TC -3'
ENPP2	Forward: 5'- GGA TTA CAG CCA CCA AGC AAG G -3' Reverse: 5'- ATC AGG CTG CTC GGA GTA GAA G -3'
STAT3	Forward: 5'- AAC GAC CTG CAG CAA TAC CA -3' Reverse: 5'- TCC ATG TCA AAC GTG AGC GA -3'
JAK1	Forward: 5'- CAA CAC AGG GGA GCA GGT AG -3' Reverse: 5'- CCC GAA GGC AGA AAC TCC AT -3'
JAK2	Forward: 5'- GCA GCA GCA GAA CCT ACA GA -3' Reverse: 5'- GTC TAA CAC CGC CAT CCC AA -3'
Galc	Forward: 5'- GTG TTG CGG TGC CCT TAT TG -3' Reverse: 5'- AGA ACG ATA GGG CTC TGG GTA -3'
MBP	Forward: 5'- GTCACCATCTCTCCT CAGTGGCTC -3' Reverse: 5'- GTTCTCAGCTCCTCA TCCCTGGAG -3'
NpuN	Forward: 5'- CGT GGA GAA GAG GAT CGA GTG -3' Reverse: 5'- CTC CTG CTC TCC CCT ATC GT -3'
NpuC	Forward: 5'- ACG GAA ATA CCT GGG AAA GCA -3' Reverse: 5'- TAA AGC CAT TCT TCA GGG CGA -3'
GAPDH	Forward: 5'- GTG GAG CCA AAA GGG TCA TCA -3' Reverse: 5'- CCC TTC CAC AAT GCC AAA GTT -3'

Table 2. Antibodies for immunofluorescent staining

Target	Host	Company	Catalog No.	Dilution Factor
Nestin	Mouse	R&D Systems	MAB2736	1:400 (IF)
Olig2	Rabbit	Sigma	AB9610	1:400 (IF)
GFAP	Rabbit	Neuromics	RA22101	1:400 (IF)
Tuj1	Mouse	BioLegend	801201	1:400 (IF)
BrdU	Rat	Abcam	ab6326	1:200 (IF)
MBP	Rat	Abcam	ab7349	1:400 (IF)
GALC	Rabbit	ABclonal	A3873	1:400 (IF)

3. Results

Part1. Oct4-Induced Cellular Reprogramming Promotes Remyelination in the KD Model

3.1. Oct4 overexpression in Twitcher mice preserved motor function in behavioral assessments

To assess the effect of Oct4 overexpression, AAV9-Oct4 virus was injected ICV into Twitcher mice within 24h postnatal. To evaluate the viral delivery route and transduction efficiency, immunofluorescence staining was used to analyze GFP expression. Further, qRT-PCR was performed to measure the relative mRNA levels of Oct4 in various brain regions, and the Oct4-treated group demonstrated significantly higher expression levels in the brain than the control group.

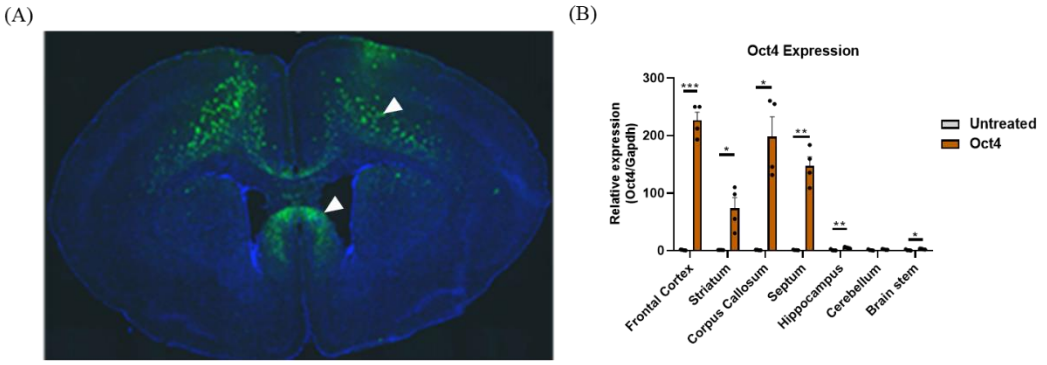

Figure 7. Confirmation of AAV9 delivery and regional Oct4 mRNA expression following intracerebroventricular injection in Twitcher mice.

(A) Representative images illustrating GFP expression in the subventricular zone (SVZ) and septal area after AAV9-GFP injection. Needle track marks were observed in the SVZ, which confirmed the injection site.

(B) Quantitative RT-PCR analysis of Oct4 mRNA levels in the frontal cortex (FC), striatum (STR), and corpus callosum (CC) after ICV AAV9-Oct4 injection. The Oct4-treated group

(Twi Oct4) demonstrated significantly higher Oct4 expression than the untreated group (Twi untreated). Data are expressed as mean ± SEM. **P < 0.05, **P < 0.01, ***P < 0.001.*

Table3. Levene's Test for Variance Heterogeneity in Oct4 mRNA Expression Across Brain Regions

Group	Frontal Cortex	Striatum	Corpus Callosum	Septum	Hippo campus	Cerebellum	Brain stem
Untreated	1.00±0.35	1.00±0.10	1.00±0.24	1.00±0.20	1.00±0.51	1.00±0.47	1.00±0.50
Oct4	226.52±14.16	73.44±18.59	198.27±34.53	147.00±16.08	5.27±0.59	1.92±0.34	2.73±0.46
F-Value	35.371	29.360	358.237	11.030	0.053	0.167	0.042
P-Value	0.001	0.002	<0.001	0.016	0.825	0.697	0.845

Note: Data is presented as mean ± SEM. Statistical analysis was performed using an independent t-test. Welch's correction was applied when the assumption of equal variances was not met, as determined by Levene's test. **P < 0.05, **P < 0.01, ***P < 0.001.*

Table4. Statistical Analysis of Oct4 mRNA Expression in Brain Regions

Regions	Comparison Groups			N	Summary	*P*-value
Frontal Cortex	Untreated	VS	Oct4	4:4	***	<0.001
Striatum	Untreated	VS	Oct4	4:4	*	0.030
Corpus Callosum	Untreated	VS	Oct4	4:4	*	0.011
Septum	Untreated	VS	Oct4	4:4	**	0.003
Hippocampus	Untreated	VS	Oct4	4:4	**	0.002
Cerebellum	Untreated	VS	Oct4	4:4	ns	0.163
Brain stem	Untreated	VS	Oct4	4:4	*	0.042

Note: Data is presented as mean ± SEM. Statistical analysis was performed using an independent t-test. Welch's correction was applied when the assumption of equal variances was not met, as determined by Levene's test. **P < 0.05, **P < 0.01, ***P < 0.001.*

3.2. Oct4-Mediated regulation of genes involved in Oligodendrocyte differentiation

To investigate the Oct4 overexpression-induced transcriptional changes, RNA sequencing was performed on the STR of Twitcher mice in two groups: GFP and Oct4. GO term enrichment analysis was conducted using the Database for Annotation, Visualization, and Integrated Discovery to compare the gene expression profiles between the Oct4 and GFP groups. The analysis revealed that Oct4 overexpression caused differential expressions of genes associated not only with cell cycle and proliferation but also with oligodendrocyte differentiation, indicating a potential role for Oct4 in promoting myelination-related pathways.

Type	Term	Fold enrichment	Term size	adjusted p-value	Genes
Differentiation	regulation of cell differentiation	1.249	1761	0.014	Trim72, Gsx2, Edn3, Il7r, Glp1r, Ctla2a, Asb4, Msx1, Oprm1, Tnfsf9, Sp7, Enpp2, Cd28, Zfp36, Drd3, Card11, Spdef, Cdkl5, Hes7, Sostdc1, Ccl19, Nkx2-2os
Differentiation	cell differentiation	0.879	4777	0.026	Trim72, Alpk3, Gsx2, Edn3, Il7r, Glp1r, Tnnt1, Col8a1, Hba-a1, Ctla2a, Slc24a5, Asb4, Msx1, Angpt2, Hba-a2, Acta2, Oprm1, Crb1, Tafa3, Tnfsf9, Sp7, Enpp2, Cd28, Zfp36, Otx2, Drd3, Spag16, Wfikkn2, Card11, Spdef, Folr1, Has2, Oca2, Cdkl5, Wnt2b, Wfikkn1, Crb3, Popdc2, Hes7, Sostdc1, Ccl19, Nkx2-2os
Differentiation	positive regulation of cell differentiation	1.443	970	0.034	Gsx2, Edn3, Il7r, Glp1r, Asb4, Oprm1, Tnfsf9, Sp7, Enpp2, Zfp36, Spdef, Cdkl5, Ccl19, Nkx2-2os
Proliferation	Cell population proliferation	1.153	2168	0.016	Edn3, Il7r, Glp1r, Col8a1, Fosl1, Aqp1, Col4a3, Msx1, Tafa3, Ecrg4, Tnfsf9, Enpp2, Cd28, Nlrc3, Zfp36, Drd3, Col8a2, Lgr6, Cxcr3, Card11, Has2, Oca2, Wnt2b, Rad51b, Ccl19
Proliferation	regulation of nuclear division	3.448	145	0.045	Edn3, Ooep, Msx1, Cd28, Drd3
Proliferation	regulation of cell population proliferation	1.112	1799	0.047	Edn3, Il7r, Glp1r, Fosl1, Aqp1, Col4a3, Msx1, Tafa3, Ecrg4, Tnfsf9, Enpp2, Cd28, Nlrc3, Zfp36, Drd3, Cxcr3, Card11, Has2, Rad51b, Ccl19
Oligodendrocyte	**regulation of oligodendrocyte differentiation**	**6.897**	58	0.02	Enpp2**, Drd3, Nkx2-2os**
Oligodendrocyte	**positive regulation of oligodendrocyte differentiation**	**8.571**	**35**	**0.039**	Enpp2**, Nkx2-2os**

Figure 8. GO term enrichment analysis reveals oligodendrocyte differentiation pathway upregulation after Oct4 overexpression.

Gene Ontology (GO) enrichment analysis was conducted on RNA sequencing data from the brains of Oct4-treated Twitcher mice to determine transcriptional changes associated with Oct4 overexpression. Among the significantly enriched GO terms, several were related to cell differentiation and proliferation, indicating that Oct4 broadly affects

developmental processes. Importantly, GO terms associated with oligodendrocyte differentiation exhibited high fold enrichment and statistically significant *p*-values, indicating a robust upregulation of myelination-related pathways in response to Oct4 treatment.

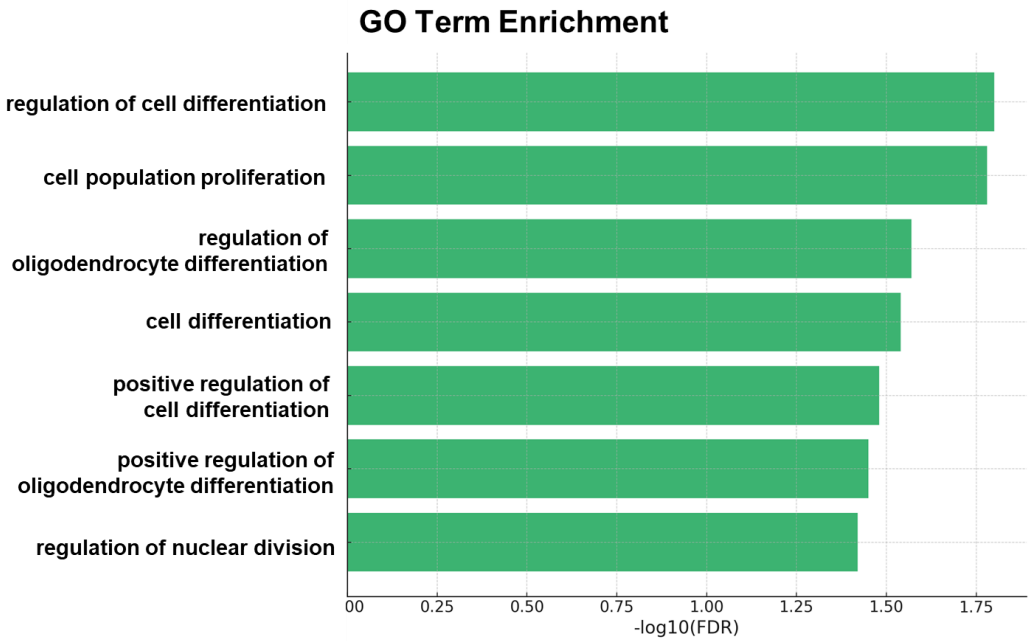

Figure 9. GO term enrichment related to oligodendrocyte differentiation in Oct4-overexpressing mice.

GO term enrichment analysis was conducted based on differentially expressed genes (DEGs) between Oct4-overexpressing and untreated Twitcher mice. The X-axis of the graph illustrates the negative log-transformed false discovery rate ($-\log_{10}$FDR), where higher values indicate greater statistical significance. Among the significantly enriched biological processes, several were associated with cell proliferation and differentiation. The GO term "positive regulation of oligodendrocyte differentiation" exhibited strong statistical significance, supporting the notion that Oct4 promotes oligodendrocyte lineage cell generation and restoration. This term includes key genes, such as Enpp2, which plays a crucial role in oligodendrocyte maturation, thereby further highlighting the biological

relevance of this finding. Fold change (FC) ≥ ±1.2, *P*-value <0.05, focusing on biological processes.

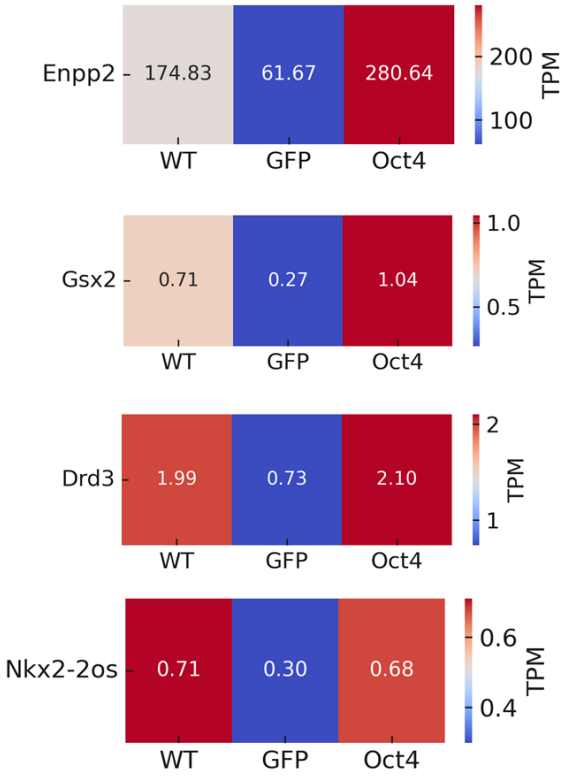

Figure 10. ENPP2 is a potential functional target of Oct4 in promoting oligodendrocyte differentiation.

This figure illustrates the expression patterns of representative genes included in the GO term-positive regulation of oligodendrocyte differentiation. Among these, ENPP2 demonstrated a marked increase in expression, specifically in the Oct4-treated group, whereas expression levels remained similar between WT and GFP Twitcher mice. The abundance of ENPP2 transcripts exceeded 280 TPM in the Oct4 group, indicating that Oct4 may directly or indirectly induce ENPP2 expression. In contrast, DRD3 and NKX2-2OS demonstrated only mild or inconsistent changes in expression, and their involvement in

oligodendrocyte function may be secondary or indirect. ENPP2 is popular for its roles in neurodevelopment, myelination, and oligodendrocyte function; therefore, it was selected as a putative functional target gene of Oct4 for further analysis.

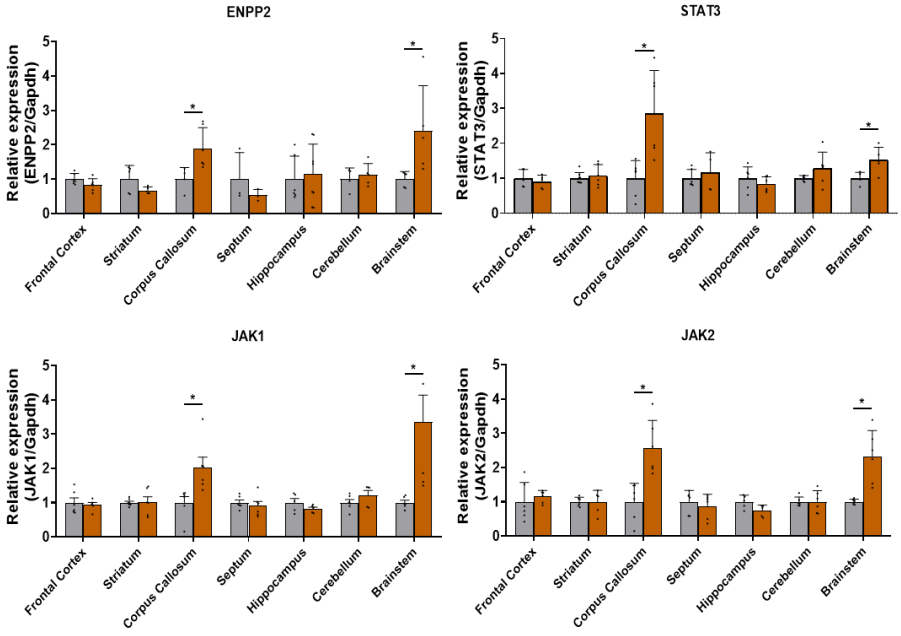

Figure 11. Oct4 promotes ENPP2 expression through JAK/STAT signaling pathway activation.

This figure illustrates qRT-PCR validation of *ENPP2* and JAK/STAT pathway gene expression after Oct4 overexpression in Twitcher mice. *ENPP*2 expression was significantly upregulated in myelin-rich regions, including the CC and BS. Notably, *STAT3*, *JAK1*, and *JAK2* expression levels were significantly increased in these regions, supporting the hypothesis that JAK/STAT signaling may activate *ENPP2* expression by Oct4. These results indicate a regulatory mechanism in which Oct4 overexpression causes JAK/STAT pathway activation, which in turn induces *ENPP2* expression, thereby promoting oligodendrocyte maturation and myelination.

Table 5. Characterization of variance heterogeneity across JACK/STAT pathway assays in Twitcher mouse.

	Group	Frontal Cortex	Striatum	Corpus Callosum	Septum	Hippocampus	Cerebellum	Brainstem
ENPP2	Untreated	1.00±0.07	1.00±0.18	1.00±0.17	1.00±0.44	1.00±0.27	1.00±0.16	1.00±0.10
	Oct4	0.83±0.08	0.67±0.04	1.90±0.25	0.53±0.10	1.14±0.31	1.12±0.15	2.41±0.59
	F-value	0.001	35.544	2.712	8.868	1.080	0.022	3.869
	P-value	0.979	<0.001	0.138	0.041	0.319	0.886	0.085
STAT3	Untreated	1.00±0.11	1.00±.057	1.00±0.21	1.00±0.10	1.00±0.13	1.00±0.03	1.00±0.07
	Oct4	0.90±0.08	1.08±0.13	2.86±0.50	1.17±0.28	0.83±0.09	1.28±0.19	1.52±0.16
	F-value	1.111	3.754	17.825	19.977	0.612	4.145	1.437
	P-value	0.323	0.077	0.002	0.002	0.452	0.069	0.265
JAK1	Untreated	1.00±0.14	1.00±0.04	1.00±0.18	1.00±0.08	1.00±0.12	1.00±0.09	1.00±0.07
	Oct4	0.93±0.08	1.02±0.15	2.02±0.31	0.91±0.13	0.82±0.05	1.22±0.14	3.36±0.78
	F-value	3.920	6.495	0.648	1.421	5.905	3.341	114.245
	P-value	0.079	0.027	0.440	0.261	0.041	0.101	<0.001
JAK2	Untreated	1.00±0.23	1.00±0.06	1.00±0.22	1.00±0.13	1.00±0.09	1.00±0.06	1.00±0.03
	Oct4	1.15±0.07	0.99±0.15	2.57±0.33	0.87±0.14	0.74±0.08	1.00±0.13	2.32±0.31
	F-value	8.216	9.230	0.995	0.045	0.046	6.496	10.313
	P-value	0.017	0.014	0.342	0.836	0.835	0.029	0.009

Note: Data is presented as mean ± SEM. Statistical analysis was performed using an independent t-test. Welch's correction was applied when the assumption of equal variances was not met, as determined by Levene's test. *$P < 0.05$, **$P < 0.01$, ***$P < 0.001$.

Table 6. Statistical analysis of JAK/STAT pathway mRNA expression in Twitcher mouse.

	Regions	Comparison Groups			N	Summary	*P*-value
ENPP2	Frontal Cortex	Untreated	VS	Oct4	6:6	ns	0.116
	Striatum	Untreated	VS	Oct4	5:5	ns	0.136
	Corpus Callosum	Untreated	VS	Oct4	4:6	*	0.028
	Septum	Untreated	VS	Oct4	3:3	ns	0.400
	Hippocampus	Untreated	VS	Oct4	6:8	ns	0.745
	Cerebellum	Untreated	VS	Oct4	4:5	ns	0.590
	Brainstem	Untreated	VS	Oct4	5:5	*	0.045
STAT3	Frontal Cortex	Untreated	VS	Oct4	5:5	ns	0.497
	Striatum	Untreated	VS	Oct4	8:6	ns	0.541
	Corpus Callosum	Untreated	VS	Oct4	6:6	*	0.012
	Septum	Untreated	VS	Oct4	6:4	ns	0.612
	Hippocampus	Untreated	VS	Oct4	6:6	ns	0.310
	Cerebellum	Untreated	VS	Oct4	6:6	ns	0.175
	Brainstem	Untreated	VS	Oct4	5:5	*	0.019
JAK1	Frontal Cortex	Untreated	VS	Oct4	6:5	ns	0.686
	Striatum	Untreated	VS	Oct4	7:6	ns	0.913
	Corpus Callosum	Untreated	VS	Oct4	6:6	*	0.016
	Septum	Untreated	VS	Oct4	6:6	ns	0.541
	Hippocampus	Untreated	VS	Oct4	5:5	ns	0.221
	Cerebellum	Untreated	VS	Oct4	6:5	ns	0.216
	Brainstem	Untreated	VS	Oct4	6:6	*	0.028
JAK2	Frontal Cortex	Untreated	VS	Oct4	6:6	ns	0.548
	Striatum	Untreated	VS	Oct4	6:5	ns	0.950
	Corpus Callosum	Untreated	VS	Oct4	6:6	**	0.003
	Septum	Untreated	VS	Oct4	6:6	ns	0.526
	Hippocampus	Untreated	VS	Oct4	5:5	ns	0.054
	Cerebellum	Untreated	VS	Oct4	6:6	ns	0.995
	Brainstem	Untreated	VS	Oct4	6:6	**	0.008

Note: Data is presented as mean ± SEM. Statistical analysis was performed using an independent t-test. Welch's correction was applied when the assumption of equal

variances was not met, as determined by Levene's test. *$P < 0.05$, **$P < 0.01$, ***$P < 0.001$.

3.3. Oct4 Overexpression significantly modulates the distribution of Olig2-, Nestin-, GFAP-, and Tuj1-Positive cells in Twitcher mice

Oct4 overexpression significantly altered the populations of Nestin-, Olig2-, GFAP-, and Tuj1-expressing cells in Twitcher mice, indicating that Oct4 broadly affects glial and neuronal lineage specification. Olig2-positive cells, which indicate the oligodendrocyte lineage, were markedly reduced in the CC and STR of Twitcher mice. Oct4 overexpression, which restored the number of Olig2-positive cells to near WT levels, notably reversed this reduction. Further, Oct4 overexpression significantly increased the number of newly generated cells, as confirmed with BrdU.

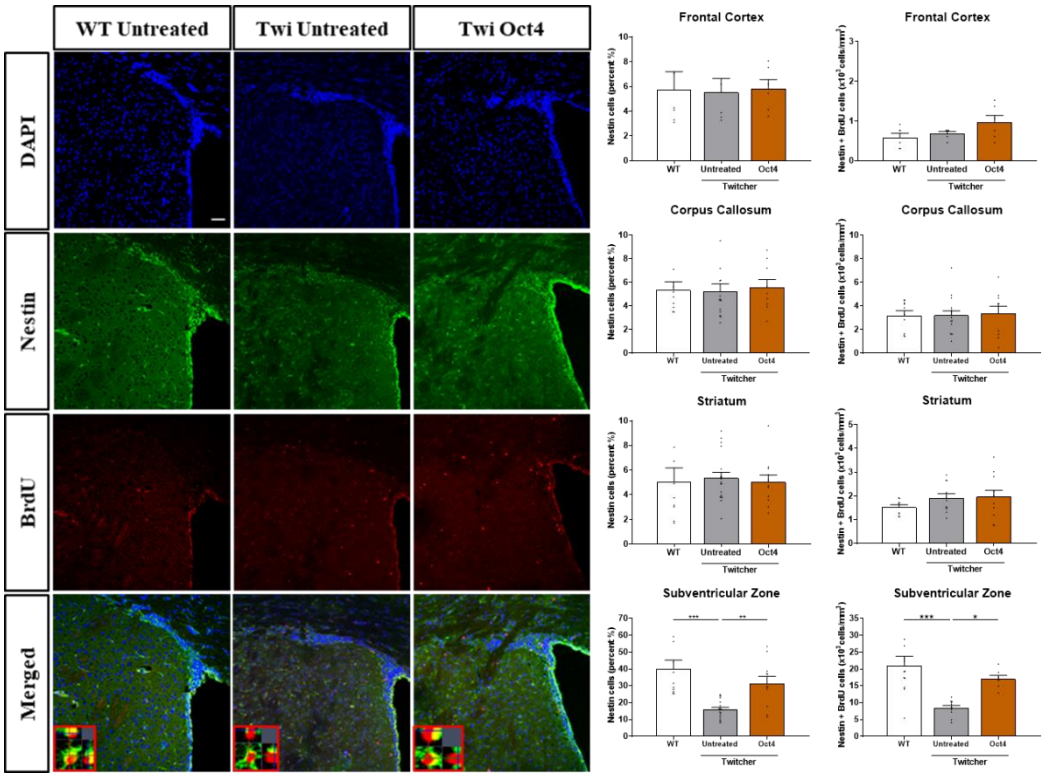

Figure 12. Oct4 overexpression significantly increases Nestin-positive cells in the subventricular zone.

Nestin immunofluorescence staining revealed a marked increase in Nestin-positive neural progenitor cells within the subventricular zone (SVZ) of Oct4-treated Twitcher mice compared with untreated controls. Quantitative analysis confirmed a statistically significant increase in Nestin-positive cell populations after Oct4 overexpression. Data are expressed as mean ± SEM. *$P < 0.05$, **$P < 0.01$, ***$P < 0.001$ with unpaired *t*-test. Scale bar = 50 μm.

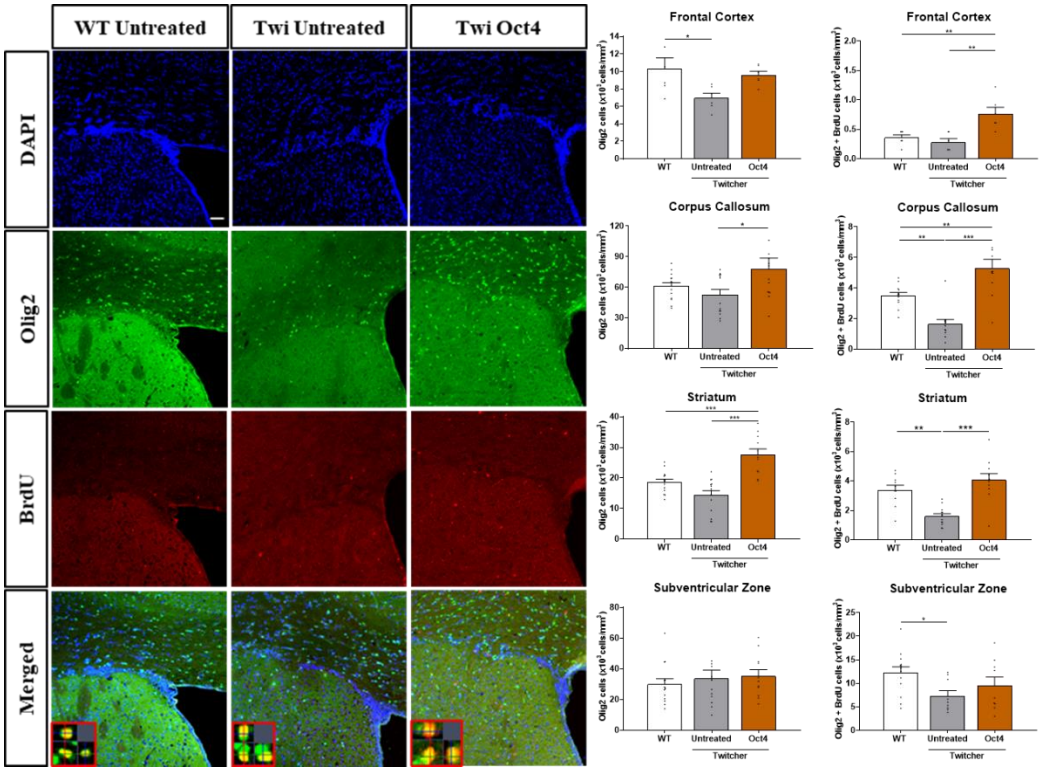

Figure 13. Restoration of Olig2-positive cells in the corpus callosum and striatum following Oct4 overexpression.

Immunofluorescence staining for Olig2 revealed a significant increase in the number of Olig2-positive cells in both the CC and STR of Oct4-overexpressing Twitcher mice compared with untreated controls. These results indicate that Oct4 contributes to the

recovery of oligodendrocyte lineage cells in demyelinated regions of the brain. *$P < 0.05$, **$P < 0.01$, ***$P < 0.001$ Scale bar = 50μm.

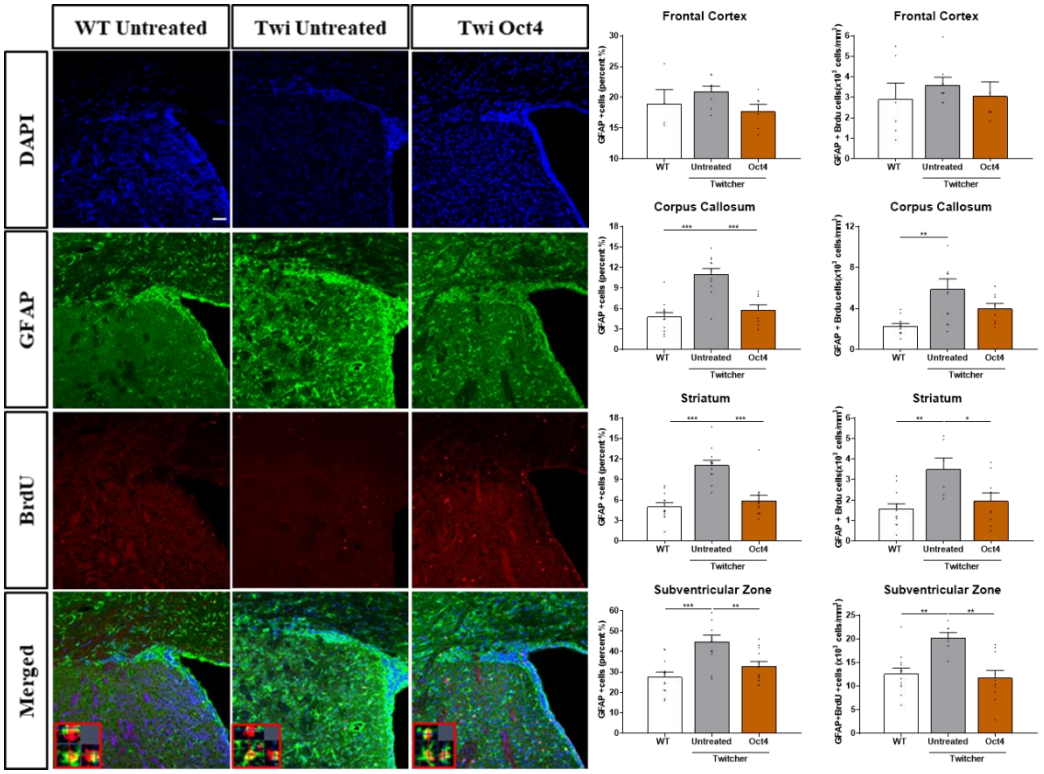

Figure 14. Oct4 overexpression reduces astrocyte reactivity and promotes new cell generation in Twitcher mice.

GFAP immunofluorescence staining revealed a significant increase in GFAP-positive reactive astrocytes in multiple brain regions of untreated Twitcher mice, consistent with gliosis and neuroinflammation. In contrast, Oct4 overexpression markedly decreases GFAP expression, indicating astrocyte activation suppression. Further, the number of newly generated BrdU-positive cells was significantly increased in the Oct4-treated group, indicating enhanced regenerative activity in response to Oct4. Scale bar = 50 μm.

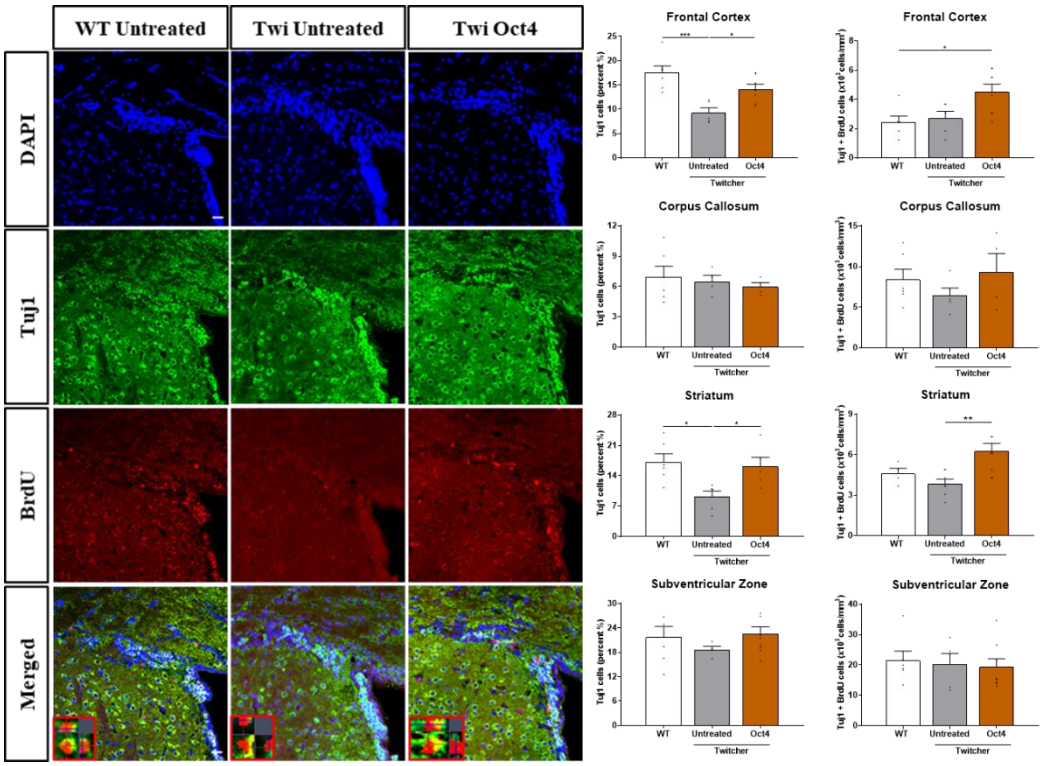

Figure 15. Oct4 overexpression promotes immature neuronal differentiation in the striatum of Twitcher mice

Tuj1, which is an early neuronal marker, was used to evaluate neuronal differentiation in the STR. The number of Tuj1-positive cells was markedly reduced in untreated Twitcher mice, indicating impaired neurogenesis. Oct4 overexpression reversed this reduction, causing a significant increase in the number of Tuj1-positive immature neurons. Consistently, newly generated BrdU-positive cells were increased after Oct4 treatment, indicating that Oct4 facilitates neuronal lineage differentiation in Twitcher mice. Scale bar = 20 μm.

Table 7. Characterization of variance heterogeneity across Nestin, Olig2, GFAP, Tuj1 staining assays in Twitcher mouse.

Antibody	Regions	WT	Untreated	Oct4	*F*-value	*P*-value
Nestin	Frontal Cortex	5.73±1.47	5.52±1.14	5.83±0.73	0.019	0.981
	Corpus Callosum	5.34±0.72	5.22±0.65	5.58±0.67	0.066	0.937
	Striatum	5.04±1.15	5.35±0.46	5.02±0.59	0.088	0.916
	Subventricular Zone	40.08±5.21	15.97±1.28	31.38±4.17	14.663	<0.001
$Nestin^{+}BrdU^{+}$	Frontal Cortex	0.58±0.11	5.52±1.14	0.97±0.17	2.616	0.106
	Corpus Callosum	3.19±0.40	3.19±0.38	3.38±0.61	0.048	0.953
	Striatum	1.52±0.11	1.90±0.18	1.96±0.28	1.212	0.313
	Subventricular Zone	21.04±2.77	8.43±0.71	17.03±1.05	11.360	<0.001
Olig2	Frontal Cortex	10.35±1.22	6.96±0.55	9.58±0.45	4.728	0.026
	Corpus Callosum	60.97±3.54	52.46±5.51	78.15±10.46	3.429	0.043
	Striatum	18.67±0.95	14.37±1.47	27.54±1.94	20.167	<0.001
	Subventricular Zone	29.97±3.53	33.57±5.58	35.23±4.25	0.354	0.704
$Olig2^{+}BrdU^{+}$	Frontal Cortex	0.36±0.05	0.28±0.06	0.76±0.11	10.793	0.001
	Corpus Callosum	3.51±0.21	1.65±0.29	5.30±0.58	22.626	<0.001
	Striatum	3.38±0.33	1.61±0.17	4.06±0.44	17.101	<0.001
	Subventricular Zone	12.30±1.19	7.32±1.13	9.53±1.82	3.478	0.044
GFAP	Frontal Cortex	18.95±2.31	20.94±0.86	17.68±1.17	1.907	0.183
	Corpus Callosum	4.77±0.63	11.04±0.80	5.74±0.78	22.120	<0.001
	Striatum	5.04±0.57	11.10±0.72	5.89±0.77	22.508	<0.001
	Subventricular Zone	27.57±2.45	44.90±3.19	32.83±2.31	11.005	<0.001
$GFAP^{+}BrdU^{+}$	Frontal Cortex	2.90±0.79	3.61±0.37	3.05±0.70	0.409	0.671
	Corpus Callosum	2.28±0.24	5.88±1.01	3.97±0.52	7.170	0.003
	Striatum	1.56±0.25	3.49±0.56	1.94±0.40	6.246	0.007
	Subventricular Zone	12.57±1.24	20.21±1.08	11.70±1.62	9.256	<0.001
Tuj1	Frontal Cortex	17.62±1.28	9.29±1.01	14.42±0.83	12.237	<0.001
	Corpus Callosum	6.97±1.02	6.47±0.65	5.97±0.41	0.346	0.715
	Striatum	17.15±1.90	9.24±1.21	16.13±2.14	6.29	0.011
	Subventricular Zone	21.69±2.71	18.62±0.88	22.57±1.71	0.794	0.469

$Tuj1^{+}BrdU^{+}$	Frontal Cortex	2.45±0.42	2.69±0.50	4.51±0.53	5.520	0.015
	Corpus Callosum	8.38±1.27	6.47±0.90	9.29±2.29	0.907	0.430
	Striatum	4.59±0.39	3.84±0.35	6.25±0.58	6.499	0.008
	Subventricular Zone	21.41±3.17	20.29±3.46	19.30±2.74	0.127	.882

Note: Data is presented as mean ± SEM. Statistical analysis was performed using one-way ANOVA, followed by Bonferroni's post hoc test. *$P < 0.05$, **$P < 0.01$, ***$P < 0.001$.

Table 8. Statistical Analysis of Nestin, Olig2, Tuj1 and GFAP Immunofluorescence in Twitcher mouse.

Antibody	Regions	Comparison Groups			N	Summary	*P*-value
Nestin	Frontal Cortex	WT	VS	Untreated	6:6	ns	1.000
		WT	VS	Oct4	6:6	ns	1.000
		Untreated	VS	Oct4	6:6	ns	1.000
	Corpus Callosum	WT	VS	Untreated	9:16	ns	1.000
		WT	VS	Oct4	9:9	ns	1.000
		Untreated	VS	Oct4	16:9	ns	1.000
	Striatum	WT	VS	Untreated	9:18	ns	1.000
		WT	VS	Oct4	9:11	ns	1.000
		Untreated	VS	Oct4	18:11	ns	1.000
	Subventricular Zone	WT	VS	Untreated	11:18	ns	<0.001
		WT	VS	Oct4	11:11	ns	0.299
		Untreated	VS	Oct4	18:11	**	0.006
$Nestin^{+}BrdU^{+}$	Frontal Cortex	WT	VS	Untreated	6:6	ns	1.000
		WT	VS	Oct4	6:6	ns	0.130
		Untreated	VS	Oct4	6:6	ns	0.378
	Corpus Callosum	WT	VS	Untreated	10:16	ns	1.000
		WT	VS	Oct4	10:10	ns	1.000
		Untreated	VS	Oct4	16:10	ns	1.000
	Striatum	WT	VS	Untreated	9:11	ns	0.646
		WT	VS	Oct4	9:11	ns	0.473
		Untreated	VS	Oct4	11:11	ns	1.000

	Subventricular Zone	WT	VS	Untreated	12:11	***	<0.001
		WT	VS	Oct4	12:7	ns	0.600
		Untreated	VS	Oct4	11:7	*	0.030
Olig2	Frontal Cortex	WT	VS	Untreated	6:6	*	0.031
		WT	VS	Oct4	6:6	ns	1.000
		Untreated	VS	Oct4	6:6	ns	0.115
	Corpus Callosum	WT	VS	Untreated	14:13	ns	0.664
		WT	VS	Oct4	14:13	ns	0.201
		Untreated	VS	Oct4	13:13	*	0.037
	Striatum	WT	VS	Untreated	14:14	ns	0.105
		WT	VS	Oct4	14:11	***	<0.001
		Untreated	VS	Oct4	14:11	***	<0.001
	Subventricular Zone	WT	VS	Untreated	14:13	ns	1.000
		WT	VS	Oct4	14:11	ns	1.000
		Untreated	VS	Oct4	13:11	ns	1.000
$Olig2^{+}BrdU^{+}$	Frontal Cortex	WT	VS	Untreated	6:6	ns	1.000
		WT	VS	Oct4	6:6	**	0.007
		Untreated	VS	Oct4	6:6	**	0.002
	Corpus Callosum	WT	VS	Untreated	12:12	**	0.004
		WT	VS	Oct4	12:11	**	0.007
		Untreated	VS	Oct4	12:11	***	<0.001
	Striatum	WT	VS	Untreated	10:13	**	0.001
		WT	VS	Oct4	10:11	ns	0.463
		Untreated	VS	Oct4	13:11	***	<0.001
	Subventricular Zone	WT	VS	Untreated	14:9	*	0.044
		WT	VS	Oct4	14:9	ns	0.478
		Untreated	VS	Oct4	9:9	ns	0.916
GFAP	Frontal Cortex	WT	VS	Untreated	4:8	ns	0.947
		WT	VS	Oct4	4:6	ns	1.000
		Untreated	VS	Oct4	8:6	ns	0.221
	Corpus Callosum	WT	VS	Untreated	12:12	***	<0.001
		WT	VS	Oct4	12:8	ns	1.000

		Untreated	VS	Oct4	12:8	***	<0.001
	Striatum	WT	VS	Untreated	12:12	***	<0.001
		WT	VS	Oct4	12:12	ns	1.000
		Untreated	VS	Oct4	12:12	***	<0.001
	Subventricular Zone	WT	VS	Untreated	12:12	***	<0.001
		WT	VS	Oct4	12:12	ns	0.523
		Untreated	VS	Oct4	12:12	**	0.009
$GFAP^+BrdU^+$	Frontal Cortex	WT	VS	Untreated	6:8	ns	1.000
		WT	VS	Oct4	6:6	ns	1.000
		Untreated	VS	Oct4	8:6	ns	1.000
	Corpus Callosum	WT	VS	Untreated	12:12	**	0.002
		WT	VS	Oct4	12:8	ns	0.370
		Untreated	VS	Oct4	12:8	ns	0.247
	Striatum	WT	VS	Untreated	12:6	**	0.006
		WT	VS	Oct4	12:9	ns	1.000
		Untreated	VS	Oct4	6:9	*	0.042
	Subventricular Zone	WT	VS	Untreated	12:7	**	0.003
		WT	VS	Oct4	12:10	ns	1.000
		Untreated	VS	Oct4	7:10	**	0.001
Tuj1	Frontal Cortex	WT	VS	Untreated	7:5	***	<0.001
		WT	VS	Oct4	7:11	ns	0.097
		Untreated	VS	Oct4	5:11	*	0.011
	Corpus Callosum	WT	VS	Untreated	6:4	ns	1.000
		WT	VS	Oct4	6:4	ns	1.000
		Untreated	VS	Oct4	4:4	ns	1.000
	Striatum	WT	VS	Untreated	6:6	*	0.016
		WT	VS	Oct4	6:5	ns	1.000
		Untreated	VS	Oct4	6:5	*	.048
	Subventricular Zone	WT	VS	Untreated	6:4	ns	1.000
		WT	VS	Oct4	6:9	ns	1.000
		Untreated	VS	Oct4	4:9	ns	0.683
$Tuj1^+BrdU^+$	Frontal Cortex	WT	VS	Untreated	6:5	ns	1.000

		WT	VS	Oct4	6:8	*	0.025
		Untreated	VS	Oct4	5:8	ns	0.069
	Corpus Callosum	WT	VS	Untreated	6:5	ns	1.000
		WT	VS	Oct4	6:4	ns	1.000
		Untreated	VS	Oct4	5:4	ns	0.664
	Striatum	WT	VS	Untreated	4:7	ns	1.000
		WT	VS	Oct4	4:9	ns	0.172
		Untreated	VS	Oct4	7:9	**	0.008
	Subventricular Zone	WT	VS	Untreated	6:5	ns	1.000
		WT	VS	Oct4	6:8	ns	1.000
		Untreated	VS	Oct4	5:8	ns	1.000

Note: Data is presented as mean ± SEM. Statistical analysis was performed using one-way ANOVA, followed by Bonferroni's post hoc test. *$P < 0.05$, **$P < 0.01$, ***$P < 0.001$.

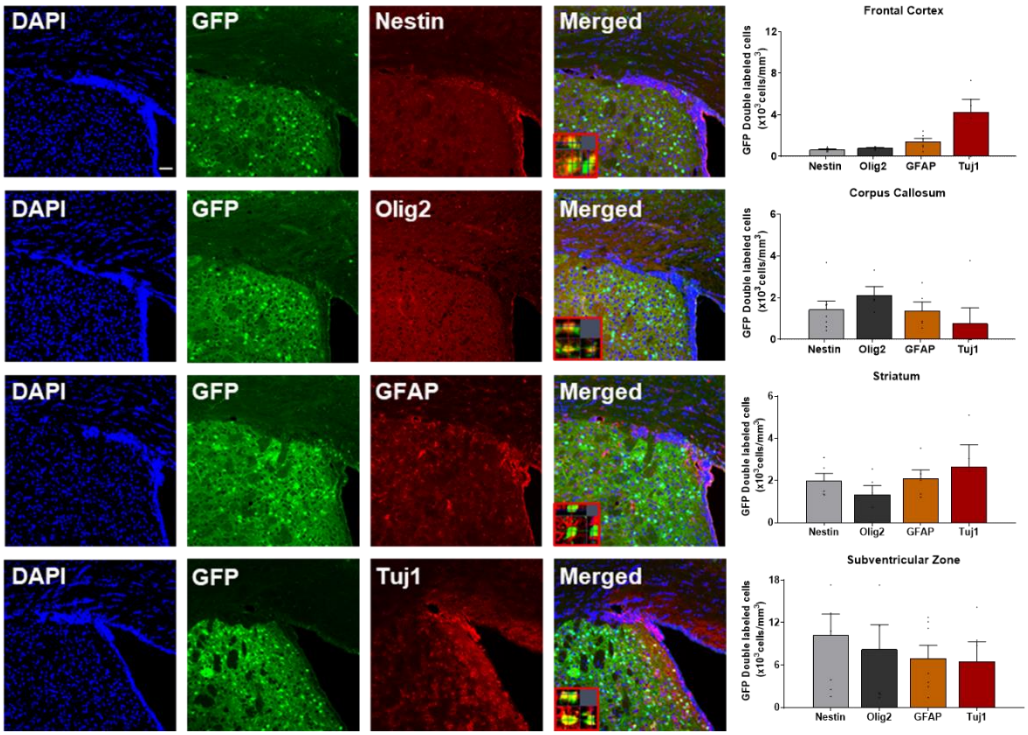

Figure 16. Lineage analysis of GFP⁺ cells after intracerebroventricular injection of AAV-GFP.

To trace the cell fate of GFP-expressing cells following ICV injection of AAV-GFP, immunofluorescence staining was performed using lineage-specific markers: Nestin (neural progenitors), Olig2 (oligodendrocyte-lineage), GFAP (astrocytes), and Tuj1 (neurons). DAPI (blue) was used for nuclear counterstaining. Merged images show co-localization of GFP (green) with each marker (red). Insets highlight representative double-positive cells. Quantification of the proportion of GFP^+ cells co-expressing each marker is shown in the bar graphs.

3.4. Oct4 overexpression helps maintain myelin structure and restore MBP levels in Twitcher mice

MBP plays a crucial role in the myelination process in the nervous system by maintaining the structural integrity of the myelin sheath through interactions with membrane lipids. Previous studies have revealed that reduced MBP expression induces demyelination in the CNS, causing tremors, seizures, and early mortality. MBP immunostaining was conducted to assess myelin sheath restoration with Oct4 treatment. MBP-positive cells were observed along the corpus callosum (CC) under fluorescence microscopy in paraffin-embedded brain sections 38 days post injection. The MBP staining intensity was higher in the Oct4-treated group than in the control group, indicating increased myelin density and thickness in the CC after Oct4 treatment.

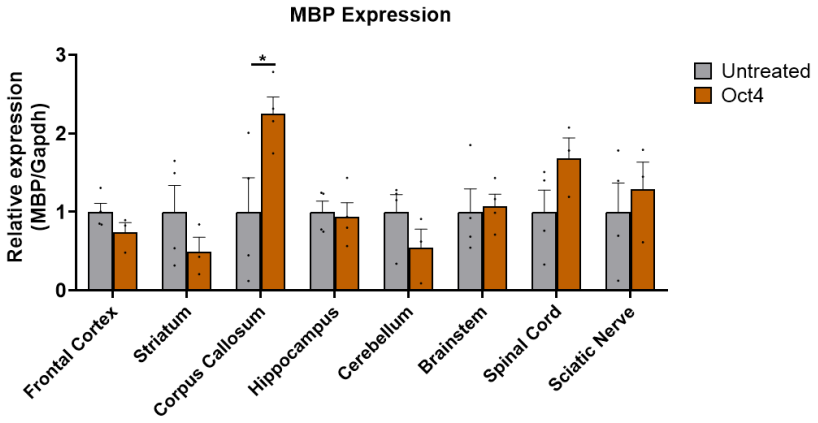

Figure 17. Oct4 treatment increases MBP mRNA expression in the corpus callosum of Twitcher mice

Quantitative RT-PCR analysis of MBP mRNA expressions in various regions of the central and PNS at 38 days post injection. Compared with untreated Twitcher mice, the Oct4-treated group demonstrated a statistically significant increase in MBP mRNA levels only in the CC. No significant differences were observed in other regions, including the FC, STR, thalamus, cerebellum, spinal cord (SC), and sciatic nerve (SN). Data are expressed as mean ± SEM. *$P < 0.05$, **$P < 0.01$, ***$P < 0.001$ by unpaired *t*-test.

Table 9. Characterization of variance heterogeneity across MBP assays in Twitcher mouse.

Group	Frontal Cortex	Striatum	Corpus Callosum	Hippocampus	Cerebellum	Brain stem	Spinal cord	Sciatic nerve
Untreated	1±0.102	1±0.314	1±0.435	1±0.148	1±0.196	1±0.254	1±0.385	1±0.275
Oct4	0.3658±0.038	0.676±0.272	2.5855±0.385	1.1162±0.653	0.7606±0.123	1.2151±0.03	0.8352±0.096	1.1398±0.443
F-value	1.576	3.508	2.358	12.436	1.288	11.244	2.460	0.085
P-value	0.278	0.134	0.199	0.024	0.320	0.028	0.192	0.785

Note: Statistical analysis was performed using an independent t-test. Welch's correction was applied when the assumption of equal variances was not met, as determined by Levene's test. *$P < 0.05$, **$P < 0.01$, ***$P < 0.001$.

Table 10. Statistical analysis of MBP mRNA expression in Twitcher mouse

Regions	Comparison Groups			N	Summary	*P*-value
Frontal Cortex	Untreated	VS	Oct4	4:2	ns	.015
Striatum	Untreated	VS	Oct4	4:2	ns	.552
Corpus Callosum	Untreated	VS	Oct4	4:2	*	.048
Hippocampus	Untreated	VS	Oct4	4:2	ns	.889
Cerebellum	Untreated	VS	Oct4	4:2	ns	.474
Brain stem	Untreated	VS	Oct4	4:2	ns	.461
Spinal cord	Untreated	VS	Oct4	4:2	ns	.791
Sciatic nerve	Untreated	VS	Oct4	4:2	ns	.791

Note: Statistical analysis was performed using an independent t-test. Welch's correction was applied when the assumption of equal variances was not met, as determined by Levene's test. **P < 0.05, **P < 0.01, ***P < 0.001.*

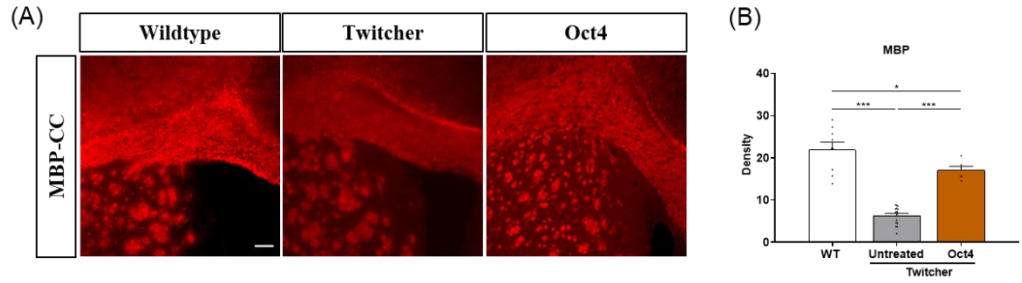

Figure 18. Oct4 improves MBP expression in the corpus callosum of Twitcher mice.

Representative images of MBP immunofluorescence in the CC at 38 days post injection in wild-type (WT), untreated twitcher, and Oct4-treated Twitcher mice. MBP-positive signals (red) were found along the CC. Quantitative analysis revealed a significant increase in MBP immunoreactivity in the Oct4-treated group compared with the untreated twitcher group, although it remained lower than that in WT mice. Data are expressed as mean ± SEM. **P* < 0.05 with one-way analysis of variance (ANOVA) followed by Bonferroni post hoc test.

Table 11. Characterization of variance heterogeneity across MBP staining assays in Twitcher mouse.

Regions	WT	Untreated	Oct4	*F*-value	*P*-value
Corpus callosum	21.97±1.77	6.41±0.47	17.10±0.90	76.087	<0.001

Data is presented as mean ± SEM. Statistical analysis was performed using one-way ANOVA, followed by Bonferroni's post hoc test. *$P < 0.05$, **$P < 0.01$, ***$P < 0.001$.

Table 12. Statistical Analysis of MBP Immunofluorescence in Twitcher mouse.

Regions	Comparison Groups			N	Summary	*P*-value
Corpus callosum	WT	VS	Untreated	9:18	***	<0.001
	WT	VS	Oct4	9:6	*	0.023
	Untreated	VS	Oct4	18:6	***	<0.001

Note: Data is presented as mean ± SEM. Statistical analysis was performed using one-way ANOVA, followed by Bonferroni's post hoc test. *$P < 0.05$, **$P < 0.01$, ***$P < 0.001$.

Luxol fast blue in combination with periodic acid-Schiff (LFB-PAS) staining was conducted on the CC across all groups to assess myelin integrity and macrophage-mediated inflammation. Untreated Twitcher mice exhibited PAS-positive foamy macrophage infiltration and severe myelin loss, whereas Oct4-treated mice demonstrated noticeably improved myelin preservation, as indicated by enhanced blue staining and increased myelin layer thickness. The structural integrity did not reach wild-type levels; however, Oct4 treatment promoted partial recovery of myelin in the CC.

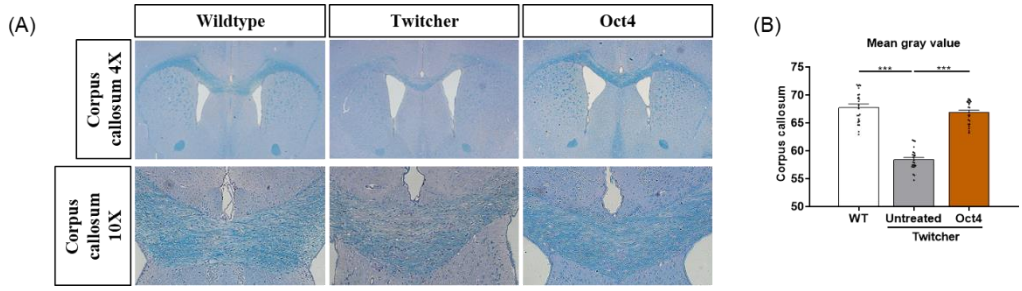

Figure 19. Oct4 treatment improves myelin preservation in the corpus callosum of Twitcher mice, as shown in LFB-PAS staining.

Representative images of LFB-PAS staining of the CC in WT, untreated, and Oct4-treated Twitcher mice at 38 days postinjection. Blue staining corresponding to intact myelin was stronger and more continuous in the Oct4-treated group than in the untreated twitcher group. Quantitative analysis based on the mean gray value revealed increased myelin density in the Oct4-treated group, although not to the level observed in WT mice. Data are expressed as mean ± SEM. $*P < 0.05$ with one-way ANOVA.

Table 13. Characterization of variance heterogeneity across Luxol Fast Blue staining assays in Twitcher mouse.

	WT	**Untreated**	**Oct4**	***F*-value**	***P*-value**
LFB Mean gray value	67.7950±0.58139	58.4100±0.38999	66.8737±0.41296	121.519	<.001

Note: Data is presented as mean ± SEM. Statistical analysis was performed using one-way ANOVA, followed by Bonferroni's post hoc test. *$*P < 0.05, **P < 0.01, ***P < 0.001$*.

Table 14. Statistical analysis details of Luxol Fast Blue staining evaluations in Twitcher mouse.

	Comparison Groups			**N**	**Summary**	***P*-value**
LFB Mean gray value	WT	vs	Untreated	24:24	***	<.001
	WT	vs	Oct4	24:24	ns	.509
	Untreated	vs	Oct4	24:24	**	<.001

Note: Data is presented as mean ± SEM. Statistical analysis was performed using one-way ANOVA, followed by Bonferroni's post hoc test. *$*P < 0.05, **P < 0.01, ***P < 0.001$*.

Transmission EM (TEM) was used to visualize myelinated fibers in the CC and SN. Instead of counting the number of myelin sheath turns, myelin structure was quantitatively

assessed using the g-ratio, which is a well-established index of myelin thickness and functional integrity. The g-ratio, defined as the ratio of the inner axonal diameter to the total outer fiber diameter, reflects axonal conduction efficiency. Oct4-treated mice demonstrated a significantly lower g-ratio than untreated Twitcher mice, thereby indicating thicker and more functionally restored myelin sheaths.

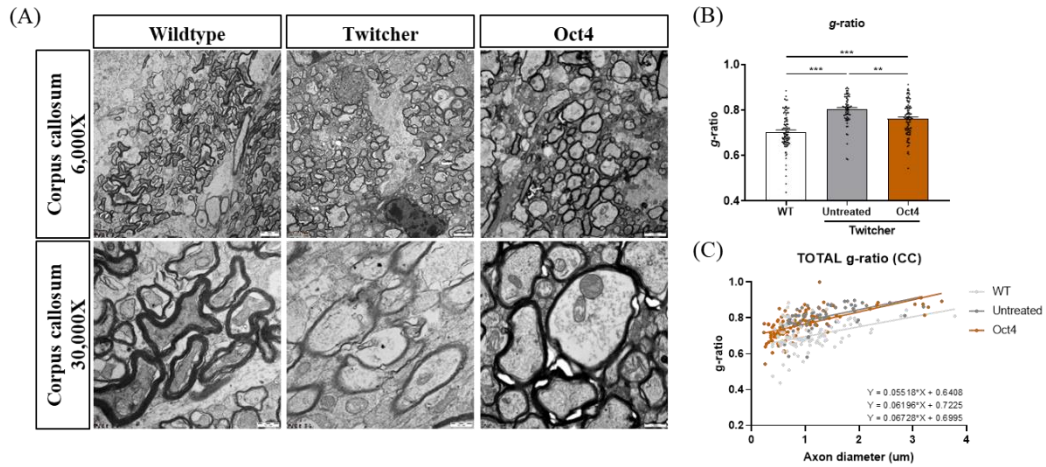

Figure 20. Oct4 treatment enhances myelin thickness in the corpus callosum and sciatic nerve as shown by transmission electron microscopy.

Representative TEM images of myelinated axons in the CC (top row) and SN (bottom row) of WT, untreated, and Oct4-treated Twitcher mice at 38 days post injection. Myelinated fibers appeared more intact and compact in the Oct4-treated group than in the untreated twitcher group, especially in the CC.

Quantitative analysis of g-ratio (axon diameter/fiber diameter) revealed a significant reduction in the Oct4-treated group, indicating thicker and functionally improved myelin sheaths. Scatter plots illustrate the g-ratio distribution in each group.

Data are expressed as mean ± SEM. *$P < 0.05$, **$P < 0.01$, ***$P < 0.001$ with one-way ANOVA.

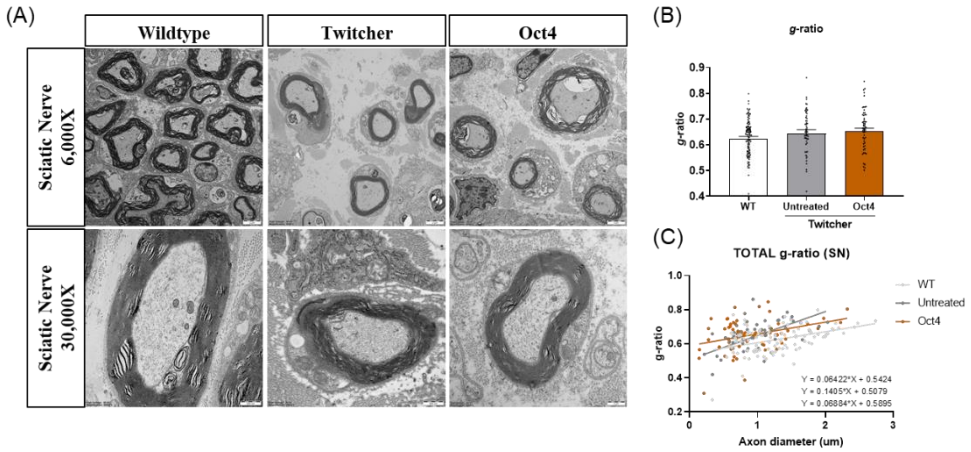

Figure 21. TEM analysis of the sciatic nerve revealing no significant difference in myelin thickness among the groups.

Representative TEM images of myelinated axons in the SN of WT, untreated, and Oct4-treated Twitcher mice at 38 days postinjection. Oct4-treated mice demonstrated slightly improved myelin morphology compared with untreated Twitcher mice; however, the overall g-ratio values demonstrated no statistically significant differences among the groups. Quantitative analysis of the g-ratio is expressed as mean ± SEM. One-way ANOVA followed by a Bonferroni post hoc test was used for statistical analysis.

Table 15. Characterization of variance heterogeneity across TEM in Twitcher mouse.

Regions	WT	Untreated	Oct4	*F*-value	*P*-value
Corpus callosum	0.70±0.00	0.80±0.01	0.76±0.001	36.114	<0.001
Sciatic nerve	0.63±0.01	0.65±0.01	0.65±0.01	1.946	0.145

Note: Data is presented as mean ± SEM. Statistical analysis was performed using one-way ANOVA, followed by Bonferroni's post hoc test. *$P < 0.05$, **$P < 0.01$, ***$P < 0.001$.

Table 16. Statistical Analysis of TEM in Twitcher mouse.

Regions	Comparison Groups			N	Summary	*P*-value
Corpus callosum	WT	VS	Untreated	96:65	***	<0.001
	WT	VS	Oct4	96:96	***	<0.001
	Untreated	VS	Oct4	65:96	**	0.003
Sciatic nerve	WT	VS	Untreated	98:55	ns	0.586
	WT	VS	Oct4	98:61	ns	0.192
	Untreated	VS	Oct4	55:61	ns	1.000

Note: Data is presented as mean ± SEM. Statistical analysis was performed using one-way ANOVA, followed by Bonferroni's post hoc test. *$P < 0.05$, **$P < 0.01$, ***$P < 0.001$.

Following previous findings, the degree of myelination in Twitcher mice was assessed using MRI, specifically through diffusion tensor imaging (DTI). DTI enables brain microstructure assessment based on diffusivity values (λ1, λ2, and λ3), predominantly summarized as scalar metrics: fractional anisotropy (FA), axial diffusivity (AD), mean diffusivity (MD), and radial diffusivity (RD). A detailed DTI analysis was conducted to investigate microstructural alterations in both white and gray matter.

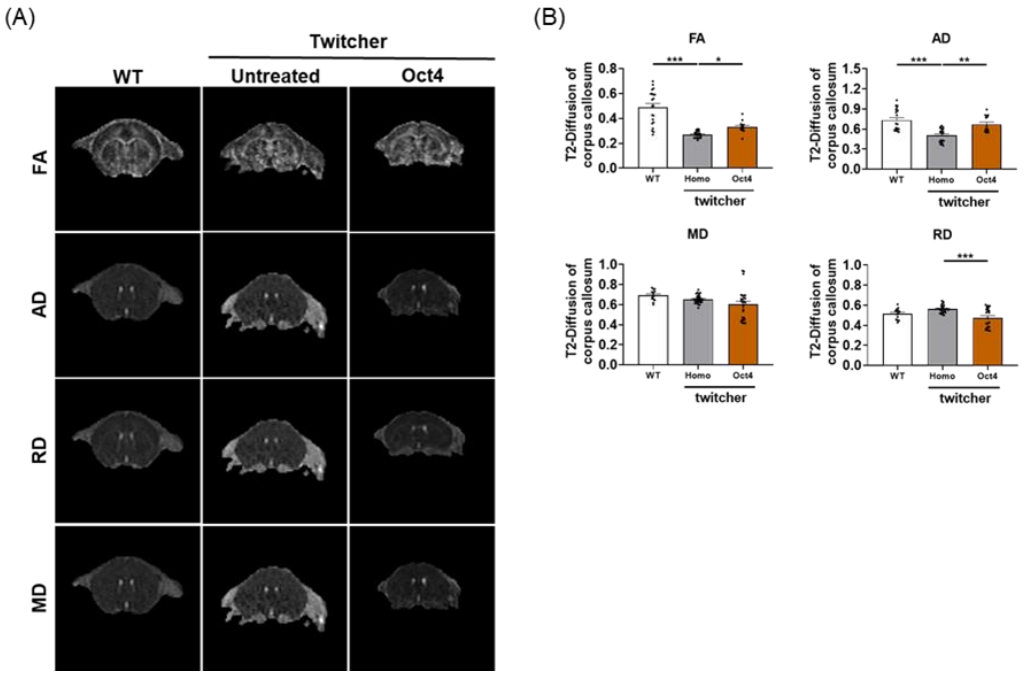

Figure 22. DTI analysis reveals improved white matter integrity in the corpus callosum of Oct4-treated Twitcher mice

Representative DTI maps of FA, AD, MD, and RD in the CC of WT, untreated, and Oct4-treated Twitcher mice at 38 days post-injection.

Quantitative analysis revealed increased FA and AD levels and decreased RD levels in the Oct4-treated group compared with the untreated twitcher group, indicating improved white matter organization and reduced demyelination.

These changes indicate that Oct4 treatment may promote remyelination or structural stabilization of the CC. Data are expressed as mean ± SEM. *$P < 0.05$, **$P < 0.01$, ***$P < 0.001$ with one-way ANOVA.

Table 17. Characterization of variance heterogeneity across MRI-DTI Analysis in Twitcher mouse.

Region	DTI	WT	Untreated	Oct4	*F*-value	*P*-value
Corpus callosum	FA	0.49±0.03	0.27±0.01	0.33±0.01	36.117	<0.001
	AD	0.73±0.04	0.51±0.02	0.67±0.03	16.565	<0.001
	MD	0.69±0.01	0.65±0.01	0.60±0.03	3.947	0.024
	RD	0.51±0.01	0.56±0.01	0.48±0.02	10.722	<0.001

Note: Data is presented as mean ± SEM. Statistical analysis was performed using one-way ANOVA, followed by Bonferroni's post hoc test. **P < 0.05, **P < 0.01, ***P < 0.001.*

Table 18. Statistical analysis details of MRI-DTI evaluations in Twitcher mouse

Region	DTI	Comparison Groups			N	Summary	*P*-value
Corpus callosum	FA	WT	VS	Untreated	21:23	***	<0.001
		WT	VS	Oct4	21:14	***	<0.001
		Untreated	VS	Oct4	23:14	ns	0.127
	AD	WT	VS	Untreated	21:21	***	<0.001
		WT	VS	Oct4	21:15	ns	0.528
		Untreated	VS	Oct4	21:15	**	0.001
	MD	WT	VS	Untreated	14:33	ns	0.642
		WT	VS	Oct4	14:27	*	0.026
		Untreated	VS	Oct4	33:27	ns	0.192
	RD	WT	VS	Untreated	14:30	ns	0.112
		WT	VS	Oct4	14:24	ns	0.277
		Untreated	VS	Oct4	30:24	***	<0.001

Note: Data is presented as mean ± SEM. Statistical analysis was performed using one-way ANOVA, followed by Bonferroni's post hoc test. **P < 0.05, **P < 0.01, ***P < 0.001.*

3.5. Overexpression of Oct4 in Twitcher mouse preserved motor function in the behavioral assessments

Following the confirmation of myelin restoration induced by Oct4 overexpression, a series of behavioral assessments were conducted to evaluate whether functional recovery had occurred in the Twitcher mouse model. The tests performed included the rotarod test, hanging wire test, clasping test, cylinder test which collectively assessed motor coordination, muscle strength, postural abnormalities, and general locomotor activity.

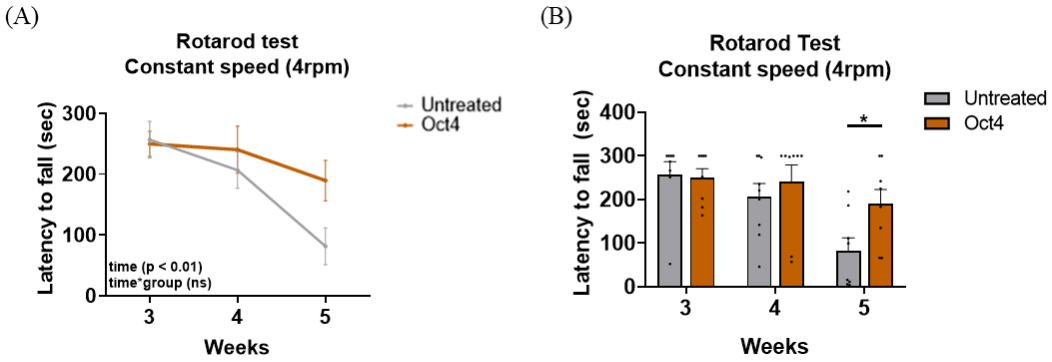

Figure 23. Oct4 overexpression preserves motor coordination in the 4rpm constant speed rotarod test.

(A) Latency to fall was assessed weekly in Twitcher mouse from 3 to 5 weeks of age using a rotarod rotating at a constant speed of 4 rpm. Two-way ANOVA revealed significant main effects of time ($P<0.001$), indicating that Oct4-treated mice maintained better motor function compared to untreated controls over time, although the interaction effect was not statistically significant.

(B) Bar graph shows group-wise comparisons at each timepoint. Oct4-treated mice exhibited significantly higher latency to fall at 5 weeks. Data is presented as mean ± SEM. *$P < 0.05$, **$P < 0.01$, ***$P < 0.001$.

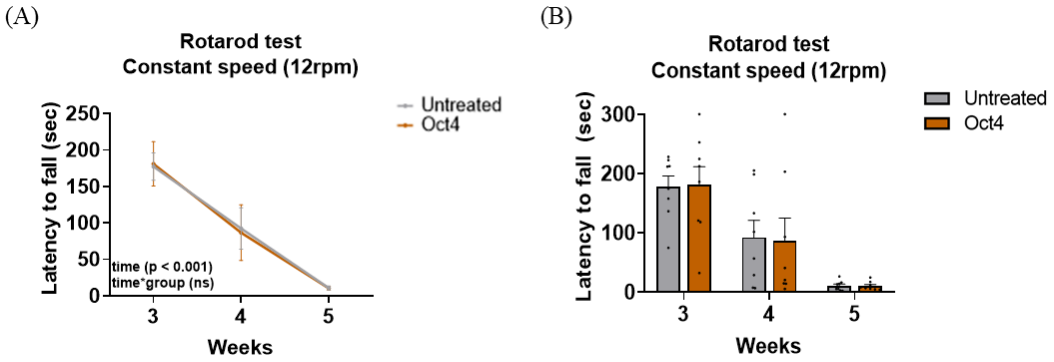

Figure 24. Oct4 overexpression does not significantly affect performance in the 12rpm constant speed rotarod test.

(A) Latency to fall was assessed weekly in Twitcher mouse from 3 to 5 weeks of age on a constant-speed rotarod rotating at 12 rpm. Two-way ANOVA revealed a significant time effect ($P < 0.001$), but no significant group or interaction effects.

(B) Bar graph displaying group-wise performance at each timepoint. No statistically significant differences were observed between Oct4-treated and untreated groups. Data is presented as mean ± SEM. *$P < 0.05$, **$P < 0.01$, ***$P < 0.001$

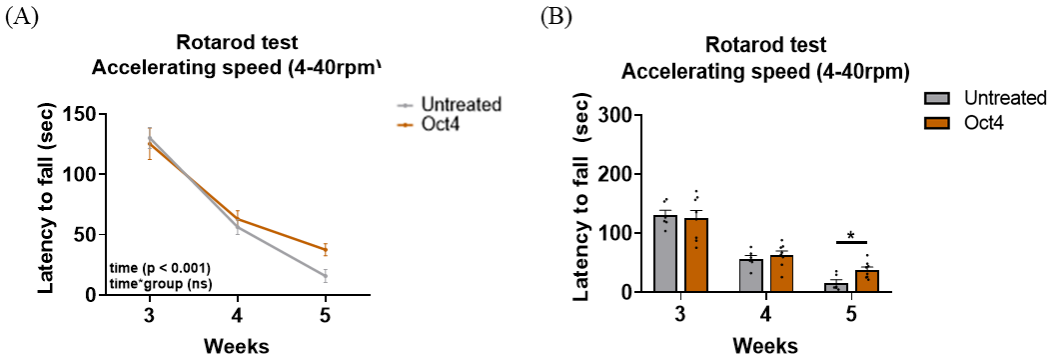

Figure 25. Oct4 overexpression partially improves motor performance in the accelerating rotarod test (4–40 rpm)

(A) Latency to fall was assessed in Twitcher mouse on an accelerating rotarod (4–40 rpm) from 3 to 5 weeks of age. Two-way ANOVA revealed a significant time effect ($P < 0.001$), but no significant group or interaction effect.

(B) Despite the lack of interaction effect, Oct4-treated mice showed significantly higher latency to fall in 5 weeks compared to untreated controls. Data is presented as mean ± SEM. *$P < 0.05$, **$P < 0.01$, ***$P < 0.001$.

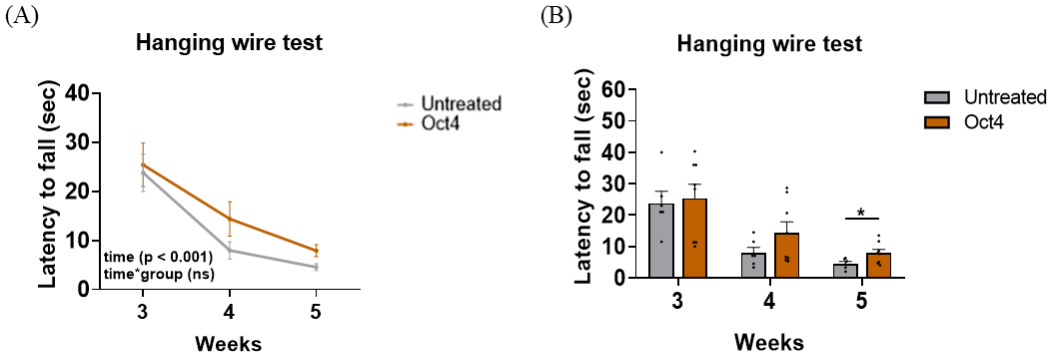

Figure 26. Oct4 overexpression preserves neuromuscular strength in the hanging wire test.

(A) Twitcher mice were subjected to the hanging wire test from 3 to 5 weeks of age to evaluate muscle strength and neuromuscular endurance. Two-way ANOVA revealed a significant time effect ($P < 0.001$), but no significant group or interaction effects.

(B) Bar graphs show that Oct4-treated mice maintained higher hanging times than untreated mice across all timepoints. Notably, a significant difference was observed at 5 weeks ($P < 0.05$), suggesting that Oct4 may mitigate the decline in neuromuscular function. Data is presented as mean ± SEM. *$P < 0.05$, **$P < 0.01$, ***$P < 0.001$.

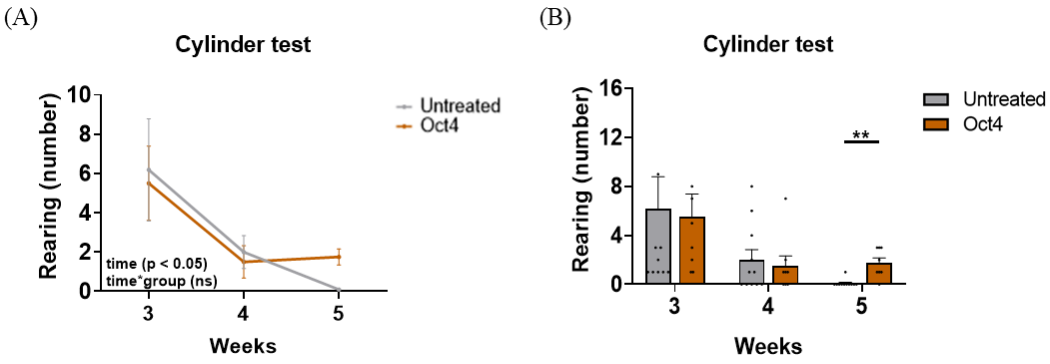

Figure 27. Oct4 overexpression improves spontaneous forelimb use in the cylinder test

at later timepoints.

(A) Cylinder test was performed weekly from 3 to 5 weeks of age to evaluate asymmetrical forelimb use during vertical exploration. The percentage of wall contacts made with the impaired forelimb was calculated. Two-way ANOVA revealed a significant main effect of time ($P < 0.001$), with no significant group or interaction effects.

(B) Bar graphs show that Oct4-treated mice exhibited higher percentages of spontaneous forelimb use compared to untreated mice across all timepoints. Notably, a significant difference was observed at 5 weeks ($P< 0.01$), suggesting that Oct4 may help preserve motor function and reduce asymmetry in forelimb use. Data is presented as mean ± SEM. *$P < 0.05$, **$P < 0.01$, ***$P < 0.001$.

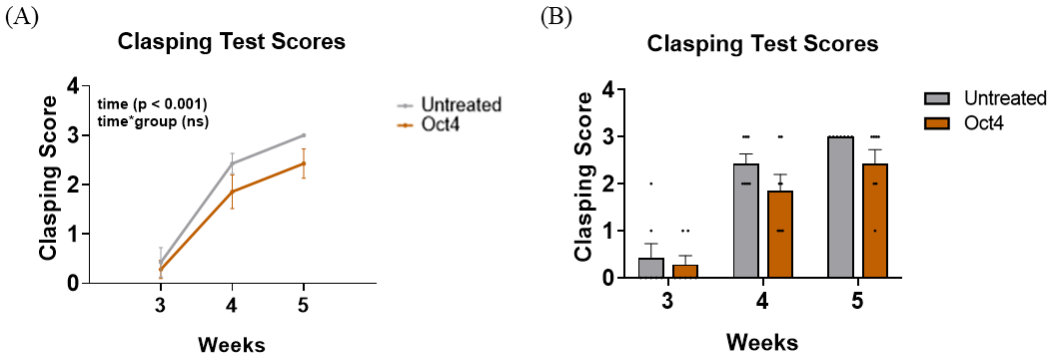

Figure 28. Oct4 overexpression shows a trend toward improved motor phenotype in the clasping score test.

(A) Clasping scores were recorded weekly from 3 to 5 weeks of age to evaluate hindlimb dystonia and neurodegeneration severity. Two-way ANOVA revealed a significant main effect of time ($p < 0.001$), indicating progressive motor deficits in both groups. No significant group or interaction effects were observed.

(B) Oct4-treated mice exhibited consistently lower clasping scores than untreated controls, especially at later timepoints, although these differences did not reach statistical significance. Bonferroni post-hoc analysis was performed. Data is presented as mean ± SEM. *$P < 0.05$, **$P < 0.01$, ***$P < 0.001$.

Table 19. Characterization of variance heterogeneity across behavioral assays in Twitcher mouse.

Test	Week	Untreated	Oct4	*F*-value	*P*-value
Rotarod constant 4rpm	3	256.96±30.01	249.93±20.86	0.009	0.928
	4	203.05±33.64	240.39±38.79	0.234	0.636
	5	81.38±30.52	189.55±33.29	0.050	0.826
Rotarod constant 12rpm	3	177.15±18.72	180.79±30.48	1.873	0.193
	4	92.21±28.55	86.38±38.42	0.450	0.513
	5	10.50±2.97	10.19±2.55	0.359	0.559
Rotarod accelerated 4-40rpm	3	130.07±8.63	125.25±12.98	3.189	0.099
	4	56.22±6.09	62.92±6.93	0.357	0.561
	5	15.75±5.39	37.54±5.01	0.028	0.870
Hanging wire test	3	23.75±3.81	25.38±4.45	2.455	0.143
	4	7.97±1.74	14.38±3.52	6.768	0.023
	5	4.56±0.68	7.90±1.20	2.005	0.182
Cylinder test	3	6.18±2.61	5.50±1.89	1.734	0.205
	4	2.00±0.842	1.50±0.824	0.802	0.383
	5	0.09±0.09	1.75±0.41	26.017	<0.001
Clasping test	3	0.43±0.30	0.29±0.18	1.293	0.278
	4	2.43±0.20	1.86±0.34	2.262	0.158
	5	3.00±0.00	2.43±0.30	24.576	<0.001

Note: Data is presented as mean ± SEM. Statistical analysis was performed using an independent t-test. Welch's correction was applied when the assumption of equal variances was not met, as determined by Levene's test. *$P < 0.05$, **$P < 0.01$, ***$P < 0.001$.

Table 20. Statistical analysis details of behavioral evaluations in Twitcher mouse

Test	Weeks	Comparison Groups			N	Summary	*P*-value
Rotarod constant 4rpm	3 weeks	Untreated	vs	Oct4	8:8	ns	0.850
	4 weeks	Untreated	vs	Oct4	8:8	ns	0.479
	5 weeks	Untreated	vs	Oct4	8:8	*	0.031
	3 weeks	Untreated	vs	Oct4	8:8	ns	0.920

Rotarod constant 12rpm	4 weeks	Untreated	vs	Oct4	8:8	ns	0.905
	5 weeks	Untreated	vs	Oct4	8:8	ns	0.937
Rotarod accelerated 4-40rpm	3 weeks	Untreated	vs	Oct4	6:8	ns	0.078
	4 weeks	Untreated	vs	Oct4	6:8	ns	0.499
	5 weeks	Untreated	vs	Oct4	6:8	*	0.013
Hanging wire test	3 weeks	Untreated	vs	Oct4	6:8	ns	0.795
	4 weeks	Untreated	vs	Oct4	6:8	ns	0.134
	5 weeks	Untreated	vs	Oct4	6:8	*	0.024
Cylinder test	3 weeks	Untreated	vs	Oct4	11:8	ns	0.847
	4 weeks	Untreated	vs	Oct4	11:8	ns	0.686
	5 weeks	Untreated	vs	Oct4	11:8	**	0.005
Clasping test	3 weeks	Untreated	vs	Oct4	**7:7**	ns	0.690
	4 weeks	Untreated	vs	Oct4	**7:7**	ns	0.174
	5 weeks	Untreated	vs	Oct4	**7:7**	ns	0.103

Note: Data is presented as mean ± SEM. Statistical analysis was performed using an independent t-test. Welch's correction was applied when the assumption of equal variances was not met, as determined by Levene's test. *$P < 0.05$, **$P < 0.01$, ***$P < 0.001$.

3.6. Oct4 overexpression significantly extends the lifespan of Twitcher mouse.

The survival and lifespan of Twitcher mouse were assessed on a daily basis. Although there was no statistically significant difference in overall lifespan between the groups (Figure 15), survival rate analysis revealed distinct differences. The Gehan–Breslow–Wilcoxon test indicated a significant divergence in survival curves . Furthermore, Pearson's chi-square analysis identified significant differences between the groups specifically during the period from day 33 to day 40.

(A)

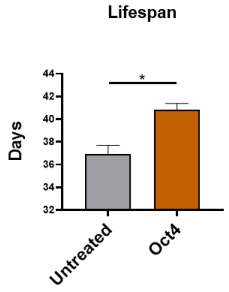

(B)

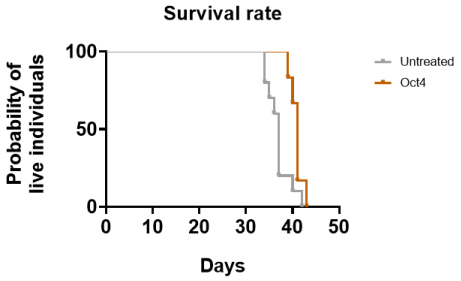

(C)

	Untreated	Oct4	Chi square	*p* value
33 days	100%	100%	-	-
34 days	80%	100%	109.499	0.018
35 days	70%	100%	91.577	0.018
36 days	60%	100%	85.714	0.012
37 days	20%	100%	197.280	0.001
38 days	20%	100%	131.597	< 0.001
39 days	20%	83.33%	143.672	< 0.001
40 days	10%	66.66%	164.705	< 0.001
41 days	10%	16.66%	218.181	< 0.001
42 days	0%	16.66%	92.307	< 0.001
43 days	0%	0%	42.857	< 0.001
44 days	0%	0%	42.857	< 0.001
45 days	0%	0%	42.857	< 0.001
46 days	0%	0%	42.857	< 0.001
47 days	0%	0%	42.857	< 0.001
48 days	0%	0%	-	-

Figure 29. Lifespan and survival rate in the Twitcher mouse.

(A)Median lifespan of each group was calculated and displayed in a bar graph. Oct4-treated mice showed a longer median survival than untreated mice, further supporting the protective role of Oct4. Data is presented as median ± range.

(B) Kaplan–Meier survival curves of Twitcher mouse demonstrate a significant increase in survival in the Oct4-treated group compared to the untreated group.

(C) Box plots represent the distribution of survival days in individual mice across both groups. Although variability exists, Oct4-treated mice demonstrated an overall rightward shift in survival compared to untreated mice. Statistical comparisons were performed using appropriate non-parametric tests, and results showed significant improvement in the Oct4 group.

3.7. Preservation of body weight in Twitcher mouse through Oct4 treatment

To assess the clinical effects of Oct4 overexpression therapy, we monitored both behavioral and physiological parameters in Twitcher mouse. Krabbe disease is characterized by severe seizures, tremors, progressive weight loss, muscle stiffness, and eventual limb paralysis. However, affected mice typically do not exhibit overt neurological symptoms until postnatal day 20 (P20). Therefore, we conducted behavioral assessments on P21, P28, and P35 to capture early-stage functional decline and compare performance between groups. In addition, body weight was measured on P21, P28, and P35 to track general health and disease progression, and brain weight was recorded at P38 immediately after sacrifice. Mice treated with Oct4 showed significantly higher body weight compared to controls, and a two-way ANOVA revealed a significant interaction between time and treatment group.

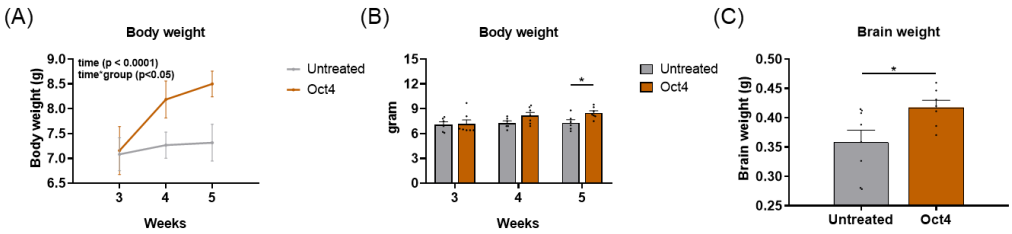

Figure 30. Assessment of Body and Brain Weights in Twitcher mouse.

(A) Body weight was measured at P21, P28, and P35 to assess the progression of general health status. Oct4-treated Twitcher mouse exhibited a significantly greater increase in body weight over time compared to untreated controls. Two-way ANOVA revealed both a significant group effect and a significant interaction between time and treatment ($*P < 0.05$).

(B) Bar graph representing body weights at each time point (P21, P28, and P35). Oct4-treated mice consistently showed higher body weights compared to untreated mice, indicating improved physiological condition.

(C) Brain weight was measured at P38 immediately after sacrifice. Oct4-treated mice

exhibited significantly higher brain weights than untreated mice (*$P < 0.05$), suggesting a protective effect on brain development and neurodegeneration.

Table 21. Characterization of variance heterogeneity across body weight and brain weight assays in Twitcher mouse.

Test	Week	Untreated	Oct4	*F*-value	*P*-value
Body weight	3	7.0833±0.33208	7.1571±0.48347	1.027	0.333
	4	7.2667±0.26162	8.1857±0.37316	1.860	0.200
	5	7.3167±0.36916	8.5000±0.25912	0.343	0.570
Brain weight	5	0.3584±0.02026	0.4178 ±0.01200	3.812	0.073

Note: Data is presented as mean ± SEM. Statistical analysis was performed using an independent t-test. Welch's correction was applied when the assumption of equal variances was not met, as determined by Levene's test. *$P < 0.05$, **$P < 0.01$, ***$P < 0.001$.

Table 22. Statistical analysis details of body weight and brain weight evaluations in Twitcher mouse

Test	Weeks	Comparison Groups			N	Summary	*P*-value
Body weight	3 weeks	Untreated	vs	Oct4	6:8	ns	0.906
	4 weeks	Untreated	vs	Oct4	6:8	ns	0.077
	5 weeks	Untreated	vs	Oct4	6:8	*	0.021
Brain weight	5 weeks	Untreated	vs	Oct4	8:7	*	0.030

Note: Data is presented as mean ± SEM. Statistical analysis was performed using an independent t-test. Welch's correction was applied when the assumption of equal variances was not met, as determined by Levene's test. *$P < 0.05$, **$P < 0.01$, ***$P < 0.001$.

3.8. No Significant Change in GALC Expression Following Oct4 Treatment

The mRNA expression and enzyme activity of GALC were analyzed to determine the changes that contributed to improved behaviors in Twitcher mice. No changes were observed between the Oct4 group and others. These results indicate that the improvement in motor function may be attributed to GALC activity restoration, but rather to alternative mechanisms such as improved myelination or neurogenesis.

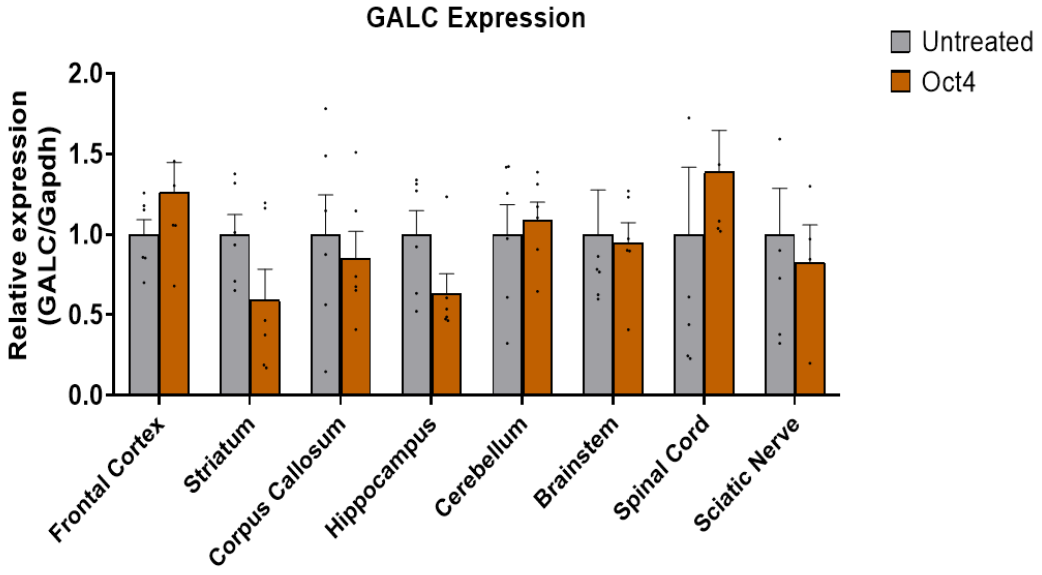

Figure 31. Oct4 overexpression does not alter the expression of endogenous *Galc* mRNA in the CNS.

Quantitative RT-PCR analysis revealed no statistically significant increase in *Galc* mRNA expression in the Oct4-overexpression group compared with the control group across multiple brain regions (FC, STR, CC, brain stem [BS], CB, and SC). Unpaired two-tailed t-tests were conducted, with no significant differences observed ($P > 0.05$). These results indicate that Oct4 overexpression alone does not upregulate endogenous *Galc* expression at the mRNA level.

Table 23. Summary of *Galc* mRNA Expression Levels in Twitcher mouse

Group	Frontal Cortex	Striatum	Corpus Callosum	Hippocampus	Cerebellum	Brainstem	Spinal Cord	Sciatic Nerve
Untreated	1.00±0.09	1.00±0.12	1.00±0.25	1.00±0.15	1.00±0.19	1.00±0.28	1.00±0.42	1.00±0.29
Oct4	1.26±0.19	0.59±0.19	0.85±0.16	0.63±0.12	1.09±0.11	0.95±0.13	1.39±0.26	0.83±0.23
F-value	1.352	2.434	1.093	1.170	2.130	1.414	2.620	1.370
P-value	0.272	0.15	0.32	0.305	0.175	0.262	0.140	0.276

Note: Data is presented as mean ± SEM. Statistical analysis was performed using an independent t-test. Welch's correction was applied when the assumption of equal variances was not met, as determined by Levene's test. *$P < 0.05$, **$P < 0.01$, ***$P < 0.001$.

Table 24. Statistical Analysis of *Galc* mRNA Expression in Twitcher mice

Regions	Comparison Groups			N	Summary	*P*-value
Frontal Cortex	Untreated	vs	Oct4	6:6	ns	0.236
Striatum	Untreated	vs	Oct4	6:6	ns	0.103
Corpus Callosum	Untreated	vs	Oct4	6:6	ns	0.633
Hippocampus	Untreated	vs	Oct4	6:6	ns	0.085
Cerebellum	Untreated	vs	Oct4	6:6	ns	0.694
Brainstem	Untreated	vs	Oct4	6:6	ns	0.863
Spinal Cord	Untreated	vs	Oct4	6:5	ns	0.471
Sciatic Nerve	Untreated	vs	Oct4	6:4	ns	0.680

Note: Data is presented as mean ± SEM. Statistical analysis was performed using an independent t-test. Welch's correction was applied when the assumption of equal variances was not met, as determined by Levene's test. *$P < 0.05$, **$P < 0.01$, ***$P < 0.001$.

Immunofluorescence staining was conducted in the FC and striatum (STR) to identify whether the behavioral improvements in Oct4-treated Twitcher mice were associated with the recovery of GALC expression. GALC levels were markedly reduced in Twitcher mice compared with wild-type controls, and Oct4 treatment did not restore GALC expression in either region (Figure 32). These results indicate that the therapeutic effects of Oct4 are independent of GALC reconstitution.

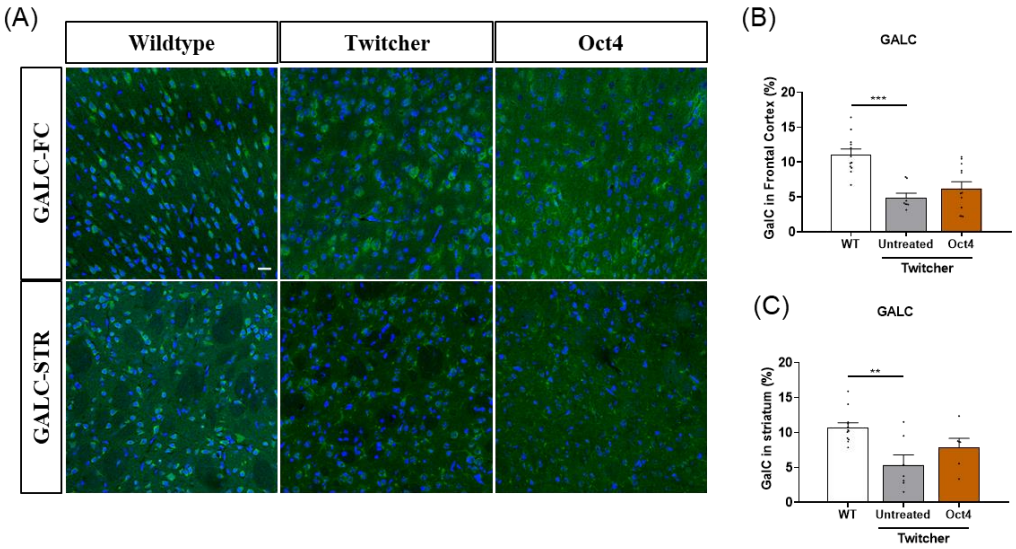

Figure 32. GALC expression is not restored in Oct4-treated Twitcher mice frontal cortex and striatum

(A) Representative immunofluorescence images illustrating GALC (green) and DAPI (blue) staining in the cortex and Striatum. No significant increase in GALC signal was observed in the Oct4-treated group compared with that in the untreated Twitcher mice.

(B–C) Quantification of GALC immunoreactivity in the Frontal Cortex (B) and Striatum (C). No significant differences were detected between the groups. These results indicate that the Oct4-mediated functional improvements are not attributable to the restoration of GALC expression levels. Data are expressed as mean ± SEM. *$P < 0.05$, **$P < 0.01$, *$P < 0.001$.

Table 25. Characterization of variance heterogeneity across GALC staining assays in Twitcher mice

Regions	WT	Untreated	Oct4	*F*-value	*P*-value
Frontal cortex	11.10±0.79	4.90±0.64	6.22±0.96	14.591	<0.001
Striatum	10.74±0.66	5.37±1.42	7.91±1.26	7.614	0.003

Note: Data is presented as mean ± SEM. Statistical analysis was performed using one-way ANOVA, followed by Bonferroni's post hoc test. **P < 0.05, **P < 0.01, ***P < 0.001.*

Table 26. Statistical Analysis of GALC Immunofluorescence in Twitcher mice

Regions	Comparison Groups			N	Summary	*P*-value
Frontal Cortex	WT	VS	Untreated	12:8	***	<0.001
	WT	VS	Oct4	12:12	***	<0.001
	Untreated	VS	Oct4	8:12	ns	0.932
Striatum	WT	VS	Untreated	12:7	**	0.002
	WT	VS	Oct4	12:6	ns	0.151
	Untreated	VS	Oct4	7:6	ns	0.289

Note: Data is presented as mean ± SEM. Statistical analysis was performed using one-way ANOVA, followed by Bonferroni's post hoc test. **P < 0.05, **P < 0.01, ***P < 0.001.*

To assess GALC enzymatic activity, we used HMU-β-gal, which is a synthetic substrate cleaved by β-galactosidase enzymes, including GALC for a fluorometric assay. Enzymatic cleavage of HMU-β-gal releases a fluorescent product (HMU), enabling the quantitative measurement of GALC activity. However, no significant difference in GALC enzymatic activity was observed in the Oct4-treated group compared with the controls, indicating that Oct4-mediated improvements are not associated with the restoration of GALC enzymatic function.

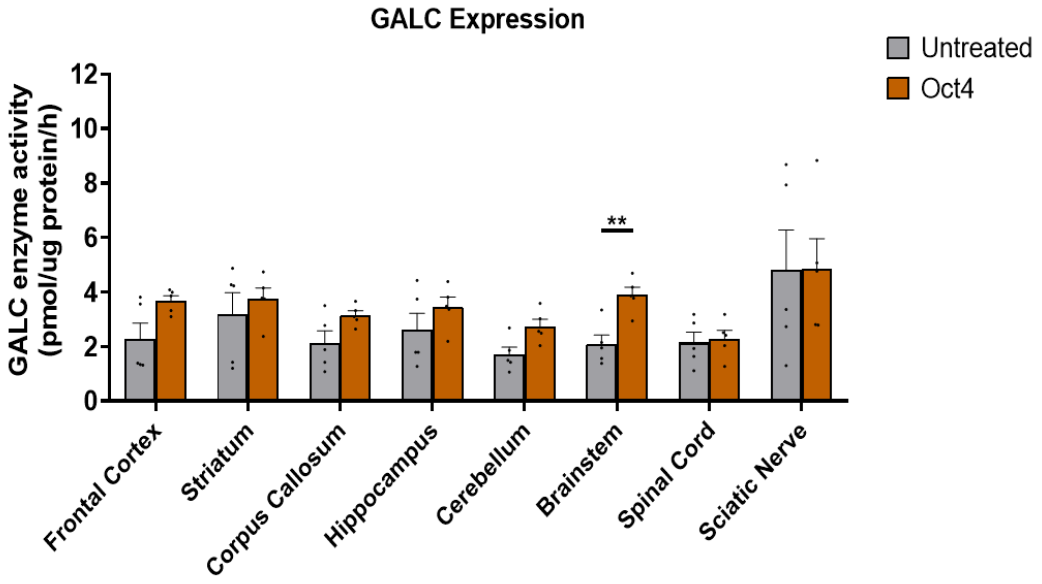

Figure 33. Quantification of GALC Enzymatic Activity using HMU-β-gal assay

To evaluate GALC enzymatic activity, a fluorometric assay using HMU-β-gal was performed across various brain regions. Each sample was incubated with the substrate, and fluorescence signal intensity was measured to quantify GALC activity. No statistically significant differences were observed between the control and Oct4-treated groups in any of the assessed brain regions, including the FC, STR, hippocampus (HC), cerebellum, and BS. These results indicate that Oct4 treatment does not restore the enzymatic function of GALC. An unpaired two-tailed t-test was conducted for statistical analysis. Data are expressed as mean ± SEM.

Table 27. Characterization of variance heterogeneity across GALC activity assays in Twitcher mice

Group	Frontal Cortex	Striatum	Corpus Callosum	Hippocampus	Cerebellum	Brainstem	Spinal Cord	Sciatic Nerve
Untreated	2.284±0.573	3.198±0.778	2.132±0.444	2.604±0.622	1.702±0.276	2.076±0.344	2.144±0.384	4.800±1.474
Oct4	3.670±0.194	3.758±0.390	3.142±0.170	3.448±0.361	2.736±0.263	3.890±0.286	2.280±0.313	4.854±1.102
F-value	3.593	8.474	1.778	3.307	0.828	0.254	0.275	14.509
P-value	0.087	0.016	0.212	0.099	0.384	0.625	0.611	0.009

Note: Data is presented as mean ± SEM. Statistical analysis was performed using an independent t-test. Welch's correction was applied when the assumption of equal variances was not met, as determined by Levene's test. *$P < 0.05$, **$P < 0.01$, ***$P < 0.001$.

Table 28. Statistical analysis details of GALC activity evaluations in Twitcher mice

Regions	Comparison Groups			N	Summary	*P*-value
Frontal Cortex	Untreated	VS	Oct4	5:5	ns	0.072
Striatum	Untreated	VS	Oct4	5:5	ns	0.545
Corpus Callosum	Untreated	VS	Oct4	5:5	ns	0.086
Hippocampus	Untreated	VS	Oct4	5:5	ns	0.274
Cerebellum	Untreated	VS	Oct4	5:5	ns	0.026
Brain stem	Untreated	VS	Oct4	5:5	**	0.004
Spinal cord	Untreated	VS	Oct4	5:5	ns	0.791
Sciatic nerve	Untreated	VS	Oct4	5:5	ns	0.977

Note: Data is presented as mean ± SEM. Statistical analysis was performed using an independent t-test. Welch's correction was applied when the assumption of equal variances was not met, as determined by Levene's test. *$P < 0.05$, **$P < 0.01$, ***$P < 0.001$.

Part2 Combination Therapy of AAV Vector-Mediated *In Vivo* Reprogramming and Gene Editing in a KD Mouse Model

3.9. Assessment of Viral Distribution and PE2max Expression after Facial Vein Injection in Mice

To assess the delivery and tissue distribution of the AAV vector, a fluorescently labeled AAV construct was intravenously administered through the facial vein in neonatal mice. Fluorescence imaging revealed widespread expression throughout the brain, with particularly strong signals observed in the FC, HC, and brain stem (BS), indicating efficient penetration and dissemination within the CNS. Further, qRT-PCR was performed to assess the mRNA expression levels of PE2max-NT and PE2max-CT and the N-terminal and C-terminal components of the split PE2max system. The robust expression of both components was detected in various brain regions, supporting the successful delivery and transcriptional activity of the vector. These results confirm the effective systemic distribution of the AAV construct and its ability to mediate gene expression in targeted CNS regions after neonatal facial vein injection.

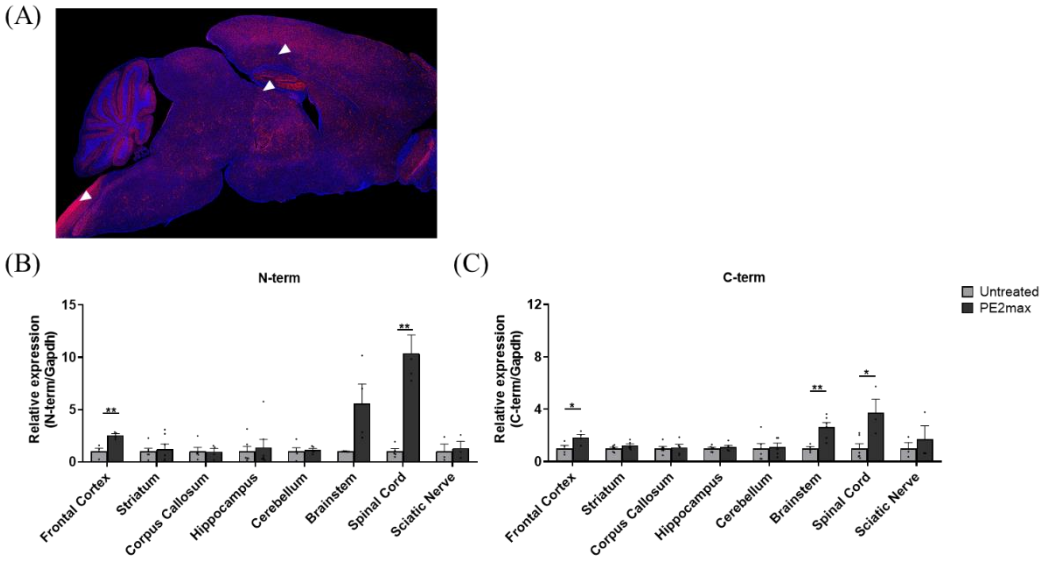

Figure 34. Brain-wide distribution and expression of split PE2max components after facial vein injection.

(A) Representative sagittal brain section demonstrating widespread fluorescence distribution after facial vein injection of fluorescently labeled AAV-PHP.eB vector. Strong signals were detected in the FC, HC, and BS (arrowheads), indicating efficient CNS transduction.

(B) Quantitative analysis of PE2max-NT mRNA expression using qRT-PCR revealed robust expression in multiple CNS regions, particularly in the FC with minimal expression in peripheral organs.

(C) PE2max-CT mRNA expression was highest in the FC, BS, and SC, exhibiting expression patterns consistent with the NT component. Both components demonstrated region-specific enrichment in CNS but very low or undetectable expression in PNS tissues, such as the SN. These results confirm that the facial vein administration of split PE2max via AAV-PHP.eB enables selective CNS-targeted delivery and efficient expression of both gene-editing components.

Table 29. Characterization of variance heterogeneity across NT and CT assays in Twitcher mice.

Split PE2max	Group	Frontal Cortex	Striatum	Corpus Callosum	Hippocampus	Cerebellum	Brain stem	Spinal cord	Sciatic nerve
NT	Untreated	1.00±0.28	1.00±0.29	1.00±0.38	1.00±0.48	1.00±0.34	1.00±0.02	1.00±0.25	1.00±0.69
	PE2max	2.53±0.16	1.19±0.48	0.95±0.32	1.37±0.78	1.13±0.15	5.58±1.86	10.39±1.76	1.30±0.66
	F-value	0.560	5.176	0.076	0.907	0.667	20.771	6.321	0.030
	P-value	0.483	0.044	0.791	0.361	0.438	0.004	0.040	0.870
CT	Untreated	1.00±0.23	1.00±.098	1.00±0.16	1.00±0.09	1.00±0.37	1.00±0.15	1.00±0.36	1.00±0.46
	PE2max	1.84±0.24	1.22±0.12	1.07±0.24	1.11±0.12	1.11±0.30	2.63±0.35	3.71±1.06	1.68±1.05
	F-value	0.033	0.194	0.627	0.015	0.111	3.732	2.993	4.175
	P-value	0.862	0.669	0.449	0.905	0.746	0.089	0.127	0.111

Note: Data is presented as mean ± SEM. Statistical analysis was performed using an independent t-test. Welch's correction was applied when the assumption of equal variances was not met, as determined by Levene's test. *$P < 0.05$, **$P < 0.01$, ***$P < 0.001$.

Table 30. Statistical analysis details of NT and CT evaluations in Twitcher mice

Split PE2max	Regions	Comparison Groups			N	Summary	*P*-value
NT	Frontal Cortex	Untreated	VS	PE2max	4:4	**	0.003
	Striatum	Untreated	VS	PE2max	6:7	ns	0.738
	Corpus Callosum	Untreated	VS	PE2max	5:4	ns	0.930
	Hippocampus	Untreated	VS	PE2max	6:7	ns	0.709
	Cerebellum	Untreated	VS	PE2max	5:5	ns	0.728
	Brain stem	Untreated	VS	PE2max	4:4	ns	0.090
	Spinal cord	Untreated	VS	PE2max	5:4	*	0.012
	Sciatic nerve	Untreated	VS	PE2max	3:3	ns	0.771
CT	Frontal Cortex	Untreated	VS	PE2max	4:4	*	0.044
	Striatum	Untreated	VS	PE2max	6:6	ns	0.177
	Corpus Callosum	Untreated	VS	PE2max	6:5	ns	0.817
	Hippocampus	Untreated	VS	PE2max	6:6	ns	0.466
	Cerebellum	Untreated	VS	PE2max	6:5	ns	0.835
	Brain stem	Untreated	VS	PE2max	4:6	**	0.007
	Spinal cord	Untreated	VS	PE2max	6:3	*	0.017
	Sciatic nerve	Untreated	VS	PE2max	3:3	ns	0.581

Note: Data is presented as mean ± SEM. Statistical analysis was performed using an independent t-test. Welch's correction was applied when the assumption of equal variances was not met, as determined by Levene's test. *$*P < 0.05$, **$P < 0.01$, ***$P < 0.001$.*

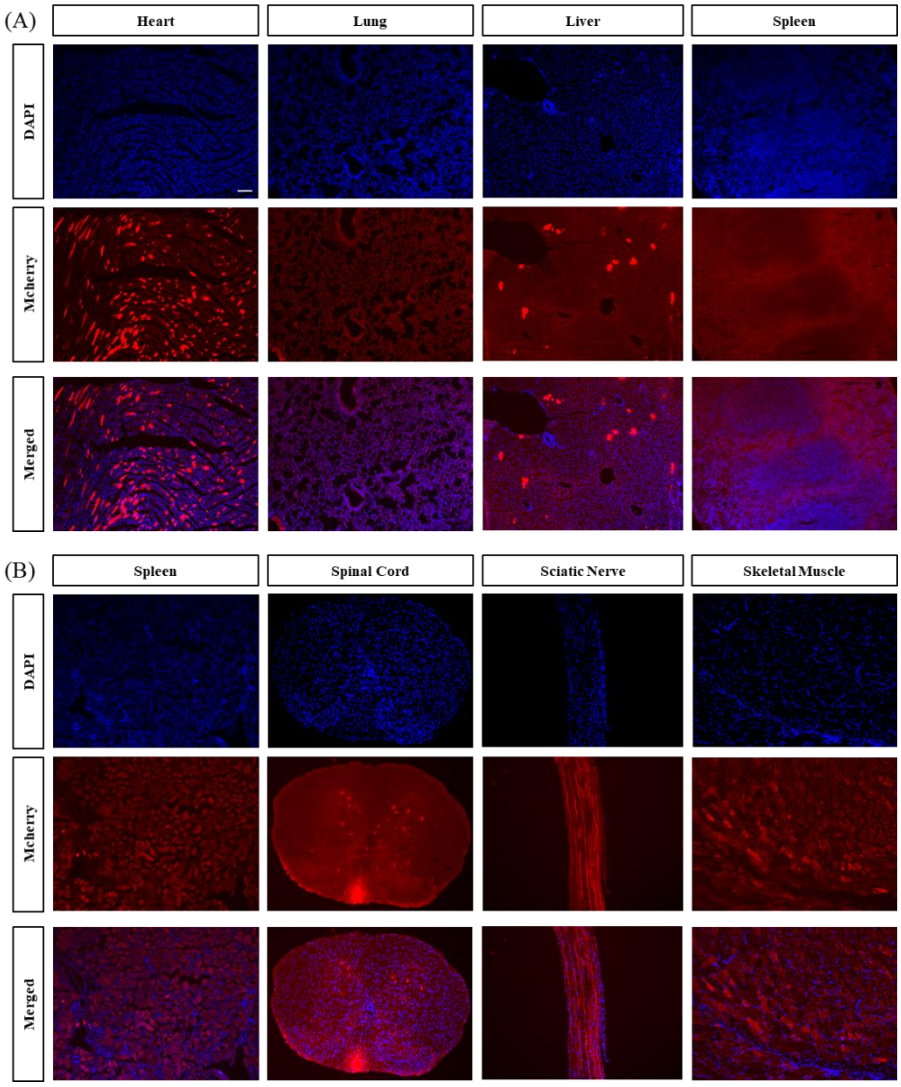

Figure 35. Systemic distribution of PE2max-mCherry expression after AAV-PHP.eB administration.

AAV-PHP.eB that expresses PE2max fused with mCherry was intravenously administered via the facial vein in neonatal mice to evaluate the peripheral distribution of the gene-editing construct. Fluorescence imaging revealed detectable mCherry expression not only in the CNS but also in selected peripheral tissues. Strong signals were observed in the heart, liver, SC, and SN, indicating partial peripheral transduction of the vector. These results

indicate that systemic leakage or limited transduction of peripheral organs may occur, particularly in highly vascularized tissues, although AAV-PHP.eB exhibits CNS tropism.

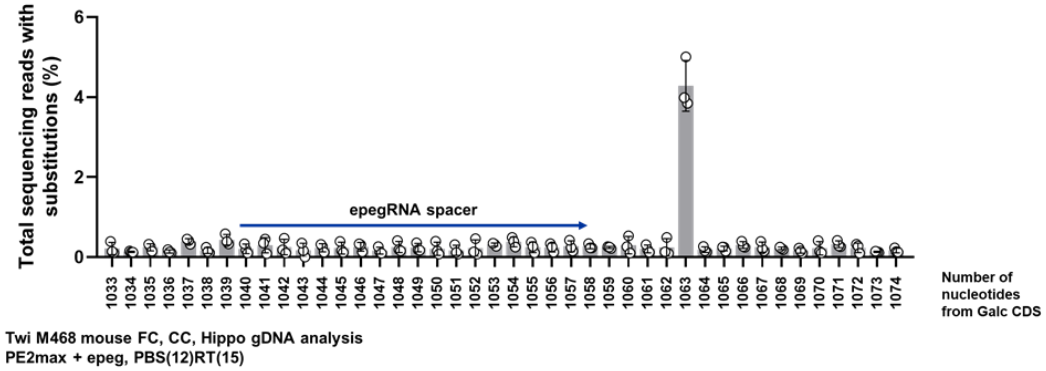

Figure 36. Optimization of the epegRNA design and indel frequency analysis at off-target sites.

Among different combinations of PBS and reverse transcription template (RT) lengths, the epegRNA design, which contains a 12-nucleotide PBS and a 15-nucleotide RT, demonstrated the highest editing efficiency, achieving up to 8% correction at the target site. Further, this optimal condition caused minimal unintended indel formation at the target locus. We further analyzed indel frequencies at predicted off-target sites to assess the specificity of the prime editing system. The results revealed negligible indel generation across most off-target regions, supporting the high precision and safety of the selected epegRNA and PE2max system.

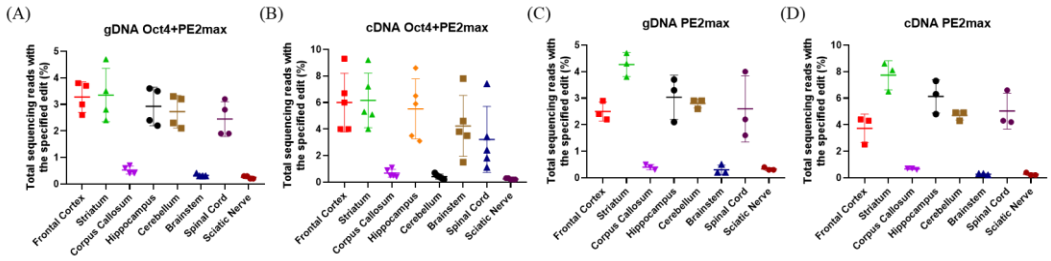

Figure 37. Regional editing efficiency of PE2max vectors in the brain

To assess the performance of prime editing across tissues, A-to-G conversion rates were measured using next-generation sequencing as an indicator of editing efficiency.

(A,C) Genomic DNA (gDNA) from the dissected brain regions was analyzed, revealing region-specific editing patterns.

(B,D) Corresponding complementary DNA (cDNA) from the same samples confirmed consistent transcriptional-level editing. The highest editing efficiencies were observed in select brain regions.

3.10. PE2max-Mediated prime editing restores *Galc* expression in Twitcher mice

A key pathological hallmark of KD is early CC and FC degeneration, accompanied by rapid white matter deterioration and a developmental block in oligodendrocyte maturation. To address this, we administered PE2max intravenously on PD 1 with the hypothesis that precise base correction of the G1065A mutation would not only restore *Galc* expression but also promote myelination-related recovery in the CNS. To validate mutation correction and subsequent *Galc* expression, we employed both molecular and histological methods. Quantitative RT-PCR analysis revealed a significant *Galc* mRNA upregulation in most brain regions, with the highest expression observed in the BS. All regions except the HC demonstrated a notable increase, whereas the SN exhibited an upward trend that did not reach statistical significance. These results confirm that PE2max successfully corrected the target mutation, thereby restoring *Galc* expression at both the RNA and protein levels.

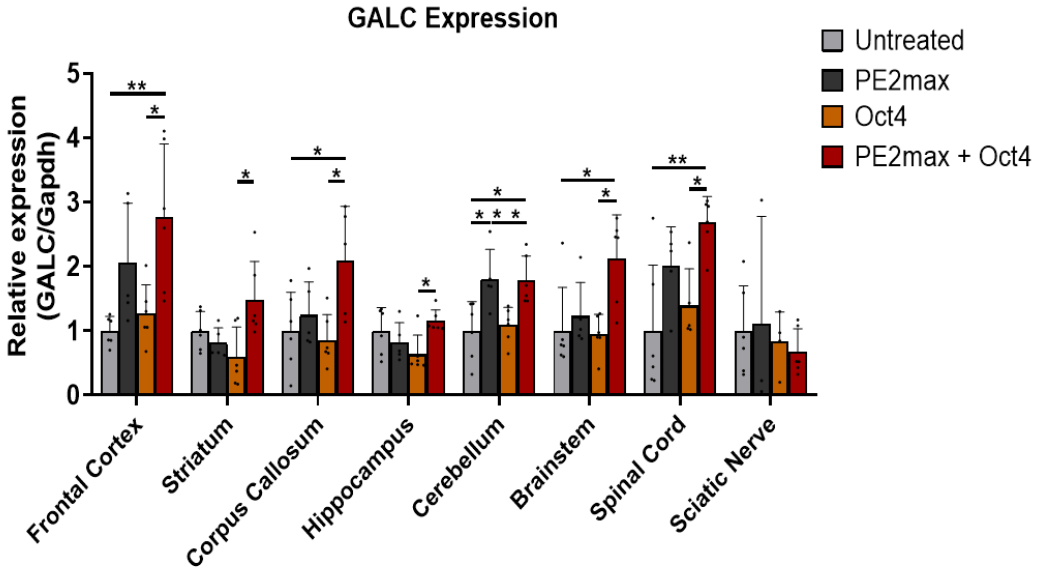

Figure 38. Quantification of *Galc* mRNA expression across the CNS and peripheral tissues after PE2max treatment.

Quantitative real-time polymerase chain reaction (qRT-PCR) was used to measure *Galc* mRNA expression levels across multiple brain regions and peripheral organs in PE2max-treated Twitcher mice. Compared with the untreated group, *Galc* expression was significantly increased in the FC, cerebellum, BS, and SC in the PE2max-treated group. The SN demonstrated a trend toward increased expression; however, the difference did not reach statistical significance.

Table 31. Characterization of variance heterogeneity across *Galc* assays in Twitcher mice

Group	Frontal Cortex	Striatum	Corpus Callosum	Hippocampus	Cerebellum	Brainstem	Spinal Cord	Sciatic Nerve
Untreated	1.00±0.09	1.00±0.12	1.00±0.25	1.00±0.15	1.00±0.19	1.00±0.28	1.00±0.42	1.00±0.29
PE2max	2.05±0.42	0.81±0.11	1.25±0.23	0.82±0.14	1.80±0.21	1.23±0.23	2.01±0.27	1.11±0.96
Oct4	1.26±0.19	0.59±0.19	0.85±0.16	0.63±0.12	1.09±0.11	0.95±0.13	1.39±0.26	0.83±0.23
PE2max+Oct4	2.77±0.46	1.48±0.24	2.09±0.38	1.15±0.07	1.78±0.16	2.13±0.27	2.68±0.17	0.67±0.15
F-value	6.570	4.508	4.491	3.524	6.832	5.640	6.496	0.270
P-value	0.003	0.015	0.016	0.035	0.003	0.006	0.004	0.846

Note: Data is presented as mean ± SEM. Statistical analysis was performed using one-way ANOVA, followed by Bonferroni's post hoc test. *$P < 0.05$, **$P < 0.01$, ***$P < 0.001$.

Table 32. Statistical analysis details of *Galc* qRT-PCR evaluations in Twitcher mice

Regions	Comparison Groups			N	Summary	*P*-value
Frontal Cortex	Untreated	VS	PE2max	6:5	ns	0.210
	Untreated	VS	Oct4	6:6	ns	1.000
	Untreated	VS	PE2max+Oct4	6:6	**	0.004
	PE2max	VS	Oct4	5:6	ns	0.625
	PE2max	VS	PE2max+Oct4	5:6	ns	0.817
	Oct4	VS	PE2max+Oct4	6:6	*	0.017
Striatum	Untreated	VS	PE2max	6:5	ns	1.000
	Untreated	VS	Oct4	6:6	ns	0.722
	Untreated	VS	PE2max+Oct4	6:6	ns	0.423
	PE2max	VS	Oct4	5:6	ns	1.000
	PE2max	VS	PE2max+Oct4	5:6	ns	0.118
	Oct4	VS	PE2max+Oct4	6:6	*	0.013
Corpus Callosum	Untreated	VS	PE2max	6:5	ns	1.000
	Untreated	VS	Oct4	6:6	ns	1.000
	Untreated	VS	PE2max+Oct4	6:5	*	0.046
	PE2max	VS	Oct4	5:6	ns	1.000
	PE2max	VS	PE2max+Oct4	5:5	ns	0.232
	Oct4	VS	PE2max+Oct4	6:5	*	0.019
Hippocampus	Untreated	VS	PE2max	6:5	ns	1.000
	Untreated	VS	Oct4	6:6	ns	.255
	Untreated	VS	PE2max+Oct4	6:6	ns	1.000
	PE2max	VS	Oct4	5:6	ns	1.000
	PE2max	VS	PE2max+Oct4	5:6	ns	.458
	Oct4	VS	PE2max+Oct4	6:6	*	.037
Cerebellum	Untreated	VS	PE2max	6:5	*	.021
	Untreated	VS	Oct4	6:6	ns	1.000
	Untreated	VS	PE2max+Oct4	6:6	*	.017
	PE2max	VS	Oct4	5:6	*	.047
	PE2max	VS	PE2max+Oct4	5:6	ns	1.000

	Oct4	VS	PE2max+Oct4	6:6	*	.041
Brainstem	Untreated	VS	PE2max	6:5	ns	1.000
	Untreated	VS	Oct4	6:6	ns	1.000
	Untreated	VS	PE2max+Oct4	6:6	*	0.016
	PE2max	VS	Oct4	5:6	ns	1.000
	PE2max	VS	PE2max+Oct4	5:6	ns	.099
	Oct4	VS	PE2max+Oct4	6:6	*	.011
Spinal Cord	Untreated	VS	PE2max	6:5	ns	0.171
	Untreated	VS	Oct4	6:5	ns	1.000
	Untreated	VS	PE2max+Oct4	6:6	**	0.004
	PE2max	VS	Oct4	5:5	ns	1.000
	PE2max	VS	PE2max+Oct4	5:6	ns	0.785
	Oct4	VS	PE2max+Oct4	5:6	*	0.041
Sciatic nerve	Untreated	VS	PE2max	6:3	ns	1.000
	Untreated	VS	Oct4	6:4	ns	1.000
	Untreated	VS	PE2max+Oct4	6:6	ns	1.000
	PE2max	VS	Oct4	3:4	ns	1.000
	PE2max	VS	PE2max+Oct4	3:6	ns	1.000
	Oct4	VS	PE2max+Oct4	4:6	ns	1.000

Note: Data is presented as mean ± SEM. Statistical analysis was performed using one-way ANOVA, followed by Bonferroni's post hoc test. *$P < 0.05$, **$P < 0.01$, ***$P < 0.001$.

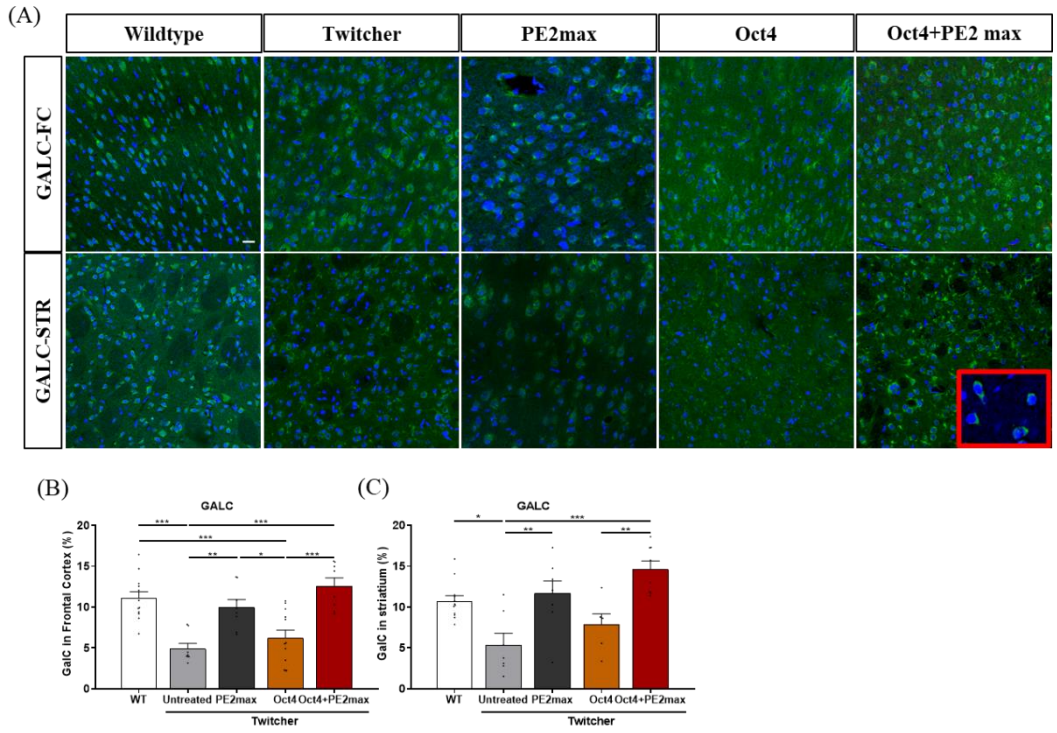

Figure 39. Immunohistochemical analysis of GALC protein expression in the brain after PE2max treatment.

IHC staining was performed to assess GALC protein expression in various brain regions of Twitcher mice. Representative images showing GALC -positive cells (green) with DAPI nuclear counterstain (blue) in the FC and BS across all treatment groups. Quantitative analysis revealed significantly increased GALC protein levels in the PE2max-treated group compared with those in the untreated controls. In particular, GALC expression in the PE2max-only group was comparable to or exceeded that of the Oct4-only and combination treatment groups. The inset image emphasizes strong cytoplasmic GALC expression in individual cells. Data are expressed as mean ± SEM. Statistical significance was identified with one-way ANOVA with a Bonferroni post hoc test.

Table 33. Characterization of variance heterogeneity across GALC staining assays in Twitcher mouse.

Regions	WT	Untreated	PE2max	Oct4	PE2max+Oct4	*F*-value	*P*-value
Frontal cortex	11.10±0.79	4.90±0.64	9.97±0.94	6.21±0.96	12.58±0.10	12.638	<.001
Striatum	10.74±0.66	5.37±1.42	11.71±1.49	7.90±1.26	14.61±1.04	8.926	<.001

Note: Data is presented as mean ± SEM. Statistical analysis was performed using one-way ANOVA, followed by Bonferroni's post hoc test. *$P < 0.05$, **$P < 0.01$, ***$P < 0.001$.

Table 34. Statistical Analysis of GALC Immunofluorescence in Twitcher mice

Regions	Comparison Groups			N	Summary	*P*-value
Frontal Cortex	WT	VS	Untreated	12:8	***	<.001
	WT	VS	PE2max	12:8	ns	1.000
	WT	VS	Oct4	12:12	***	<.001
	WT	VS	PE2max+Oct4	12:8	ns	1.000
	Untreated	VS	PE2max	8:8	**	.007
	Untreated	VS	Oct4	8:12	ns	1.000
	Untreated	VS	PE2max+Oct4	8:8	***	<.001
	PE2max	VS	Oct4	8:12	*	0.050
	PE2max	VS	PE2max+Oct4	8:8	ns	0.669
	Oct4	VS	PE2max+Oct4	12:8	***	<.001
Striatum	WT	VS	Untreated	12:7	*	0.012
	WT	VS	PE2max	12:8	ns	1.000
	WT	VS	Oct4	12:6	ns	0.860
	WT	VS	PE2max+Oct4	12:8	ns	0.126
	Untreated	VS	PE2max	7:8	**	.005
	Untreated	VS	Oct4	7:6	ns	1.000
	Untreated	VS	PE2max+Oct4	7:8	***	<.001
	PE2max	VS	Oct4	8:6	ns	.353
	PE2max	VS	PE2max+Oct4	8:8	ns	.803
	Oct4	VS	PE2max+Oct4	6:8	**	.005

Note: Data is presented as mean ± SEM. Statistical analysis was performed using one-way ANOVA, followed by Bonferroni's post hoc test. *$P < 0.05$, **$P < 0.01$, ***$P < 0.001$.

Building on prior observations of increased GALC expression in the FC, BS, and SC, we next aimed to identify whether these molecular changes translated into functional recovery. To assess GALC enzymatic activity, we performed a fluorometric assay using HMU-β-gal, which is a synthetic substrate cleaved by β-galactosidase enzymes, including GALC Enzymatic cleavage of HMU-β-gal releases a fluorescent product (HMU), enabling quantitative measurement of activity. PE2max-treated mice demonstrated significantly increased GALC activity, with the most robust increases observed in the BS and SC regions, indicating that increased protein expression was accompanied by restored enzymatic function.

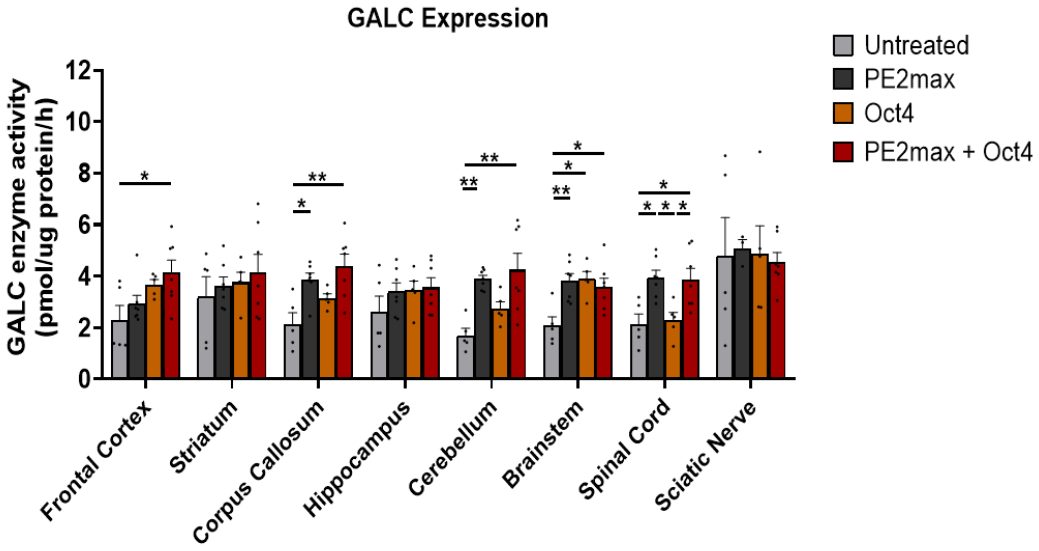

Figure 40. Enzymatic activity of GALC across various brain and peripheral tissues.
This graph illustrates a quantitative comparison of GALC enzymatic activity across treatment groups in Twitcher mice. A fluorescence-based assay was used to measure the activity, revealing the following results. The PE2max-treated group demonstrated a significant increase in GALC activity in regions, such as the FC, BS, and SC, compared

with the untreated group. The BS and SC exhibited the highest GALC activity in the PE2max group, indicating that functional recovery was most prominent in these regions. These findings indicate that PE2max-mediated gene correction not only restored GALC expression at the protein level but also led to functional enzymatic recovery. Furthermore, the overlap between regions with high editing efficiency (FC, BS, and SC) and those with increased GALC activity supports a consistent therapeutic pathway from genetic correction → protein expression → enzymatic function restoration.

Table 35. Characterization of variance heterogeneity across GALC activity assays in Twitcher mouse.

Group	Frontal Cortex	Striatum	Corpus Callosum	Hippocampus	Cerebellum	Brainstem	Spinal Cord	Sciatic Nerve
Untreated	2.2840±0.5734	3.1980±0.7798	2.1320±0.4444	2.6040±0.6216	1.7020±0.2755	2.0760±0.3442	2.1440±0.3843	4.8000±1.4741
PE2max	2.9329±0.3258	3.6343±0.3402	3.8600±0.2587	3.3943±0.3414	3.8857±0.1452	3.8071±0.2884	3.9371±0.2908	5.0733±0.3524
Oct4	3.6700±.19416	3.7580±0.3902	3.1420±0.1698	3.4480±0.3611	2.7360±0.2629	3.8900±0.2863	2.2800±0.3132	4.8540±1.1022
PE2max+Oct4	4.1400±0.4801	4.1629±0.6813	4.3957±0.4613	3.5600±0.3777	4.2471±0.6361	3.5743±0.3459	3.8686±0.4348	4.5443±0.3762
F-value	3.642	0.471	6.765	0.962	7.391	6.032	6.800	0.048
P-value	.030	.706	.002	.430	.002	.004	.002	.985

Note: Data is presented as mean ± SEM. Statistical analysis was performed using one-way ANOVA, followed by Bonferroni's post hoc test. *$P < 0.05$, **$P < 0.01$, ***$P < 0.001$.

Table 36. Statistical analysis details of GALC activity evaluations in Twitcher mouse

Regions	Comparison Groups			N	Summary	*P*-value
Frontal Cortex	Untreated	VS	PE2max	5:7	ns	1.000
	Untreated	VS	Oct4	5:5	ns	0.283
	Untreated	VS	PE2max+Oct4	5:7	*	0.037
	PE2max	VS	Oct4	7:5	ns	1.000
	PE2max	VS	PE2max+Oct4	7:7	ns	0.248
	Oct4	VS	PE2max+Oct4	5:7	ns	1.000
Striatum	Untreated	VS	PE2max	5:7	ns	1.000
	Untreated	VS	Oct4	5:5	ns	1.000
	Untreated	VS	PE2max+Oct4	5:7	ns	1.000
	PE2max	VS	Oct4	7:5	ns	1.000
	PE2max	VS	PE2max+Oct4	7:7	ns	1.000
	Oct4	VS	PE2max+Oct4	5:7	ns	1.000
Corpus Callosum	Untreated	VS	PE2max	5:7	*	0.023
	Untreated	VS	Oct4	5:5	ns	0.552
	Untreated	VS	PE2max+Oct4	5:7	**	0.002
	PE2max	VS	Oct4	7:5	ns	1.000
	PE2max	VS	PE2max+Oct4	7:7	ns	1.000
	Oct4	VS	PE2max+Oct4	5:7	ns	0.167
Hippocampus	Untreated	VS	PE2max	5:7	ns	1.000
	Untreated	VS	Oct4	5:5	ns	1.000
	Untreated	VS	PE2max+Oct4	5:7	ns	0.772
	PE2max	VS	Oct4	7:5	ns	1.000
	PE2max	VS	PE2max+Oct4	7:7	ns	1.000
	Oct4	VS	PE2max+Oct4	5:7	ns	1.000
Cerebellum	Untreated	VS	PE2max	5:7	**	0.009
	Untreated	VS	Oct4	5:5	ns	0.747
	Untreated	VS	PE2max+Oct4	5:7	**	0.002
	PE2max	VS	Oct4	7:5	ns	0.410
	PE2max	VS	PE2max+Oct4	7:7	ns	1.000

	Oct4	VS	PE2max+Oct4	5:7	ns	0.119
Brainstem	Untreated	VS	PE2max	5:7	**	0.008
	Untreated	VS	Oct4	5:5	**	0.010
	Untreated	VS	PE2max+Oct4	5:7	*	0.025
	PE2max	VS	Oct4	7:5	ns	1.000
	PE2max	VS	PE2max+Oct4	7:7	ns	1.000
	Oct4	VS	PE2max+Oct4	5:7	ns	1.000
Spinal cord	Untreated	VS	PE2max	5:7	*	0.018
	Untreated	VS	Oct4	5:5	ns	1.000
	Untreated	VS	PE2max+Oct4	5:7	*	0.024
	PE2max	VS	Oct4	7:5	*	0.032
	PE2max	VS	PE2max+Oct4	7:7	ns	1.000
	Oct4	VS	PE2max+Oct4	5:7	*	0.043
Sciatic nerve	Untreated	VS	PE2max	5:3	ns	1.000
	Untreated	VS	Oct4	5:5	ns	1.000
	Untreated	VS	PE2max+Oct4	5:7	ns	1.000
	PE2max	VS	Oct4	3:5	ns	1.000
	PE2max	VS	PE2max+Oct4	3:7	ns	1.000
	Oct4	VS	PE2max+Oct4	5:7	ns	1.000

Note: Data is presented as mean ± SEM. Statistical analysis was performed using one-way ANOVA, followed by Bonferroni's post hoc test. *$P < 0.05$, **$P < 0.01$, ***$P < 0.001$.

3.11. Combined PE2max and Oct4 treatment maximizes Myelin integrity and MBP restoration in Twitcher mice

MBP plays a crucial role in the myelination process in the nervous system by maintaining the structural integrity of the myelin sheath through interactions with membrane lipids. Previous studies have revealed that reduced MBP expression induces demyelination in the CNS, causing tremors, seizures, and early mortality. MBP immunostaining was conducted in paraffin-embedded brain sections 38 days postinjection to assess myelin sheath restoration. MBP-positive cells were observed along the CC under fluorescence

microscopy. The PE2max + Oct4 combination treatment resulted in the strongest MBP staining intensity among all groups, indicating the highest degree of myelin restoration. These findings indicate that PE2max and Oct4 have a synergistic effect in improving MBP expression and myelin integrity in Twitcher mice.

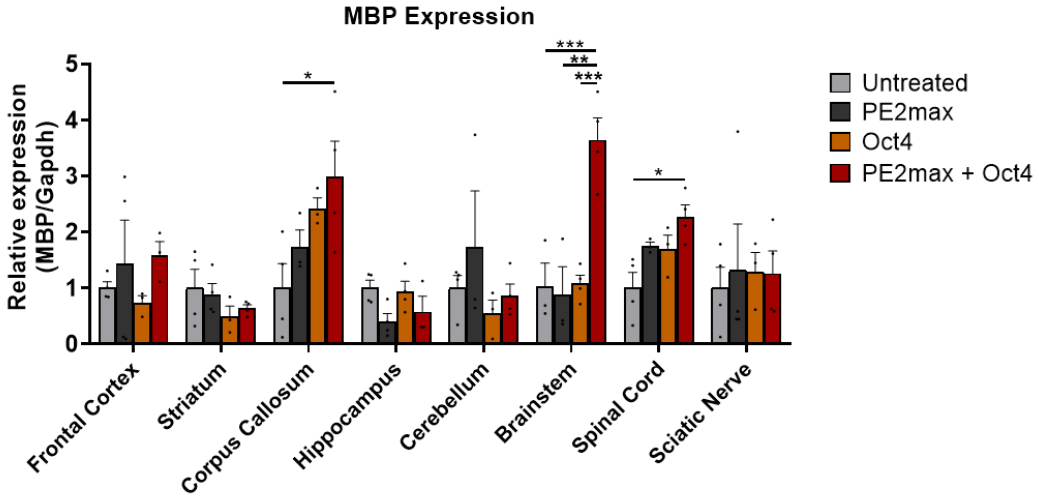

Figure 41. Quantitative analysis of MBP mRNA expression across the brain and spinal regions after Oct4 and PE2max treatment.

MBP mRNA expression was quantified using qRT-PCR to assess myelination levels across various CNS regions in Twitcher mice treated with Oct4, PE2max, or both. The PE2max + Oct4 combination group demonstrated the highest MBP expression levels, with statistically significant increases observed in the FC, CC, BS, and SC compared with the untreated group. Oct4 or PE2max monotherapy also improved MBP expression in some regions, whereas the combined treatment exhibited the most prominent synergistic effect. Data are expressed as mean ± SEM (n = 4–5 per group). Statistical analysis was conducted using one-way ANOVA followed by a Bonferroni post hoc test. *$p < 0.05$, **$p < 0.01$ versus untreated group.

Table 37. Characterization of variance heterogeneity across MPB assays in Twitcher mouse.

Group	Frontal Cortex	Striatum	Corpus Callosum	Hippocampus	Cerebellum	Brain stem	Spinal cord	Sciatic nerve
Untreated	1.00±0.11	1.00±0.33	1.00±0.44	1.00±0.14	1.00±0.22	1.00±0.29	1.00±0.28	1.00±0.37
PE2max	1.44±0.77	0.88±0.19	1.53±0.29	0.40±0.14	1.72±1.00	0.88±050	1.75±0.07	1.31±0.83
Oct4	0.74±0.13	0.49±0.19	2.42±0.19	0.94±0.18	0.54±0.24	1.07±0.15	1.68±0.26	1.28±0.35
PE2max+Oct4	1.58±0.25	0.64±0.06	2.99±0.63	0.58±0.27	0.86±0.20	3.65±0.39	2.27±0.22	1.26±0.40
F-value	0.622	1.012	4.103	2.689	1.008	16.319	5.646	0.073
P-value	0.617	0.424	0.035	0.098	0.429	<0.001	0.016	0.973

Note: Data is presented as mean ± SEM. Statistical analysis was performed using one-way ANOVA, followed by Bonferroni's post hoc test. *$P < 0.05$, **$P < 0.01$, ***$P < 0.001$.

Table 38. Statistical analysis details of MBP qRT-PCR evaluations in Twitcher mouse

Regions	Comparison Groups			N	Summary	*P*-value
Frontal Cortex	Untreated	VS	PE2max	4:4	ns	1.000
	Untreated	VS	Oct4	4:3	ns	1.000
	Untreated	VS	PE2max+Oct4	4:3	ns	1.000
	PE2max	VS	Oct4	4:3	ns	1.000
	PE2max	VS	PE2max+Oct4	4:3	ns	1.000
	Oct4	VS	PE2max+Oct4	3:3	ns	1.000
Striatum	Untreated	VS	PE2max	4:4	ns	1.000
	Untreated	VS	Oct4	4:3	ns	0.909
	Untreated	VS	PE2max+Oct4	4:4	ns	1.000
	PE2max	VS	Oct4	4:3	ns	1.000
	PE2max	VS	PE2max+Oct4	4:4	ns	1.000
	Oct4	VS	PE2max+Oct4	3:4	ns	1.000
Corpus callosum	Untreated	VS	PE2max	4:4	ns	1.000
	Untreated	VS	Oct4	4:3	ns	0.335
	Untreated	VS	PE2max+Oct4	4:4	*	0.047
	PE2max	VS	Oct4	4:3	ns	1.000
	PE2max	VS	PE2max+Oct4	4:4	ns	0.221
	Oct4	VS	PE2max+Oct4	3:4	ns	1.000
Hippocampus	Untreated	VS	PE2max	4:4	ns	.192
	Untreated	VS	Oct4	4:4	ns	1.000
	Untreated	VS	PE2max+Oct4	4:3	ns	.831
	PE2max	VS	Oct4	4:4	ns	.306
	PE2max	VS	PE2max+Oct4	4:3	ns	1.000
	Oct4	VS	PE2max+Oct4	4:3	ns	1.000
Cerebellum	Untreated	VS	PE2max	4:3	ns	1.000
	Untreated	VS	Oct4	4:3	ns	1.000
	Untreated	VS	PE2max+Oct4	4:4	ns	1.000
	PE2max	VS	Oct4	3:3	ns	0.754
	PE2max	VS	PE2max+Oct4	3:4	ns	1.000

	Oct4	VS	PE2max+Oct4	3:4	ns	1.000
Brain stem	Untreated	VS	PE2max	4:3	ns	1.000
	Untreated	VS	Oct4	4:4	ns	1.000
	Untreated	VS	PE2max+Oct4	4:4	***	<0.001
	PE2max	VS	Oct4	3:4	ns	1.000
	PE2max	VS	PE2max+Oct4	3:4	**	0.001
	Oct4	VS	PE2max+Oct4	4:4	***	<0.001
Spinal cord	Untreated	VS	PE2max	4:3	ns	0.295
	Untreated	VS	Oct4	4:3	ns	0.412
	Untreated	VS	PE2max+Oct4	4:4	*	0.013
	PE2max	VS	Oct4	3:3	ns	1.000
	PE2max	VS	PE2max+Oct4	3:4	ns	0.907
	Oct4	VS	PE2max+Oct4	3:4	ns	0.661
Sciatic nerve	Untreated	VS	PE2max	4:4	ns	1.000
	Untreated	VS	Oct4	4:3	ns	1.000
	Untreated	VS	PE2max+Oct4	4:4	ns	1.000
	PE2max	VS	Oct4	4:3	ns	1.000
	PE2max	VS	PE2max+Oct4	4:4	ns	1.000
	Oct4	VS	PE2max+Oct4	3:4	ns	1.000

Note: Data is presented as mean ± SEM. Statistical analysis was performed using one-way ANOVA, followed by Bonferroni's post hoc test. *$P < 0.05$, **$P < 0.01$, ***$P < 0.001$.

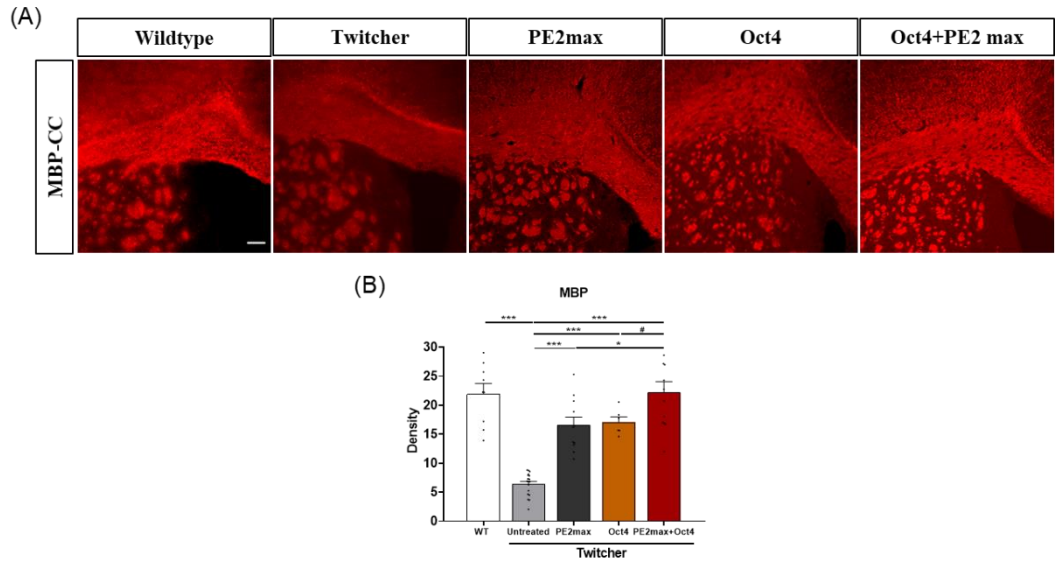

Figure 42. MBP immunofluorescence analysis in the corpus callosum after Oct4 and PE2max treatment.

Immunofluorescent staining for MBP was performed to assess myelin restoration in the CC of Twitcher mice. Representative images illustrate the MBP-positive signal (red) 38 days after treatment in each group. Quantitative analysis of MBP fluorescence intensity revealed that the PE2max + Oct4 combination group demonstrated the highest MBP signal among all groups. Further, significant increases were observed in the Oct4-only and PE2max-only groups compared with the untreated controls. These findings indicate that Oct4 and PE2max promote myelin recovery in the CC, and their combination further improves this effect. Data are expressed as mean ± SEM (n = 4–5 per group). Statistical analysis was conducted using one-way ANOVA with a Bonferroni post hoc test.

Table 39. Characterization of variance heterogeneity across MBP staining assays in Twitcher mouse.

Regions	WT	Untreated	PE2max	Oct4	PE2max+Oct4	*F*-value	*P*-value
Corpus callosum	21.97±1.77	6.41±0.47	16.57±1.38	17.10±0.90	22.20±1.88	31.160	<0.001

Note: Data is presented as mean ± SEM. Statistical analysis was performed using one-way ANOVA, followed by Bonferroni's post hoc test. *$P < 0.05$, **$P < 0.01$, ***$P < 0.001$.

Table 40. Statistical Analysis of MBP Immunofluorescence in Twitcher mouse

Regions	Comparison Groups			N	Summary	*P*-value
Corpus callosum	WT	VS	Untreated	9:18	***	<0.001
	WT	VS	PE2max	9:11	ns	0.089
	WT	VS	Oct4	9:6	ns	0.412
	WT	VS	PE2max+Oct4	9:12	ns	1.000
	Untreated	VS	PE2max	18:11	***	<0.001
	Untreated	VS	Oct4	18:6	***	<0.001
	Untreated	VS	PE2max+Oct4	18:12	***	<0.001
	PE2max	VS	Oct4	11:6	ns	1.000
	PE2max	VS	PE2max+Oct4	11:12	*	0.036
	Oct4	VS	PE2max+Oct4	6:12	ns	0.251

Note: Data is presented as mean ± SEM. Statistical analysis was performed using one-way ANOVA, followed by Bonferroni's post hoc test. *$P < 0.05$, **$P < 0.01$, ***$P < 0.001$.

3.12. Improved corpus callosum myelin preservation after PE2max and Oct4 combination therapy

LFB-PAS staining was performed on the CC across all groups to assess myelin integrity and macrophage-mediated inflammation. Untreated Twitcher mice demonstrated severe myelin loss and PAS-positive foamy macrophage infiltration, whereas mice treated with Oct4 or PE2max exhibited improved myelin preservation. The PE2max + Oct4

combination group demonstrated the most significant recovery, as indicated by intense blue staining and increased myelin layer thickness. Full restoration to wild-type levels was not achieved; however, the combination treatment promoted greater structural recovery of myelin in the CC than either monotherapy.

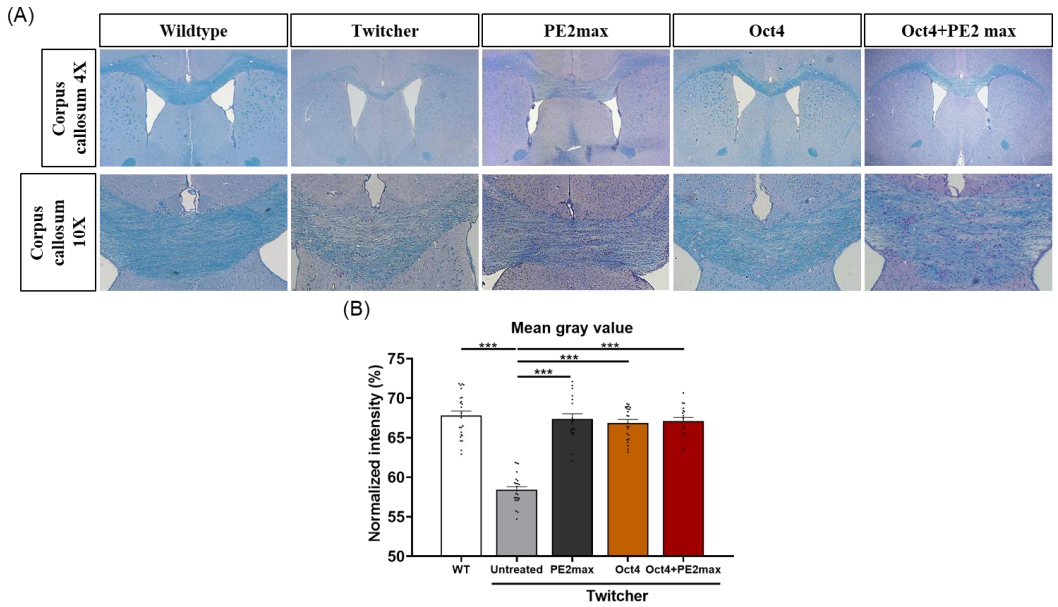

Figure 43. PE2max and Oct4 combination therapy most effectively improves corpus callosum myelin preservation.

LFB-PAS staining was performed to assess myelin preservation and tissue structure in the CC of Twitcher mice. Severe myelin loss and infiltration of PAS-positive foamy macrophages were prominently observed in the untreated group, reflecting the pathological hallmarks of KD. In contrast, Oct4 or PE2max monotherapy caused partial recovery of myelin, as evidenced by increased blue staining intensity and thicker myelin layers. Notably, the PE2max + Oct4 combination group demonstrated the strongest blue staining and most distinct restoration of myelin structure, indicating that the combination therapy produced the greatest effect on CC myelin preservation. Quantitative analysis was based on mean gray value, and statistical significance was identified using one-way ANOVA followed by Bonferroni post hoc test.

Table 41. Characterization of variance heterogeneity across Luxol Fast Blue staining assays in Twitcher mice

	WT	Untreated	PE2max	Oct4	PE2max+Oct4	*F*-value	*P*-value
LFB Mean gray value	67.80±0.58	58.41±0.39	67.37±0.67	66.87±0.41	67.09±0.47	67.14	<0.001

Note: Data is presented as mean ± SEM. Statistical analysis was performed using one-way ANOVA, followed by Bonferroni's post hoc test. *$P < 0.05$, **$P < 0.01$, ***$P < 0.001$.

Table 42. Statistical analysis details of Luxol Fast Blue staining evaluations in Twitcher mice

	Comparison Groups			N	Summary	*P*-value
LFB Mean gray value	WT	vs	Untreated	24:24	***	<.001
	WT	vs	PE2max	24:18	ns	1.000
	WT	vs	Oct4	24:24	ns	1.000
	WT	vs	PE2mac+Oct4	24:18	ns	1.000
	Untreated	vs	PE2max	24:18	***	<.001
	Untreated	vs	Oct4	24:24	***	<.001
	Untreated	vs	PE2max+Oct4	24:18	***	<.001
	PE2max	vs	Oct4	18:24	ns	1.000
	PE2max	vs	PE2max+Oct4	18:18	ns	1.000
	Oct4	vs	PE2max+Oct4	24:18	ns	1.000

Note: Data is presented as mean ± SEM. Statistical analysis was performed using one-way ANOVA, followed by Bonferroni's post hoc test. *$P < 0.05$, **$P < 0.01$, ***$P < 0.001$.

3.13. TEM-based assessment of myelin restoration highlights the combination therapy effect

TEM was used to assess the ultrastructure of myelinated axons in the CC and SN. Rather than counting the number of myelin sheath turns, myelin integrity was quantitatively assessed using the g-ratio, which is a widely used metric of myelin thickness and axonal insulation. The g-ratio is calculated as the ratio between the inner axonal diameter and the total outer diameter, where a lower value indicates thicker and more compact myelin. The PE2max + Oct4 combination treatment led to the lowest g-ratio values among all groups, reflecting the most robust improvement in myelin compaction. This indicates that the combined therapy most effectively restored the structural and functional integrity of myelin in Twitcher mice.

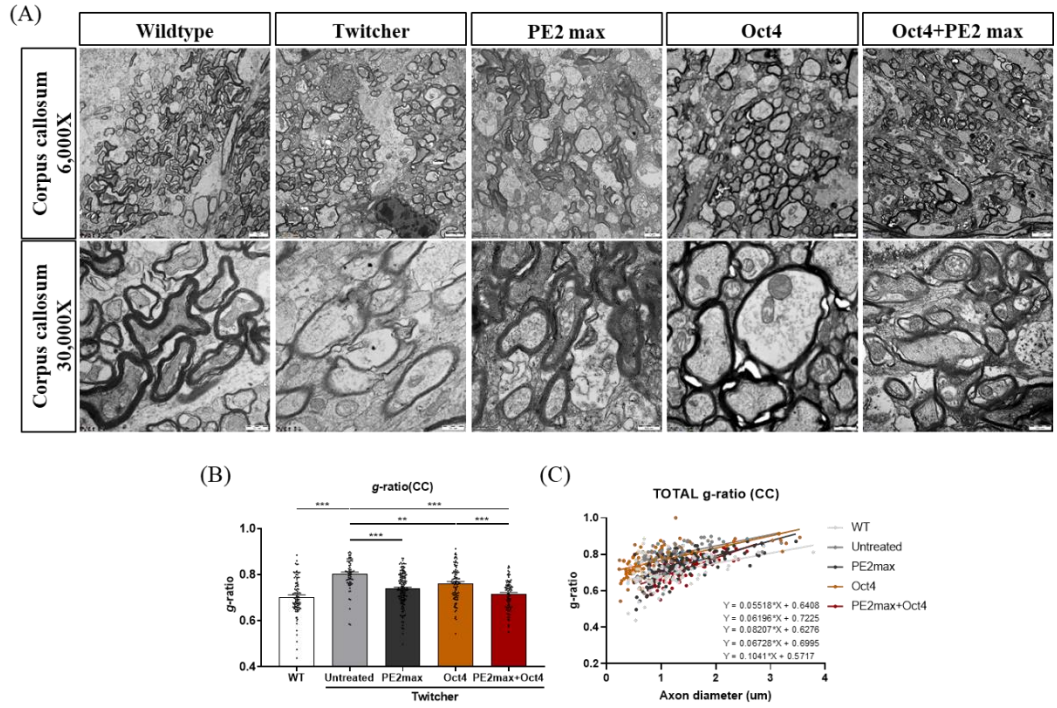

Figure 44. TEM analysis of corpus callosum reveals improved myelin compaction after combination therapy with PE2max and Oct4.

TEM was used to assess the ultrastructural features of myelinated axons in the CC of Twitcher mice across different treatment groups. Representative TEM images illustrate distinct differences in myelin sheath integrity between groups. Untreated Twitcher mice demonstrated poorly compacted or disorganized myelin, whereas PE2max- and Oct4-treated groups showed moderate sheath structure improvement. Notably, the PE2max + Oct4 combination group demonstrated densely packed and well-organized myelin layers, which closely resembled the structure observed in WT mice. Quantitative analysis using the g-ratio (inner axonal diameter/total outer diameter) was conducted to assess myelin thickness. A significantly lower g-ratio was observed in the PE2max + Oct4 group than in the other groups, indicating thicker and more functionally mature myelin sheaths. These findings indicate that combination therapy most effectively restores CC myelin integrity. Data are expressed as mean ± SEM. Statistical analysis was conducted using one-way ANOVA followed by a Bonferroni post hoc test.

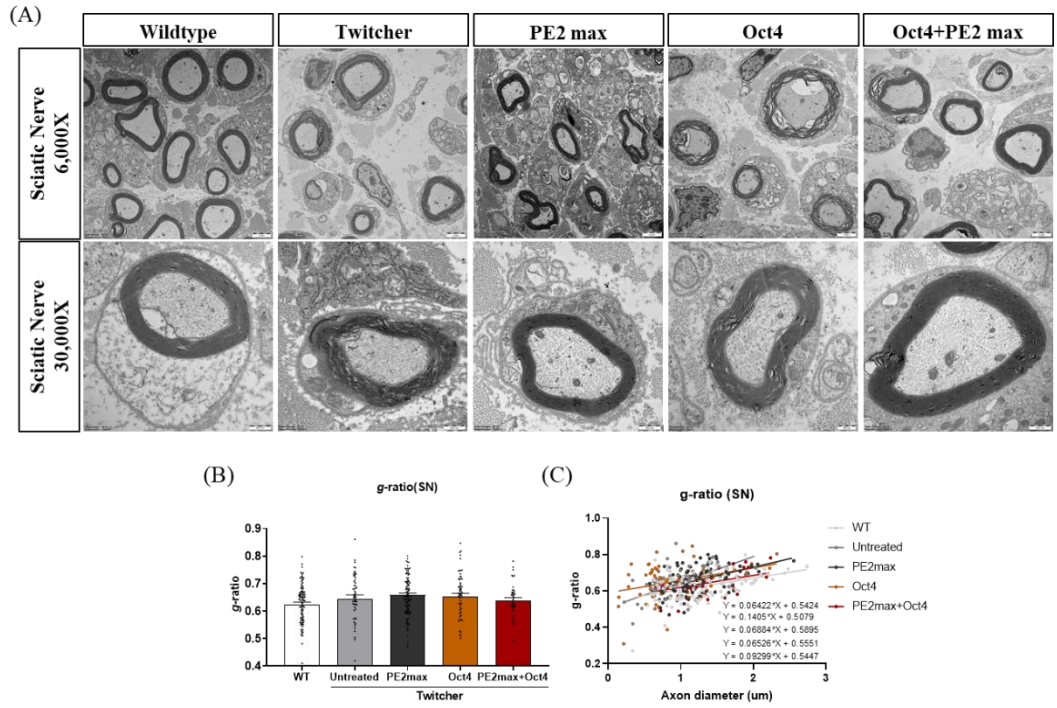

Figure 45. TEM analysis of the sciatic nerve reveals limited myelin recovery after PE2max and Oct4 treatment.

TEM was utilized to assess the ultrastructural features of myelinated axons in the SN of Twitcher mice across treatment groups. Untreated Twitcher mice displayed severe myelin disruption and axonal distortion, whereas mice treated with Oct4 or PE2max alone demonstrated partial improvements in myelin morphology. The PE2max + Oct4 combination group exhibited relatively more compact and aligned myelin sheaths; however, the degree of structural restoration was less pronounced compared with the CNS. Quantitative assessment using the g-ratio (inner axonal diameter/total outer diameter) indicated a trend toward reduced g-ratio in the combination group, indicating improved myelin thickness. However, these differences did not reach statistical significance, implying that functional myelin recovery was more limited in the PNS. Data are expressed as mean ± SEM. Statistical analysis was conducted using one-way ANOVA with a Bonferroni post hoc test.

Table 43. Characterization of variance heterogeneity across TEM assays in Twitcher mice

Regions	WT	Untreated	PE2max	Oct4	PE2max+Oct4	*F*-value	*P*-value
Corpus callosum	0.70±0.01	0.80±0.01	0.74±0.01	0.76±0.01	0.72±0.01	23.140	<.001
Sciatic nerve	0.63±0.01	0.65±0.01	0.66±0.01	0.65±0.01	0.64±0.01	2.149	0.074

Note: Data is presented as mean ± SEM. Statistical analysis was performed using one-way ANOVA, followed by Bonferroni's post hoc test. *$P < 0.05$, **$P < 0.01$, ***$P < 0.001$.

Table 44. Statistical Analysis of TEM assays in Twitcher mice

Regions	Comparison Groups			N	Summary	*P*-value
Corpus callosum	WT	VS	Untreated	96:65	***	<0.001
	WT	VS	PE2max	96:150	**	0.002
	WT	VS	Oct4	96:96	***	<0.001

	WT	VS	PE2max+Oct4	96:82	ns	1.000
	Untreated	VS	PE2max	65:150	***	<0.001
	Untreated	VS	Oct4	65:96	**	0.006
	Untreated	VS	PE2max+Oct4	65:82	***	<0.001
	PE2max	VS	Oct4	150:96	ns	0.137
	PE2max	VS	PE2max+Oct4	150:82	ns	0.162
	Oct4	VS	PE2max+Oct4	96:82	***	<0.001
Sciatic nerve	WT	VS	Untreated	98:55	ns	1.000
	WT	VS	PE2max	98:94	ns	0.062
	WT	VS	Oct4	98:61	ns	0.438
	WT	VS	PE2max+Oct4	98:40	ns	1.000
	Untreated	VS	PE2max	55:94	ns	1.000
	Untreated	VS	Oct4	55:61	ns	1.000
	Untreated	VS	PE2max+Oct4	55:40	ns	1.000
	PE2max	VS	Oct4	94:61	ns	1.000
	PE2max	VS	PE2max+Oct4	94:40	ns	1.000
	Oct4	VS	PE2max+Oct4	61:40	ns	1.000

Note: Data is presented as mean ± SEM. Statistical analysis was performed using one-way ANOVA, followed by Bonferroni's post hoc test. *$P < 0.05$, **$P < 0.01$, ***$P < 0.001$.

3.14. Galc Gene Correction Ameliorates Psychosine Accumulation

Psychosine (also known as galactosylsphingosine) is a toxic metabolite that is generated during sphingolipid metabolism. Under normal conditions, the enzyme GALC (galactocerebrosidase) degraded psychosine. However, enzymatic activity is lost in disorders that involve *Galc* gene deficiency, such as KD, resulting in the accumulation of psychosine within neural cells. Psychosine is particularly toxic to oligodendrocytes and neurons, causing myelin damage and neuronal cell death.

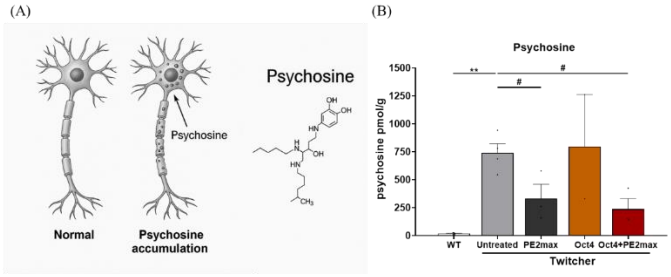

Figure 46. Combined treatment with PE2max and Oct4 significantly reduces psychosine accumulation in Twitcher mice.

(A) The panel illustrates the pathological changes associated with psychosine accumulation compared with normal neurons. Normal neurons maintain continuous myelin structures, whereas psychosine accumulates in *Galc*-deficient neurons, resulting in intracellular vacuolation and axonal demyelination—hallmark pathological features of KD.

(B) Graph quantifies psychosine levels (pmol/g) across experimental groups in the Twitcher mouse model. The untreated twitcher group demonstrated a significant increase in psychosine levels. PE2max treatment alone caused a statistically significant reduction in psychosine accumulation. In contrast, Oct4 alone did not reduce psychosine levels. Notably, the combination of PE2max and Oct4 led to the most significant decrease in psychosine accumulation compared with the untreated group. Statistical analysis was conducted using one-way ANOVA followed by post hoc tests. Bonferroni-corrected *p*-values are indicated as ** ($p < 0.05$), ** ($p < 0.01$), and *** ($p < 0.001$),* whereas LSD test results are indicated as *# ($p < 0.05$), ## ($p < 0.01$), and ### ($p < 0.001$).*

Table 45. Characterization of variance heterogeneity across psychosine assays in Twitcher mice

	WT	Untreated	PE2max	Oct4	PE2max+Oct4	*F*-value	*P*-value
psychosine	17.87± 3.57	739.07± 83.58	332.35± 126.98	796.28± 465.54	238.68± 92.72	7.137	0.004

Note: Data is presented as mean ± SEM. Statistical analysis was performed using one-way ANOVA, followed by Bonferroni's post hoc test. *$P < 0.05$, **$P < 0.01$, ***$P < 0.001$.

Table 46. Statistical analysis details of psychosine evaluations in Twitcher mice

	Comparison Groups			N	Summary	*P*-value
Psychosine	WT	vs	Untreated	5:4	###	<.001
	WT	vs	PE2max	5:3	ns	0.092
	WT	vs	Oct4	5:2	##	0.002
	WT	vs	PE2mac+Oct4	5:3	ns	1.000
	Untreated	vs	PE2max	4:3	#	0.043
	Untreated	vs	Oct4	4:2	ns	0.784
	Untreated	vs	PE2max+Oct4	4:3	#	0.017
	PE2max	vs	Oct4	3:2	ns	0.052
	PE2max	vs	PE2max+Oct4	3:3	ns	0.635
	Oct4	vs	PE2max+Oct4	2:3	#	0.024

Note: Data is presented as mean ± SEM. Statistical analysis was performed using one-way ANOVA, followed by Bonferroni's post hoc test. *$P < 0.05$, **$P < 0.01$, ***$P < 0.001$.

3.15. MRI-DTI analysis of Myelin integrity and brain tissue changes in patients with KD

In line with previous findings, the myelination degree in Twitcher mice was assessed using MRI, specifically through DTI. DTI enables the assessment of brain microstructure based on diffusivity values (λ1, λ2, and λ3), predominantly summarized as scalar metrics: FA, AD, MD, and RD. A detailed DTI analysis was conducted to investigate microstructural alterations in both white and gray matter.

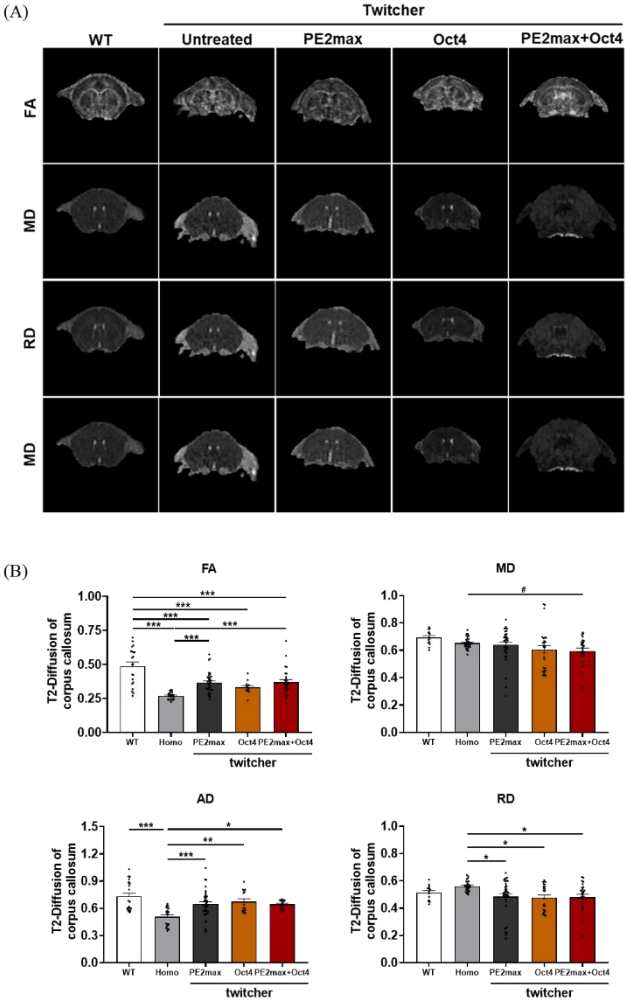

Figure 47. DSI Studio-based DTI reveals microstructural alterations in the brains of Twitcher mice.

DTI analysis was conducted using DSI Studio to assess microstructural changes in both white and gray matter of Twitcher mice. Representative maps of FA, AD, RD, and MD were obtained, along with quantitative comparisons across groups. RD and MD values were markedly increased in the untreated twitcher group, whereas FA values were decreased, indicating substantial demyelination and microstructural disruption. In contrast, the PE2max + Oct4 combination group demonstrated decreased RD and MD values and increased FA, indicating improved axonal integrity and partial remyelination. Notably, the combination treatment resulted in diffusivity metrics that were closer to those of the WT group, particularly in AD, RD, and MD, emphasizing the structural neuroprotective effects of the treatment on CNS white matter. All data are expressed as mean ± SEM, and statistical significance was assessed using one-way ANOVA followed by a Bonferroni post hoc test.

Table 47. Characterization of variance heterogeneity across MRI-DTI Analysis in Twitcher mouse.

Region	DTI	WT	Untreated	PE2max	Oct4	PE2max+Oct4	*F*-value	*P*-value
Corpus callosum	FA	0.49±0.03	0.27±0.01	0.37±0.01	0.33±0.01	0.37±0.02	18.229	<0.001
	AD	0.73±0.04	0.51±0.02	0.65±0.02	0.67±0.03	0.64±0.01	8.847	<0.001
	MD	0.69±0.01	0.65±0.01	0.64±0.02	0.60±0.03	0.59±0.02	2.826	0.027
	RD	0.51±0.01	0.56±0.01	0.48±0.02	0.48±0.02	0.48±0.02	3.860	0.005

Note: Data is presented as mean ± SEM. Statistical analysis was performed using one-way ANOVA, followed by Bonferroni's post hoc test. *$P < 0.05$, **$P < 0.01$, ***$P < 0.001$.

Table 48. Statistical analysis details of MRI-DTI evaluations in Twitcher mouse

Region	DTI	Comparison Groups			N	Summary	*P*-value
Corpus callosum	FA	WT	VS	Untreated	21:23	***	<0.001
		WT	VS	PE2max	21:36	***	<0.001
		WT	VS	Oct4	21:14	***	<0.001
		WT	VS	PE2max+Oct4	21:27	***	<0.001
		Untreated	VS	PE2max	23:36	***	<0.001
		Untreated	VS	Oct4	23:14	ns	0.391
		Untreated	VS	PE2max+Oct4	23:27	***	<0.001
		PE2max	VS	Oct4	36:14	ns	1.000
		PE2max	VS	PE2max+Oct4	36:27	ns	1.000
		Oct4	VS	PE2max+Oct4	14:27	ns	1.000
	AD	WT	VS	Untreated	21:21	***	<0.001
		WT	VS	PE2max	21:39	ns	0.171
		WT	VS	Oct4	21:15	ns	1.000
		WT	VS	PE2max+Oct4	21:16	ns	0.383
		Untreated	VS	PE2max	21:39	***	<0.001
		Untreated	VS	Oct4	21:15	**	0.002
		Untreated	VS	PE2max+Oct4	21:16	*	0.015
		PE2max	VS	Oct4	39:15	ns	1.000
		PE2max	VS	PE2max+Oct4	39:16	ns	1.000
		Oct4	VS	PE2max+Oct4	15:16	ns	1.000
	MD	WT	VS	Untreated	14:33	ns	1.000
		WT	VS	PE2max	14:36	ns	1.000
		WT	VS	Oct4	14:27	ns	0.128
		WT	VS	PE2max+Oct4	14:27	ns	0.057
		Untreated	VS	PE2max	33:36	ns	1.000
		Untreated	VS	Oct4	33:27	ns	0.807
		Untreated	VS	PE2max+Oct4	33:27	ns	0.355
		PE2max	VS	Oct4	36:27	ns	1.000
		PE2max	VS	PE2max+Oct4	36:27	ns	0.884

	Oct4	VS	PE2max+Oct4	27:27	ns	1.000
RD	WT	VS	Untreated	14:30	ns	1.000
	WT	VS	PE2max	14:37	ns	1.000
	WT	VS	Oct4	14:24	ns	1.000
	WT	VS	PE2max+Oct4	14:27	ns	1.000
	Untreated	VS	PE2max	30:37	*	0.017
	Untreated	VS	Oct4	30:24	*	0.019
	Untreated	VS	PE2max+Oct4	30:27	*	0.022
	PE2max	VS	Oct4	37:24	ns	1.000
	PE2max	VS	PE2max+Oct4	37:27	ns	1.000
	Oct4	VS	PE2max+Oct4	24:27	ns	1.000

Note: Data is presented as mean ± SEM. Statistical analysis was performed using one-way ANOVA, followed by Bonferroni's post hoc test. *$P < 0.05$, **$P < 0.01$, ***$P < 0.001$.

3.16. Combination therapy with PE2max and Oct4 preserves motor function in Twitcher mice

A series of behavioral tests was conducted on Twitcher mice to assess the neurological effects of PE2max and Oct4 combination therapy. The following tests were performed: rotarod, hanging wire, clasping, cylinder test. The rotarod test was conducted weekly from postnatal weeks 3–5 under three conditions: constant speed at 4 rpm, constant speed at 12 rpm, and accelerating speed from 4 to 40 rpm (Figure 7). At 4 rpm, only the combination group (PE2max + Oct4) maintained consistent motor performance through week 5, whereas the other groups demonstrated deteriorated performance. Further, the combination group demonstrated significantly prolonged latency time at 12 rpm, indicating a therapeutic effect under more challenging conditions. Under the accelerating condition (4–40 rpm), the combination group sustained motor function up to week 5, whereas the untreated and monotherapy groups failed to do so. Two-way ANOVA revealed significant effects of both time and treatment group across all test conditions (4 rpm, 12 rpm, and accelerating). Notably, the combination treatment of PE2max + Oct4 demonstrated the most robust preservation of motor function, indicating a synergistic and complementary neuroprotective effect.

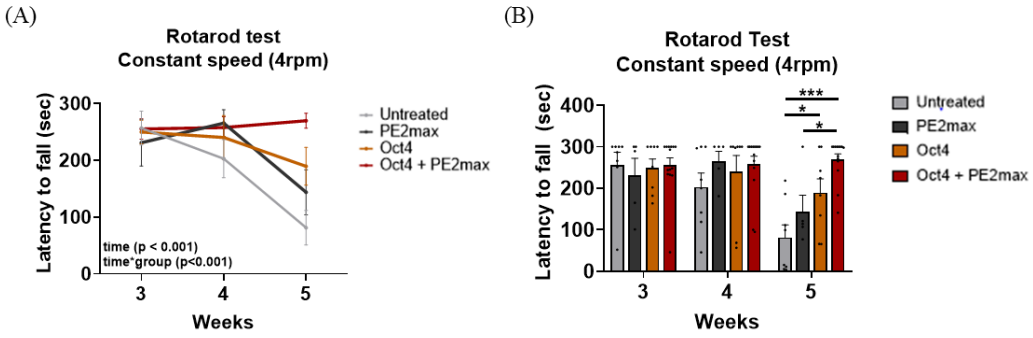

Figure 48. PE2max + Oct4 combination therapy most effectively preserves motor function in the 4-rpm fixed-speed rotarod test.

(A) Rotarod testing was conducted at a constant speed of 4 rpm from postnatal week 3–5.

The PE2max + Oct4 combination group (red line) maintained a consistent latency time without performance decline, whereas the untreated, PE2max-only, and Oct4-only groups demonstrated a significant reduction in motor performance by week 5.

(B) At week 5, comparison of latency across groups revealed that the combination group demonstrated the longest latency time, indicating that the combinational treatment most effectively preserved motor function. These findings demonstrate that motor decline in Twitcher mice can be detected even under a low-speed condition (4 rpm), and that the combination therapy exhibits the strongest neuroprotective effect among the treatment groups. Statistical analysis was conducted using two-way ANOVA, and significant effects were observed for both the time and treatment groups ($p < 0.05$).

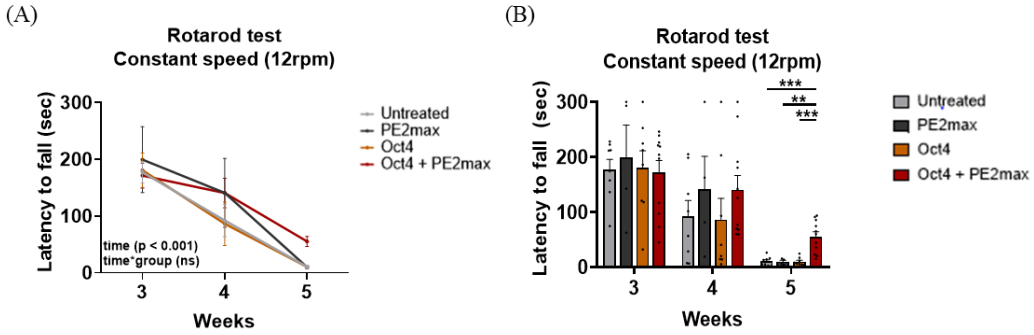

Figure 49. The Oct4 + PE2max combination therapy significantly preserves motor performance in the 12-rpm fixed-speed rotarod test.

(A) The rotarod test at a constant speed of 12 rpm was conducted weekly from postnatal weeks 3–5 to assess motor coordination and endurance. The latency to fall decreased over time in the untreated, PE2max, and Oct4 groups, indicating progressive motor impairment. In contrast, the Oct4 + PE2max combination group (red line) maintained performance with a slower rate of decline, indicating a protective effect on motor function.

(B) At week 5, the combination group demonstrated the longest latency to fall, with a statistically significant difference compared with the untreated group (*$p < 0.05$). These findings indicate that the cotreatment of Oct4 and PE2max synergistically preserves motor function under moderate motor challenge, as modeled by the 12-rpm fixed-speed rotarod

test. Statistical analysis was conducted using two-way ANOVA with a Bonferroni post hoc test, demonstrating significant effects for both time and treatment groups.

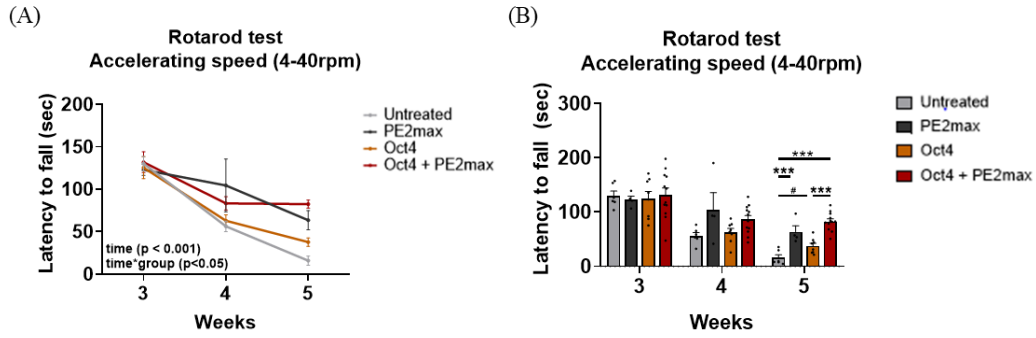

Figure 50. The Oct4 + PE2max combination treatment preserves motor endurance under accelerating rotarod conditions (4–40 rpm).

(A) The accelerating rotarod test (from 4 to 40 rpm) was conducted weekly from postnatal weeks 3–5 to assess motor coordination and endurance under increasing motor demand. The latency to fall significantly reduced by week 5 in the untreated, PE2max-only, and Oct4-only groups, indicating progressive motor dysfunction. In contrast, the Oct4 + PE2max combination group (red line) maintained motor performance over time, with minimal latency reduction.

(B) At week 5, the combination group demonstrated the longest latency to fall among all groups, exhibiting a statistically significant difference compared with the untreated group (*$p < 0.05$). These findings indicate that the combination of Oct4 and PE2max provides synergistic neuroprotective effects, especially under more challenging motor tasks that need sustained coordination and balance. Statistical analysis was conducted using two-way ANOVA with a Bonferroni post hoc correction, revealing significant effects of both time and treatment groups.

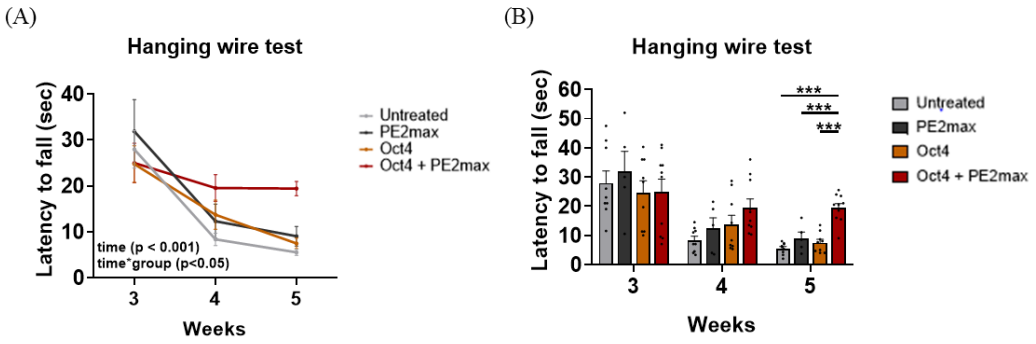

Figure 51. The combination of Oct4 and PE2max most effectively preserves neuromuscular performance in the hanging wire test.

(A) The hanging wire test was conducted weekly from postnatal weeks 3–5 to assess neuromuscular strength and coordination by measuring the time each mouse could remain suspended on a horizontal wire. The untreated, PE2max-only, and Oct4-only groups demonstrated a progressive decrease in latency to fall over time, whereas the Oct4 + PE2max combination group (red line) maintained a relatively stable latency, indicating delayed motor function decline.

(B) At week 5, the combination group demonstrated the longest hanging time among all groups, with a statistically significant improvement compared with the untreated group (*p < 0.05). These findings indicate that Oct4 and PE2max coadministration effectively preserves neuromuscular integrity and delays motor impairment in Twitcher mice. Statistical analysis was conducted using two-way ANOVA with a Bonferroni post hoc test, confirming the significant effects of both the time and treatment groups.

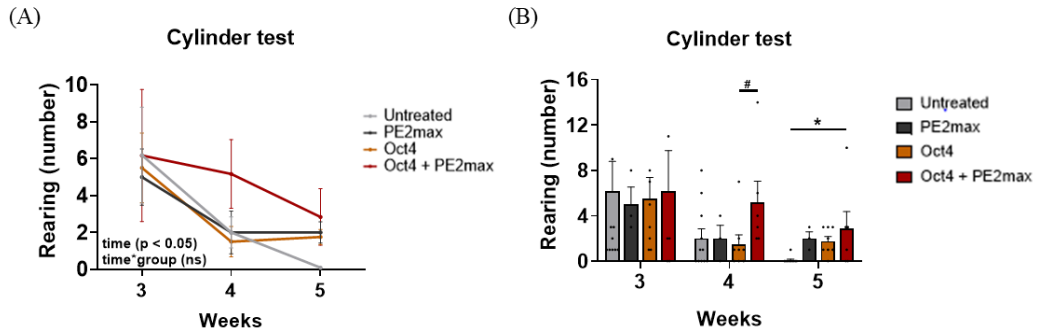

Figure 52. Oct4 + PE2max cotreatment shows a trend toward forelimb motor preservation in the cylinder test.

(A) The cylinder test was conducted weekly from postnatal weeks 3–5 to assess forelimb motor function and wall contact asymmetry. The untreated, PE2max, and Oct4 groups exhibited a general decline in forelimb usage over time. In contrast, the Oct4 + PE2max combination group (red line) maintained a relatively higher performance, indicating a partial motor decline.

(B) The combination group demonstrated the highest forelimb use score at week 5; however, the two-way ANOVA revealed no statistically significant differences for either time or group effects. These findings indicate that Oct4 + PE2max treatment has a positive trend toward functional preservation.

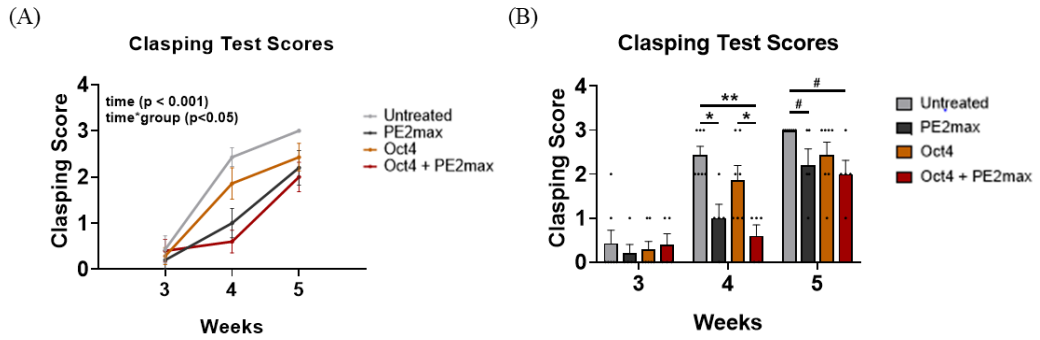

Figure 53. Clasping test reveals a delay in neurodegeneration with Oct4 + PE2max combination treatment.

(A) The clasping test was conducted weekly from postnatal weeks 3–5 to assess hindlimb

clasping behavior, which is a hallmark indicator of progressive neurodegeneration in Twitcher mice.

Clasping scores steadily increased over time in the untreated, PE2max, and Oct4 groups, reflecting worsening motor impairment. In contrast, the Oct4 + PE2max group (red line) demonstrated a slower increase in the clasping score, indicating the neuroprotective effects of the combined treatment.

(B) At week 5, the combination group maintained the lowest clasping scores among all groups, indicating a delay in symptom progression. However, the two-way ANOVA did not detect statistically significant differences across groups. These results imply that Oct4 + PE2max may help slow the progression of neurodegenerative disease. However, further studies with larger sample sizes and extended timepoints are warranted to confirm the significance of the results.

Table 49. Characterization of variance heterogeneity across behavioral assays in Twitcher mouse**.**

Test	Week	Untreated	PE2max	Oct4	PE2MAX+Oct4	*F*-value	*P*-value
Rotarod constant 4rpm	3	256.96±30.01	231.22±41.28	249.93±20.86	255.35±18.01	0.155	0.926
	4	203.05±33.64	265.74±23.48	240.39±38.79	257.97±19.28	0.846	0.479
	5	81.38±30.52	143.90±39.74	189.55±33.29	269.96±13.26	11.302	<0.001
Rotarod constant 12rpm	3	177.15±18.72	199.55±58.31	180.79±30.48	171.27±22.11	0.130	0.942
	4	92.21±28.55	140.80±60.67	86.38±38.42	140.64±26.09	0.749	0.533
	5	10.50±2.97	9.75±2.80	10.19±2.55	55.23±8.81	13.645	<0.001
Rotarod accelerated 4-40rpm	3	130.07±8.63	122.80±6.677	125.25±12.98	131.83±12.45	0.096	0.961
	4	56.22±6.09	104.45±31.085	62.92±6.93	86.25±7.47	3.124	0.043
	5	15.75±5.39	63.50±11.378	37.54±5.01	82.46±4.86	26.231	<0.001
Hanging wire test	3	23.75±3.81	31.86±6.95	25.38±4.45	25.00±4.28	0.431	0.733
	4	7.97±1.74	12.30±3.72	14.38±3.52	19.55±2.90	2.451	0.087
	5	4.56±0.68	9.04±2.13	7.90±1.20	19.40±1.55	21.79	<0.001
Cylinder test	3	6.18±2.61	5.00±1.53	5.50±1.89	6.17±3.58	0.029	0.993
	4	2.00±0.84	2.00±1.16	1.50±0.82	5.17±1.87	1.892	0.158
	5	0.09±0.091	2.00±0.58	1.75±0.41	2.83±1.54	3.189	0.042
Clasping test	3	0.43±0.30	0.20±0.20	0.29±0.18	0.40±0.24	0.178	0.910
	4	2.43±0.20	1.00±0.32	1.86±0.34	0.60±0.24	8.229	<0.001
	5	3.00±0.00	2.20±0.37	2.43±0.30	2.00±0.32	2.697	0.073

Note: Data is presented as mean ± SEM. Statistical analysis was performed using one-way ANOVA, followed by Bonferroni's post hoc test. *$P < 0.05$, **$P < 0.01$, ***$P < 0.001$.

Table 50. Statistical analysis details of behavioral evaluations in Twitcher mouse

Test	Age	Comparison Groups			N	Summary	*P*-value
Rotarod constant 4rpm	3 weeks	Untreated	vs	PE2max	8:5	ns	1.000
		Untreated	vs	Oct4	8:8	ns	1.000
		Untreated	vs	PE2max+Oct4	8:14	ns	1.000
		PE2max	vs	Oct4	5:8	ns	1.000
		PE2max	vs	PE2max+Oct4	5:14	ns	1.000
		Oct4	vs	PE2max+Oct4	8:14	ns	1.000
	4 weeks	Untreated	vs	PE2max	8:5	ns	1.000
		Untreated	vs	Oct4	8:8	ns	1.000
		Untreated	vs	PE2max+Oct4	8:14	ns	0.942
		PE2max	vs	Oct4	5:8	ns	1.000
		PE2max	vs	PE2max+Oct4	5:14	ns	1.000
		Oct4	vs	PE2max+Oct4	8:14	ns	1.000
	5weeks	Untreated	vs	PE2max	8:5	ns	0.946
		Untreated	vs	Oct4	8:8	*	0.046
		Untreated	vs	PE2max+Oct4	8:14	***	<0.001
		PE2max	vs	Oct4	5:8	ns	1.000
		PE2max	vs	PE2max+Oct4	5:14	*	0.019
		Oct4	vs	PE2max+Oct4	8:14	ns	0.137
Rotarod constant 12rpm	3 weeks	Untreated	vs	PE2max	8:4	ns	1.000
		Untreated	vs	Oct4	8:8	ns	1.000
		Untreated	vs	PE2max+Oct4	8:11	ns	1.000
		PE2max	vs	Oct4	4:8	ns	1.000
		PE2max	vs	PE2max+Oct4	4:11	ns	1.000
		Oct4	vs	PE2max+Oct4	8:11	ns	1.000
	4 weeks	Untreated	vs	PE2max	8:4	ns	1.000
		Untreated	vs	Oct4	8:8	ns	1.000
		Untreated	vs	PE2max+Oct4	8:11	ns	1.000
		PE2max	vs	Oct4	4:8	ns	1.000
		PE2max	vs	PE2max+Oct4	4:11	ns	1.000
		Oct4	vs	PE2max+Oct4	8:11	ns	1.000
	5weeks	Untreated	vs	PE2max	8:4	ns	1.000

		Untreated	vs	Oct4	8:8	ns	1.000
		Untreated	vs	PE2max+Oct4	8:11	***	<0.001
		PE2max	vs	Oct4	4:8	ns	1.000
		PE2max	vs	PE2max+Oct4	4:11	**	0.002
		Oct4	vs	PE2max+Oct4	8:11	***	<0.001
Rotarod accelerated 4-40rpm	3 weeks	Untreated	vs	PE2max	6:4	ns	1.000
		Untreated	vs	Oct4	6:8	ns	1.000
		Untreated	vs	PE2max+Oct4	6:12	ns	1.000
		PE2max	vs	Oct4	4:8	ns	1.000
		PE2max	vs	PE2max+Oct4	4:12	ns	1.000
		Oct4	vs	PE2max+Oct4	8:12	ns	1.000
	4 weeks	Untreated	vs	PE2max	6:4	ns	0.108
		Untreated	vs	Oct4	6:8	ns	1.000
		Untreated	vs	PE2max+Oct4	6:12	ns	0.317
		PE2max	vs	Oct4	4:8	ns	0.182
		PE2max	vs	PE2max+Oct4	4:12	ns	1.000
		Oct4	vs	PE2max+Oct4	8:12	ns	0.576
	5weeks	Untreated	vs	PE2max	6:4	***	<0.001
		Untreated	vs	Oct4	6:8	ns	0.123
		Untreated	vs	PE2max+Oct4	6:12	***	<0.001
		PE2max	vs	Oct4	4:8	ns	0.092
		PE2max	vs	PE2max+Oct4	4:12	ns	0.330
		Oct4	vs	PE2max+Oct4	8:12	***	<0.001
Hanging wire test	3 weeks	Untreated	vs	PE2max	6:5	ns	1.000
		Untreated	vs	Oct4	6:8	ns	1.000
		Untreated	vs	PE2max+Oct4	6:10	ns	1.000
		PE2max	vs	Oct4	5:8	ns	1.000
		PE2max	vs	PE2max+Oct4	5:10	ns	1.000
		Oct4	vs	PE2max+Oct4	8:10	ns	1.000
	4 weeks	Untreated	vs	PE2max	6:5	ns	1.000
		Untreated	vs	Oct4	6:8	ns	1.000
		Untreated	vs	PE2max+Oct4	6:10	ns	0.087
		PE2max	vs	Oct4	5:8	ns	1.000

		PE2max	vs	PE2max+Oct4	5:10	ns	0.800
		Oct4	vs	PE2max+Oct4	8:10	ns	1.000
	5weeks	Untreated	vs	PE2max	6:5	ns	0.457
		Untreated	vs	Oct4	6:8	ns	0.809
		Untreated	vs	PE2max+Oct4	6:10	***	<0.001
		PE2max	vs	Oct4	5:8	ns	1.000
		PE2max	vs	PE2max+Oct4	5:10	***	<0.001
		Oct4	vs	PE2max+Oct4	8:10	***	<0.001
Cylinder test	3 weeks	Untreated	vs	PE2max	11:3	ns	1.000
		Untreated	vs	Oct4	11:8	ns	1.000
		Untreated	vs	PE2max+Oct4	11:6	ns	1.000
		PE2max	vs	Oct4	3:8	ns	1.000
		PE2max	vs	PE2max+Oct4	3:6	ns	1.000
		Oct4	vs	PE2max+Oct4	8:6	ns	1.000
	4 weeks	Untreated	vs	PE2max	11:3	ns	1.000
		Untreated	vs	Oct4	11:8	ns	1.000
		Untreated	vs	PE2max+Oct4	11:6	ns	0.328
		PE2max	vs	Oct4	3:8	ns	1.000
		PE2max	vs	PE2max+Oct4	3:6	ns	0.959
		Oct4	vs	PE2max+Oct4	8:6	ns	0.227
	5weeks	Untreated	vs	PE2max	11:3	ns	0.772
		Untreated	vs	Oct4	11:8	ns	0.403
		Untreated	vs	PE2max+Oct4	11:6	*	0.047
		PE2max	vs	Oct4	3:8	ns	1.000
		PE2max	vs	PE2max+Oct4	3:6	ns	1.000
		Oct4	vs	PE2max+Oct4	8:6	ns	1.000
Clasping test	3 weeks	Untreated	vs	PE2max	7:5	ns	1.000
		Untreated	vs	Oct4	7:7	ns	1.000
		Untreated	vs	PE2max+Oct4	7:5	ns	1.000
		PE2max	vs	Oct4	5:7	ns	1.000
		PE2max	vs	PE2max+Oct4	5:5	ns	1.000
		Oct4	vs	PE2max+Oct4	7:5	ns	1.000
	4 weeks	Untreated	vs	PE2max	7:5	*	0.014

	Untreated	vs	Oct4	7:7	ns	0.851
	Untreated	vs	PE2max+Oct4	7:5	**	0.001
	PE2max	vs	Oct4	5:7	ns	0.295
	PE2max	vs	PE2max+Oct4	5:5	ns	1.000
	Oct4	vs	PE2max+Oct4	7:5	*	0.036
5weeks	Untreated	vs	PE2max	7:5	ns	0.295
	Untreated	vs	Oct4	7:7	ns	0.702
	Untreated	vs	PE2max+Oct4	7:5	ns	0.099
	PE2max	vs	Oct4	5:7	ns	1.000
	PE2max	vs	PE2max+Oct4	5:5	ns	1.000
	Oct4	vs	PE2max+Oct4	7:5	ns	1.000

Note: Data is presented as mean ± SEM. Statistical analysis was performed using one-way ANOVA, followed by Bonferroni's post hoc test. *$P < 0.05$, **$P < 0.01$, ***$P < 0.001$.

3.17. PE2maxOct4 overexpression significantly extends the lifespan of Twitcher mice

The survival and lifespan of Twitcher mice were assessed daily. No statistically significant difference in the overall lifespan was found between the groups; however, the survival rate analysis revealed distinct differences. The Gehan–Breslow–Wilcoxon test indicated a significant divergence in the survival curves. Furthermore, Pearson's Chi-square analysis identified significant differences between the groups, specifically from day 33 to day 40.

(A)

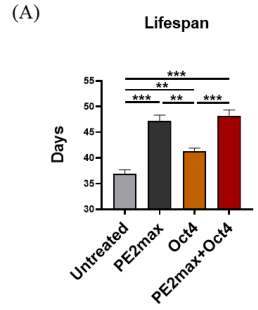

(B)

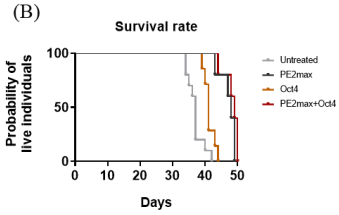

(C)

	Untreated	PE2max	Oct4	PE2max + Oct4	Chi square	*p* value
33 days	100%	100%	100%	100%	-	-
34 days	80%	100%	100%	100%	3.672	0.316
35 days	70%	100%	100%	100%	5.738	0.210
36 days	60%	100%	100%	100%	7.983	0.045
37 days	20%	100%	100%	100%	19.326	<0.001
38 days	20%	100%	100%	100%	19.326	<0.001
39 days	20%	100%	85.71%	100%	15.943	<0.001
40 days	10%	100%	71.43%	100%	17.355	<0.001
41 days	10%	100%	28.57%	100%	17.673	<0.001
42 days	0%	100%	28.57%	100%	21.214	<0.001
43 days	0%	80%	14.28%	100%	19.894	<0.001
44 days	0%	80%	0%	80%	19.326	<0.001
45 days	0%	80%	0%	80%	19.326	<0.001
46 days	0%	80%	0%	80%	19.326	<0.001
47 days	0%	60%	0%	80%	16.586	<0.001
48 days	0%	40%	0%	60%	11.095	0.005
49 days	0%	0%	0%	40%	9.504	0.057
50 days	0%	0%	0%	0%	-	-

Figure 54. Combined PE2max and Oct4 treatment extends lifespan in Twitcher mice.
The effect of PE2max and Oct4 treatment on the survival of Twitcher mice.

(A) A bar graph comparing the average lifespan of animals in each treatment group illustrates that the combination of PE2max and Oct4 caused the most pronounced increase in lifespan among all groups. The untreated group demonstrated the shortest lifespan, whereas the PE2max-only and Oct4-only groups exhibited moderate but partial improvements.

Importantly, the PE2max + Oct4 group demonstrated a greater lifespan extension than either monotherapy group, indicating a potential synergistic effect of the dual treatment.

(B) The Kaplan–Meier survival curves further support these results. Mice treated with both PE2max and Oct4 survived significantly longer than their counterparts in the other groups. The survival benefit in the combination group became more obvious after PD37, and the difference widened over time. The untreated group showed rapid mortality, with complete lethality observed around PD41, whereas the PE2max + Oct4 group maintained survival in a larger proportion of animals beyond this timepoint.

(C) The number of animals used in each group was as follows: untreated (N = 10), PE2max (N = 5), Oct4 (N = 7), and PE2max + Oct4 (N = 5). Together, these results indicate

that the coadministration of PE2max and Oct4 exhibits a more robust therapeutic effect in prolonging the lifespan of Twitcher mice compared with either treatment alone.

3.18. Body weight preservation in Twitcher mice through PE2max + Oct4 treatment.

We evaluated both behavioral and physiological parameters in Twitcher mice to assess the therapeutic efficacy of the PE2max + Oct4 combination therapy. KD is characterized by severe seizures, tremors, progressive weight loss, muscle stiffness, and eventual limb paralysis. However, affected mice typically do not demonstrate overt neurological symptoms until PD20. Therefore, we conducted behavioral assessments on PD21, PD28, and PD35 to capture early-stage functional decline and compare performance between groups. Further, body weight was measured at PD21, PD28, and PD35 to monitor general health and track disease progression. Brain weight was recorded at PD38 immediately after sacrifice. Mice treated with PE2max + Oct4 demonstrated significantly higher body weight than untreated controls across all time points. Statistical analysis using two-way ANOVA revealed a significant interaction between the time and treatment groups, indicating that the combined therapy more effectively preserved body weight over time compared with single or no treatment.

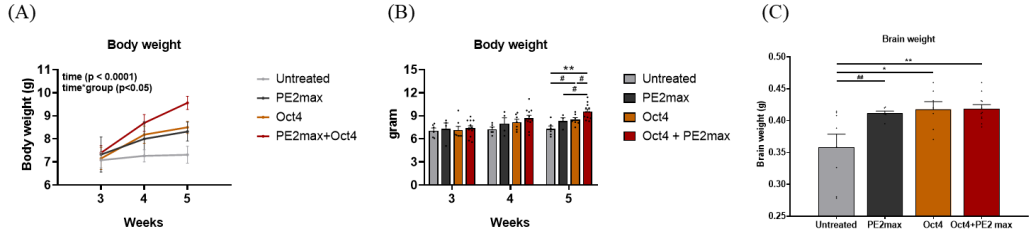

Figure 55. Combined treatment with PE2max and Oct4 prevents body weight loss in Twitcher mice.

(A) The line graph depicts changes in body weight measured on PD21, PD28, and PD35. The PE2max + Oct4 group (red line) demonstrated the most substantial increase in body weight over time. In contrast, the untreated group (light gray) demonstrated minimal weight

gain, whereas both the PE2max-only (dark gray) and Oct4-only (orange) groups exhibited less pronounced, but partial, improvements. According to two-way ANOVA with a Bonferroni post hoc correction, the PE2max + Oct4 group had significantly higher body weight than the untreated group at all time points.

(B) The bar graphs present body weight at each time point (PD21, PD28, and PD35), reinforcing the observation that the combination treatment most effectively maintained body weight. Notably, at PD35, the PE2max + Oct4 group demonstrated a statistically significant increase, indicating suppression of disease progression.

(C) Brain weight measured at PD38 post sacrifice revealed a significant increase in the PE2max + Oct4 group compared with the untreated group. This indicates that the therapeutic effect may extend beyond peripheral weight maintenance and could positively impact CNS preservation or development.

Table 51. Characterization of variance heterogeneity across body weight and brain weight assays in Twitcher mouse.

Test	Week	Untreated	PE2max	Oct4	*PE2max+Oct4*	*F*-value	*P*-value
Body weight	3	7.08±0.33	7.33±0.76	7.16±0.48	7.40±0.31	0.131	0.941
	4	7.27±0.26	8.00±0.74	8.19±0.37	8.69±0.37	2.147	0.120
	5	7.32±0.37	8.32±0.41	8.50±0.26	9.56±0.28	8.984	<0.001
Brain weight	5	0.36±0.02	0.41±0.00	0.42 ±0.01	0.42±0.01	5.634	0.004

Note: Data is presented as mean ± SEM. Statistical analysis was performed using one-way ANOVA, followed by Bonferroni's post hoc test. *$P < 0.05$, **$P < 0.01$, ***$P < 0.001$.

Table 52. Statistical analysis details of body weight and brain weight evaluations in Twitcher mice

Test	Age	Comparison Groups			N	Summary	*P*-value
Body weight	3 weeks	Untreated	vs	PE2max	6:4	ns	1.000
		Untreated	vs	Oct4	6:7	ns	1.000
		Untreated	vs	PE2max+Oct4	6:12	ns	1.000
		PE2max	vs	Oct4	4:7	ns	1.000
		PE2max	vs	PE2max+Oct4	4:12	ns	1.000
		Oct4	vs	PE2max+Oct4	7:12	ns	1.000
	4weeks	Untreated	vs	PE2max	6:4	ns	1.000
		Untreated	vs	Oct4	6:7	ns	0.945
		Untreated	vs	PE2max+Oct4	6:12	ns	0.112
		PE2max	vs	Oct4	4:7	ns	1.000
		PE2max	vs	PE2max+Oct4	4:12	ns	1.000
		Oct4	vs	PE2max+Oct4	7:12	ns	1.000
	5weeks	Untreated	vs	PE2max	6:4	ns	0.549
		Untreated	vs	Oct4	6:7	ns	0.145
		Untreated	vs	PE2max+Oct4	6:12	***	<0.001
		PE2max	vs	Oct4	4:7	ns	1.000
		PE2max	vs	PE2max+Oct4	4:12	ns	0.138
		Oct4	vs	PE2max+Oct4	7:12	ns	0.113
Brain weight	5weeks	Untreated	vs	PE2max	8:6	ns	0.054
		Untreated	vs	Oct4	8:7	*	0.016
		Untreated	vs	PE2max+Oct4	8:11	**	0.005
		PE2max	vs	Oct4	6:7	ns	1.000
		PE2max	vs	PE2max+Oct4	6:11	ns	1.000
		Oct4	vs	PE2max+Oct4	7:11	ns	1.000

Note: Data is presented as mean ± SEM. Statistical analysis was performed using one-way ANOVA, followed by Bonferroni's post hoc test. *$P < 0.05$, **$P < 0.01$, ***$P < 0.001$.

3.19. H&E Analysis Reveals No Tumor Formation in Brain After Intracerebroventricular Injection of AAV vector.

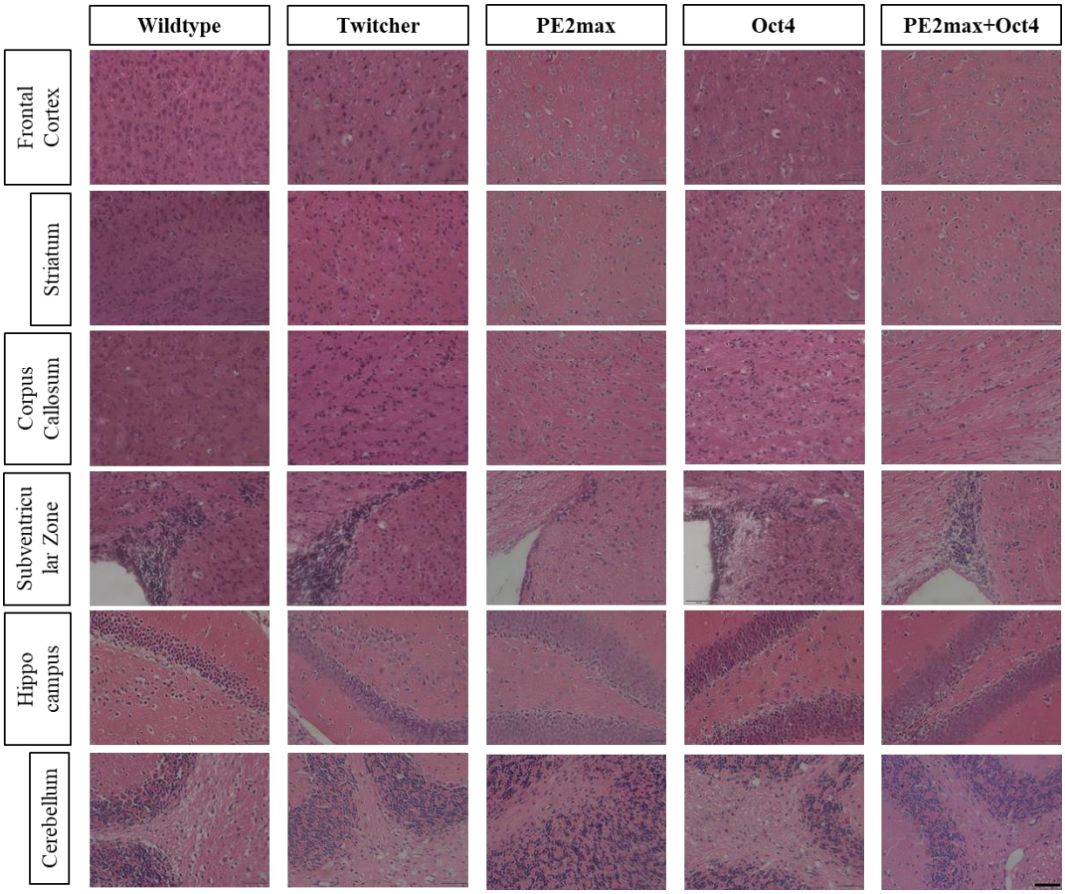

Figure 56. Hematoxylin and Eosin (H&E) Staining of Major Organs Following AAV Administration
Representative H&E-stained sections of the brain were examined to assess potential tumor formation or abnormal histopathology following systemic or intracerebroventricular administration of AAV vectors. No evidence of tumorigenesis, inflammation, or structural abnormalities was observed in any of the examined tissues, indicating the safety of AAV-based gene delivery in vivo. Scale bar = 50 μm

4. Discussion

This study assessed the therapeutic potential of Oct4 and PE2max in the KD Twitcher mouse model. We aimed to identify how these interventions mitigate disease progression by integrating transcriptomic profiling, behavioral assessments, and histological analysis. The results demonstrate that Oct4 facilitates reprogramming toward the oligodendrocyte lineage, whereas PE2max restores GALC enzymatic activity through precise gene correction. The combination of both treatments generated a synergistic effect, causing reduced demyelination and extended survival. Transcriptome analysis revealed that Oct4 administration significantly modulated gene expression associated with oligodendrocyte differentiation. Among the upregulated genes were *ENPP2, JAK1, JAK2*, and *STAT3*, all of which are involved in oligodendrocyte development and maturation.[16,17] These results are consistent with previous reports indicating that Oct4 promotes reprogramming toward the oligodendrocyte progenitor cell lineage. IHC staining corroborated these results, exhibiting increased expression of oligodendrocyte lineage markers in the Oct4-treated group, thereby supporting its role in remyelination through lineage reprogramming. PE2max, which is a next-generation prime editor engineered for efficient base editing, was designed to correct the pathogenic c.355A>G point mutation in the *Galc* gene. PE2max treatment restored GALC enzymatic activity, particularly in the spinal cord (SC) and cerebellum, which are regions most affected by twitcher pathology. This restoration contributed to myelin preservation, as evidenced by LFB-PAS staining and reduced white matter vacuolization.[18] PE2max monotherapy produced moderate benefits; however, its combination with Oct4 resulted in more pronounced functional and histological improvements. Behavioral tests, including motor function and neurobehavioral assessments, demonstrated the greatest improvements in the combined treatment group. Further, body and brain weight preservation was most evident in this group. The Chi-square test indicated that survival rates differed significantly between treatment groups, which may reflect differences in therapeutic efficacy. Despite these encouraging outcomes, the clinical translation of Oct4

remains limited because of its oncogenic potential. Recent studies have investigated alternative transcription factors with improved safety profiles to address this limitation. For instance, Sox10 and Olig2 have directly reprogrammed postnatal cortical astrocytes into MBP^+ or $PDGFR\alpha^+$ oligodendrocyte lineage cells *in vivo*, without inducing tumorigenesis. Sox10 alone efficiently drives fate conversion, whereas Olig2, either independently or in combination with Sox10, further improves oligodendrocyte lineage specification.[19,20] Moreover, EGF signaling augments Sox10-mediated reprogramming efficiency and maturation in SC injury models. These findings indicate that Sox10 and Olig2 may serve as safer and more clinically viable alternatives to Oct4 for *in vivo* remyelination strategies.[21] Future investigations should directly compare these factors with Oct4-based approaches to assess therapeutic efficacy, lineage stability, and long-term safety in disease models, such as the Twitcher mouse model.

5. Conclusion

In summary, this study reveals that the combinational treatment of PE2max and Oct4 exhibits a synergistic therapeutic effect in Twitcher mice. Oct4 improves oligodendrocyte differentiation through cellular reprogramming, whereas PE2max restores GALC enzyme function via precise gene editing. Integration of these two strategies effectively attenuates demyelination, improves behavioral and physiological outcomes, and prolongs survival. These results indicate the potential of combining gene correction and cell fate modulation as a novel therapeutic approach for lysosomal storage diseases such as KD.

6. Reference

1 Suzuki, K. & Suzuki, K. The Twitcher mouse: a model for Krabbe disease and for experimental therapies. *Brain Pathol* **5**, 249-258 (1995). https://doi.org:10.1111/j.1750-3639.1995.tb00601.x

2 Shinoda, H., Kobayashi, T., Katayama, M., Goto, I. & Nagara, H. Accumulation of Galactosylsphingosine (Psychosine) in the Twitcher mouse - Determination by Hplc. *J Neurochem* **49**, 92-99 (1987). https://doi.org:DOI 10.1111/j.1471-4159.1987.tb03399.x

3 Herdt, A. R. *et al.* Brain Targeted AAV1-GALC Gene Therapy Reduces Psychosine and Extends Lifespan in a Mouse Model of Krabbe Disease. *Genes (Basel)* **14** (2023). https://doi.org:10.3390/genes14081517

4 Tonazzini, I. *et al.* Visual System Impairment in a Mouse Model of Krabbe Disease: The Twitcher mouse. *Biomolecules* **11** (2020). https://doi.org:10.3390/biom11010007

5 Nasir, G., Chopra, R., Elwood, F. & Ahmed, S. S. Krabbe Disease: Prospects of Finding a Cure Using AAV Gene Therapy. *Front Med (Lausanne)* **8**, 760236 (2021). https://doi.org:10.3389/fmed.2021.760236

6 Bendavid, E. *et al.* Emerging Perspectives on Prime Editor Delivery to the Brain. *Pharmaceuticals-Base* **17** (2024). https://doi.org:ARTN 763
10.3390/ph17060763

7 Davis, J. R. *et al.* Efficient prime editing in mouse brain, liver and heart with dual AAVs. *Nat Biotechnol* **42**, 253-264 (2024). https://doi.org:10.1038/s41587-023-01758-z

8 Yu, J. H. *et al.* In Vivo Expression of Reprogramming Factor OCT4 Ameliorates Myelination Deficits and Induces Striatal Neuroprotection in Huntington's Disease. *Genes (Basel)* **12** (2021). https://doi.org:10.3390/genes12050712

9 Zhu, S. *et al.* Small molecules enable OCT4-mediated direct reprogramming into expandable human neural stem cells. *Cell Res* **24**, 126-129 (2014). https://doi.org:10.1038/cr.2013.156

10 Foust, K. D. *et al.* Intravascular AAV9 preferentially targets neonatal neurons and adult astrocytes. *Nat Biotechnol* **27**, 59-65 (2009). https://doi.org:10.1038/nbt.1515

11 Hu, S., Yang, T. & Wang, Y. Widespread labeling and genomic editing of the fetal central nervous system by in utero CRISPR AAV9-PHP.eB administration. *Development* **148** (2021). https://doi.org:10.1242/dev.195586

12 Olmstead, C. E. Neurological and neurobehavioral development of the mutant 'twitcher' mouse. *Behav Brain Res* **25**, 143-153 (1987). https://doi.org:10.1016/0166-4328(87)90007-6

13 Scruggs, B. A. *et al.* High-throughput screening of stem cell therapy for globoid cell leukodystrophy using automated neurophenotyping of Twitcher mice. *Behav Brain Res* **236**, 35-47 (2013). https://doi.org:10.1016/j.bbr.2012.08.020

14 Murray, M., Butler, A. M., Fiala-Beer, E. & Su, G. M. Phospho-STAT5 accumulation in nuclear fractions from vitamin A-deficient rat liver. *FEBS Lett* **579**, 3669-3673 (2005). https://doi.org:10.1016/j.febslet.2005.05.052

15 Song, I. & Huganir, R. L. Regulation of AMPA receptors during synaptic plasticity. *Trends Neurosci* **25**, 578-588 (2002). https://doi.org:10.1016/s0166-2236(02)02270-1

16 Tang, Y. & Tian, X. C. JAK-STAT3 and somatic cell reprogramming. *JAKSTAT* **2**, e24935 (2013). https://doi.org:10.4161/jkst.24935

17 Hong, H. *et al.* Suppression of the JAK/STAT pathway inhibits neuroinflammation in the line 61-PFF mouse model of Parkinson's disease. *J Neuroinflammation* **21**, 216 (2024). https://doi.org:10.1186/s12974-024-03210-8

18 Beecken, M. *et al.* The Cuprizone Mouse Model: A Comparative Study of Cuprizone Formulations from Different Manufacturers. *Int J Mol Sci* **24** (2023). https://doi.org:10.3390/ijms241310564

19 El Waly, B., Cayre, M. & Durbec, P. Promoting Myelin Repair through Neuroblast Reprogramming. *Stem Cell Rep* **10**, 1492-1504 (2018). https://doi.org:10.1016/j.stemcr.2018.02.015

20 Matjusaitis, M. *et al.* Reprogramming of Fibroblasts to Oligodendrocyte Progenitor-like Cells Using CRISPR/Cas9-Based Synthetic Transcription Factors. *Stem Cell Rep* **13**, 1053-1067 (2019). https://doi.org:10.1016/j.stemcr.2019.10.010

21 Liu, X. Y. *et al.* EGF signaling promotes the lineage conversion of astrocytes into oligodendrocytes. *Mol Med* **28** (2022). https://doi.org:ARTN 50 10.1186/s10020-022-00478-5

Abstract in Korean

Krabbe병에서 Oct4 유도 리프로그래밍과 PE2max 기반 프라임 에디팅의 병합 효과가 탈수초 및 GALC 활성 회복에 미치는 영향

크라베병(Krabbe disease, KD)은 GALC 유전자의 기능 상실 돌연변이에 의해 발생하는 치명적인 리소좀 축적 질환으로, 미엘린 대사의 장애 및 신경세포 독성 대사산물인 사이코신(psychosine)의 축적으로 이어진다. 본 연구에서는 크라베병의 대표적인 동물모델인 Twitcher 마우스에서 프라임 에디팅과 생체 내 세포 리프로그래밍을 결합한 새로운 치료 전략의 효과를 평가하고자 하였다. 이를 위해, Galc 유전자의 점돌연변이를 프라임 에디터 PE2max를 이용하여 교정하였으며, 생후 1일차(PD 1)에 AAV9-Oct4를 뇌실 내 주입(intracerebroventricular injection)하여 Oct4 과발현을 유도하였다. 또한 전신 투여를 위해 PE2max를 발현하는 AAVPHP.eB를 안면정맥을 통해 주입하였다.

운동 및 행동 기능 평가는 PD21, PD28, PD35에 걸쳐 Rotarod, Hanging wire, Cylinder, Clasping을 통해 수행되었고, PD38에 희생하여 Galc 발현, 미엘린 회복(MBP), 그리고 세포 운명 마커(Nestin, Olig2, Tuj1, GFAP)를 평가하기 위해 qRT-PCR, 면역조직화학(IHC), 전자현미경(EM), MRI 등의 분자 및 조직학적 분석을 수행하였다. 또한, PD7~PD9에 BrdU 표지법을 통해 Oct4 과발현이 신경전구세포의 증식을 유도함을 확인하였다.

그 결과, Oct4 과발현은 신경줄기세포 및 희소돌기아교세포 계열 마커의 발현을 유의하게 증가시키고, 반응성 성상교세포증(astrogliosis)은 감소시켰다. PE2max에 의한 유전자 교정은 Galc 효소 활성을 회복시키고, 사이코신 축적을 감소시켰다. 두 치료법을 병합했을 때, 미엘린 회복, 행동 기능 개선, 생존 기

간 연장 측면에서 단독 치료나 대조군보다 더 우수한 효과를 보였다.

이러한 결과는 Oct4 기반 리프로그래밍과 PE2max 기반 유전자 교정을 결합한 이중 치료 전략이 세포 재생과 효소 결핍이라는 크라베병의 두 핵심 병리 기전을 동시에 해결할 수 있는 유망한 치료 접근법임을 시사한다